10.1071/CH21313
Australian Journal of Chemistry

Supplementary Material

Heteroleptic lanthanide(III) complexes: synthetic utility and versatility of the unsubstituted bis-scorpionate ligand framework

Tajrian Chowdhury[A], *Samuel J. Horsewill*[A], *Claire Wilson*[A] and *Joy H. Farnaby*[A,*]

[A]School of Chemistry, Joseph Black Building, University of Glasgow, Glasgow G12 8QQ, UK

*Correspondence to: Email: Joy.Farnaby@glasgow.ac.uk

Contents

A. Synthesis of ligands, reagents, and starting materials 3

S **i** Synthesis of Potassium hydrotris(1-pyrazolyl)borate **K(Tp)** 3

S **ii** Synthesis of Lanthanide triflates **Ln(OTf)$_3$** (Ln = Y, Eu, Gd, Yb) 3

S **iii** Synthesis of Sodium-benzophenone ketyl-radical solution for testing dryness of Lanthanide triflates and anhydrous solvents 5

B. Spectroscopic Data for complexes 1-Ln to 5-Ln 6

S1 Nuclear magnetic resonance (NMR) 6

S**1.1** K(Tp) 6

S**1.2** Ln(OTf)$_3$ (Ln = Y, Eu, Gd, Yb) 9

S**1.3** [Ln(Tp)$_2$(OTf)] **1-Ln** (Ln = Y, Eu, Gd, Yb) 11

S**1.4** [Ln(Tp)$_2$(hfac)] **2-Ln** (Ln = Y, Eu, Yb) 20

S**1.5** [Ln(Tp)$_2$(N'')] **3-Ln** (Ln = Y, Yb) 28

S**1.6** [{Y(Tp)$_2$(μ-OH)}$_2$] **4-Y** 33

S**1.7** [Ln(Tp)$_2$(OAr)] **5-Ln** (Ln = Y, Yb) 35

S2 Infrared (IR) 40

S**2.1** K(Tp) 40

S**2.2** Ln(OTf)$_3$ (Ln = Y, Eu, Gd, Yb) 40

S**2.3** [Ln(Tp)$_2$(OTf)] **1-Ln** (Ln = Y, Eu, Gd, Yb) 42

S**2.4** [Ln(Tp)$_2$(hfac)] **2-Ln** (Ln = Y, Eu, Yb) 44

S**2.5** [Ln(Tp)$_2$(N'')] **3-Ln** (Ln = Y, Yb) 46

S**2.6** [Ln(Tp)$_2$(OAr)] **5-Ln** (Ln = Y, Yb) 47

S3 Electronic absorption (UV-Vis-NIR) of Ln(Tp)$_2$(hfac) 2-Ln (Ln = Y, Eu, Yb) 48

C. References 49

A. Synthesis of ligands, reagents, and starting materials

S i Synthesis of Potassium hydrotris(1-pyrazolyl)borate K(Tp)

Potassium hydrotris(1-pyrazolyl)borate K(Tp) (**Figure S 1**) was synthesised by adaptation of literature procedure.[1] KBH_4 (1.52 g, 28.2 mmol, 1.0 eq) and pyrazole (8.03 g, 117.9 mmol, 4.2 eq) were combined dry in a 50 mL single-necked round-bottomed flask. The flask was mounted onto a heating block on a hot plate, equipped with a thermocouple. The round-bottomed flask was fitted with a take-off, which was connected *via* a Dreschel bottle to a large, up turned measuring cylinder (1 L) filled with water and partially submerged under water to collect and measure the H_2 gas given off by the reaction. All ground glass joints were greased, and rubber bands were used to hold the apparatus in place in order to prevent leakage of H_2. The temperature of the heating block was raised gradually in stages, beginning at 120 °C and ending at 210 °C. At each stage, the gas evolved was monitored and the temperature was raised after evolution had slowed. Gentle heating of the upper half of the reaction vessel was used to re-melt condensed pyrazole into the reaction melt. Once the gas evolution was complete (1.938 L, 79.2 mmol, 2.8 eq), the reaction vessel was cooled to 130°C and boiling toluene was added (40 mL). The mixture was immediately filtered across a frit. The round-bottomed flask was rinsed with boiling toluene (40 mL) onto the frit and the filtrates were cooled to RT overnight, yielding white crystals. The crystals were isolated by filtering across a Gooch crucible and were washed with room temperature toluene (2 x 25 mL) and hexane (4 x 10 mL). The white solids were then dried *in vacuo* (60°C, 10^{-2} mbar, 3 h) yielding K(Tp) as a white powder (4.36 g, 17.3 mmol, 61%). δ_H (d_3-MeCN) 4.70 (multiplet apparent q 1:1:1:1, $^1J_{BH}$ 105.3 Hz, Tp-B*H*), 6.07 (t, $^3J_{HH}$ 1.8 Hz, 6H, Tp-C^4*H*), 7.45 (apparent d, $^3J_{HH}$ 1.4 Hz, 6H, Tp-C^3*H*), 7.56 (d, $^3J_{HH}$ 2.1 Hz, 6H, Tp-C^5*H*) ppm. $\delta_{C\{H\}}$ (d_3-MeCN) 103.93 (Tp-*C*^{4}), 135.27 (Tp-*C*^{5}), 140.24 (Tp-*C*^{3}) ppm. δ_B (d_3-MeCN) -1.58 (d, $^1J_{BH}$ 107.7 Hz, Tp-*B*) ppm. $\delta_{B\{H\}}$ (d_3-MeCN) -1.55 (s, Tp-*B*) ppm. Anal. Calc. for $C_9H_{10}BN_6K$: C 42.87, H 4.00, N 33.33. Found: C 41.83-42.13, H 3.85-3.90, N 32.74-33.02%. ν_{max} (ATR)/cm^{-1} 3120 (w, $\upsilon_{sp^2\text{-}CH}$), 2438 (w, υ_{BH}), 2404 (w, υ_{BH}), 1737 (w), 1498 (m, $\upsilon_{C=C}$), 1418 (m), 1396 (m), 1290 (m), 1210 (m), 1112 (s), 1043 (s), 960 (m), 922 (w), 891 (w), 777 (s), 761 (s), 738 (s), 723 (s), 676 (m), 660 (m), 626 (m).

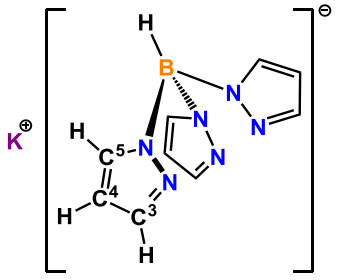

Figure S 1. Numbering system for the pyrazolyl carbon atoms.

S ii Synthesis of Lanthanide triflates Ln(OTf)$_3$ (Ln = Y, Eu, Gd, Yb)

A 200 mL rota-tap reaction ampoule was charged with a stirrer bar and the white powder of Ln_2O_3 was added. Triflic acid (10 g, 66.6 mmol) was added dropwise by pipette to 10 ml deionised H_2O at

0°C. Fumes were observed upon triflic acid addition and after fuming subsided, the diluted triflic acid solution was added dropwise to the ampoule. The ampoule was then sealed under partial vacuum and the stirred suspension was refluxed (110°C, 16 h), after which a slightly cloudy solution was obtained. Water was removed by rotary evaporation (40 mbar, 50°C) until precipitation was observed, then the mixture was filtered across a Gooch crucible/fritted Büchner funnel to obtain $Ln(OTf)_3(H_2O)_x$ as a white, wet crystalline solid. The solids were washed several times with Et_2O (at least 5 x 5 mL) until a microspatula (*ca* 3-5 mg) of solid dissolved in H_2O had neutral pH (6.5-7.0). The $Ln(OTf)_3$ were then dried overnight with heating *in vacuo* (200°C, 10^{-3} mbar) to afford $Ln(OTf)_3$ as a free-flowing white powder.

$Y(OTf)_3$ was synthesised using the following materials and quantities: Y_2O_3 (2.23 g, 9.88 mmol, 1.0 eq), HOTf (10 g, 66.6 mmol, 6.7 eq). Yield: 6.35 g, 11.85 mmol, 60%. δ_F (d_3-MeCN) -79.25 (s, OTf-C*F*$_3$) ppm. Anal. Calc. for $C_3S_3F_9O_9Y$: C 6.72, H 0.00, N 0.00. Found: C 6.64-6.96, H 0.19-0.25, N 0.00%. ν_{max} (ATR)/cm^{-1} 1636 (w), 1353 (w), 1299 (s), 1231 (s), 1196 (s), 1169 (s), 1032 (s), 777 (w), 626 (s), 581 (m).

$Eu(OTf)_3$ was synthesised using the following materials and quantities: Eu_2O_3 (3.55 g, 10.1 mmol, 1.0 eq), HOTf (10 g, 66.6 mmol, 6.6 eq). Yield: 6.54 g, 10.91 mmol, 54%. δ_F (d_3-MeCN) -80.01 (s, OTf-C*F*$_3$) ppm. Anal. Calc. for $C_3S_3F_9O_9Eu$: C 6.01, H 0.00, N 0.00. Found: C 5.79-5.94, H 0.00, N 0.00%. ν_{max} (ATR)/cm^{-1} 1624 (w), 1347 (w), 1287 (s), 1231 (s), 1215 (s), 1198 (s), 1167 (s), 1034 (s), 775 (w), 625 (s), 581 (m).

$Gd(OTf)_3$ was synthesised using the following materials and quantities: Gd_2O_3 (3.66 g, 10.1 mmol, 1.0 eq), HOTf (10 g, 66.6 mmol, 6.6 eq). Yield: 8.67 g, 14.34 mmol, 71%. δ_F (d_3-MeCN) -79.36 (s, OTf-C*F*$_3$) ppm. Anal. Calc. for $C_3S_3F_9O_9Gd$: C 5.96, H 0.00, N 0.00. Found: C 6.46-6.48, H 0.45-0.46, N 0.00%. ν_{max} (ATR)/cm^{-1} 1636 (w), 1344 (w), 1286 (s), 1232 (s), 1208 (s), 1163 (s), 1031 (s), 770 (w), 623 (s), 580 (m).

$Yb(OTf)_3$ was synthesised using the following materials and quantities: Yb_2O_3 (4.17 g, 11.0 mmol, 1.0 eq), HOTf (10 g, 66.6 mmol, 6.1 eq). Yield: 7.78 g, 12.54 mmol, 57%. δ_F (d_3-MeCN) -88.27 (s, OTf-C*F*$_3$) ppm. Anal. Calc. for $C_3S_3F_9O_9Yb$: C 5.81, H 0.00, N 0.00. Found: C 5.39-5.59, H 0.00, N 0.00%. ν_{max} (ATR)/cm^{-1} 1636 (w), 1352 (w), 1300 (s), 1231 (s), 1202 (s), 1167 (s), 1040 (s), 777 (w), 621 (s), 582 (m).

Note in the EA data, there is a range of H% seen after drying, which arises from an acceptable level of moisture and does not significantly impact the nature of the chemistry undertaken. Anal. Calc. for IR (ATR) sample of $Y(OTf)_3 \cdot xH_2O$, $C_3S_3F_9O_{x+9}H_{2x}Y$: C 5.16, H 2.60, N 0.00. Found: C 6.25-6.59%, H 1.06-1.31, N 0.00% consistent with x = 3.5-4.0. Note, the sample for ATR-IR for $Ln(OTf)_3$ was exposed to air/moisture for a maximum of 5-10 minutes and therefore is consistent with the formulation of $Ln(OTf)_3(H_2O)_x$, where x = 3.5-4.0, since $Ln(OTf)_3$ salts are very hygroscopic (see EA data for $Y(OTf)_3 \cdot xH_2O$ above for reference).

Complete dehydration was confirmed by ATR-IR, ^{1}H NMR spectroscopy, and testing with sodium-benzophenone ketyl-radical solution (see synthesis of the sodium-benzophenone ketyl-radical solution below in **S iii**). Dryness of the $Ln(OTf)_3$ was confirmed by testing a suspension of $Ln(OTf)_3$ in hexane with sodium benzophenone ketyl radical solution. In the glovebox, a spatula heap of $Ln(OTf)_3$ (*ca* 10-20 mg) was suspended in dry hexane (3 mL) in a 20 mL scintillation vial. The deep-violet sodium-benzophenone ketyl-radical solution (60 μL) was added by micropipette to the $Ln(OTf)_3$ suspension. The colour of the radical solution was retained for at least 2 minutes with vigorous shaking when $Ln(OTf)_3$ was dry. The colour gradually reduced in intensity from the original deep purple to pale-yellow over time.

S iii Synthesis of Sodium-benzophenone ketyl-radical solution for testing dryness of Lanthanide triflates and anhydrous solvents

The sodium benzophenone ketyl radical solution was synthesised using the following methodology, by adaptation of several literature procedures.[2,3] A 200 mL reaction ampoule was charged with a stirrer bar and two freshly cut Na cubes (250.0 mg, 10.8 mmol, 1.0 eq). Na was extracted from mineral oil, cut to size using a scalpel, and excess oil was removed by rinsing with dry hexane. The cubes were then placed directly in the ampoule under N_2 and dried *in vacuo*. To this ampoule, THF (90 mL) was added and stirred for 0.5 hours. A portion of this dry THF (10 mL) was used to dissolve and transfer benzophenone (1500.0 mg, 8.23 mmol, 1.2 eq) from a pencil ampoule to the reaction ampoule. The reaction mixture was stirred at ambient temperature for 4-5 hours. After few minutes, a dark-blue colour resulted, which gradually turned deep-violet over time. The deep-violet suspension was transferred to a Schlenk tube and filtered *via* filter cannula to exclude any sodium granules remaining, into a J. Young's ampoule for storage under N_2 in the glovebox.

B. Spectroscopic Data for complexes 1-Ln to 5-Ln

S1 Nuclear magnetic resonance (NMR)

S1.1 K(Tp)

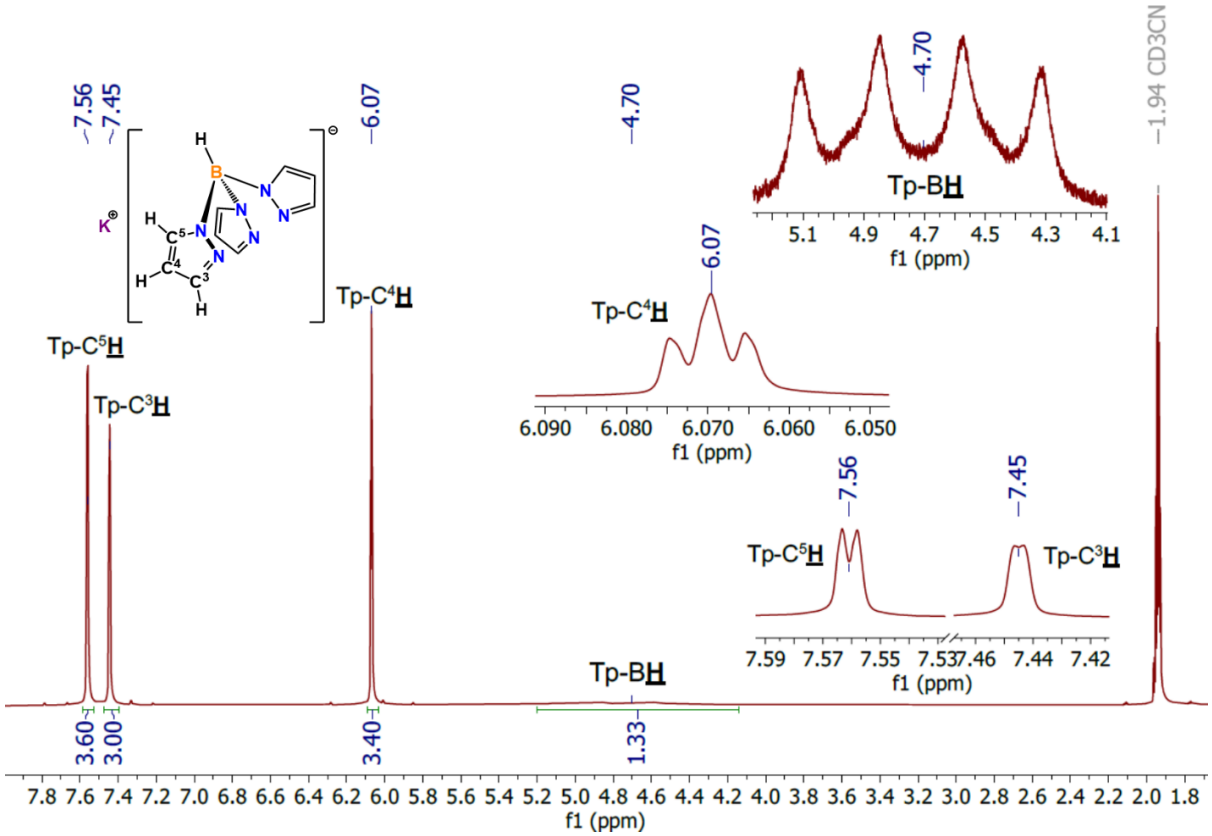

Figure S 2. ^{1}H NMR spectrum of K(Tp), recorded in d_3-MeCN. The pyrazolyl carbon atom numbering system shown here has been maintained in NMR data of all [Ln(Tp)$_2$(X)] complexes.

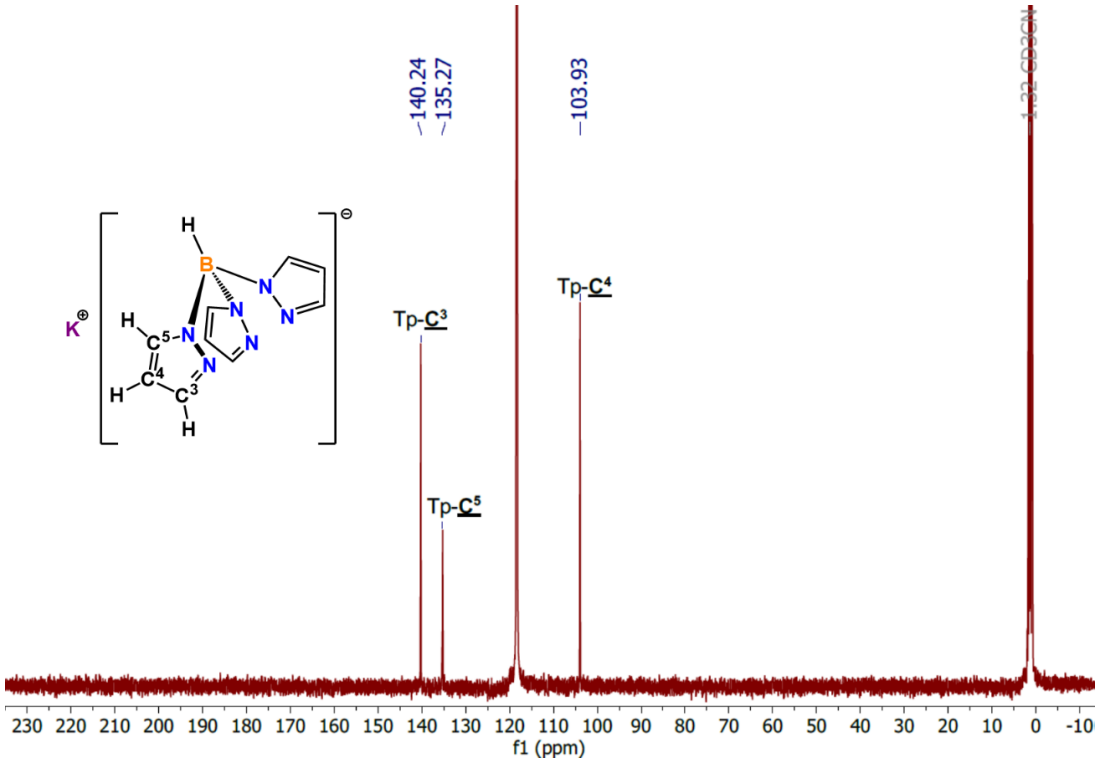

Figure S 3. ^{13}C{^{1}H} NMR spectrum of K(Tp), recorded in d_3-MeCN.

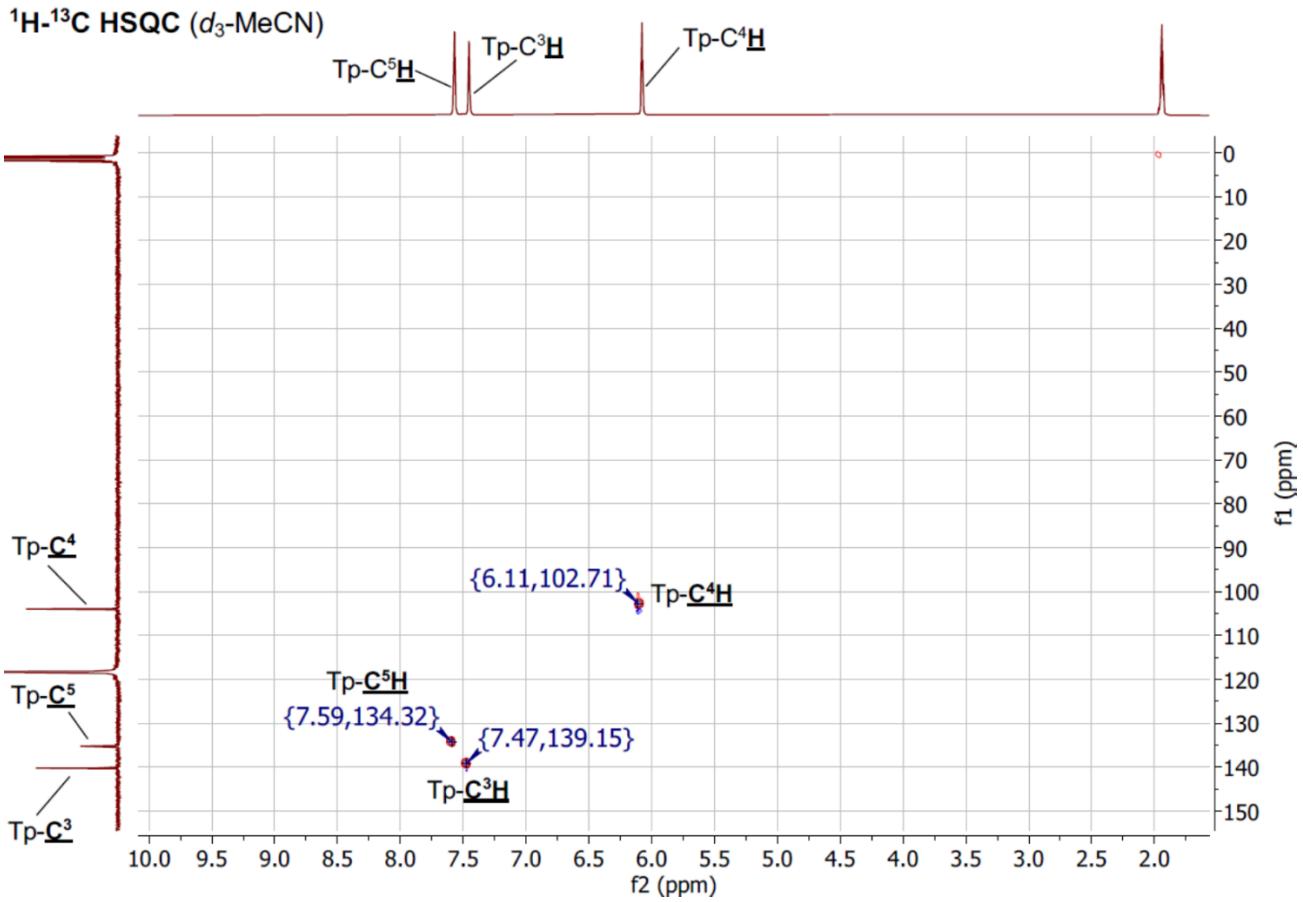

Figure S 4. ^{1}H-^{13}C HSQC NMR spectrum of K(Tp), recorded in d_3-MeCN.

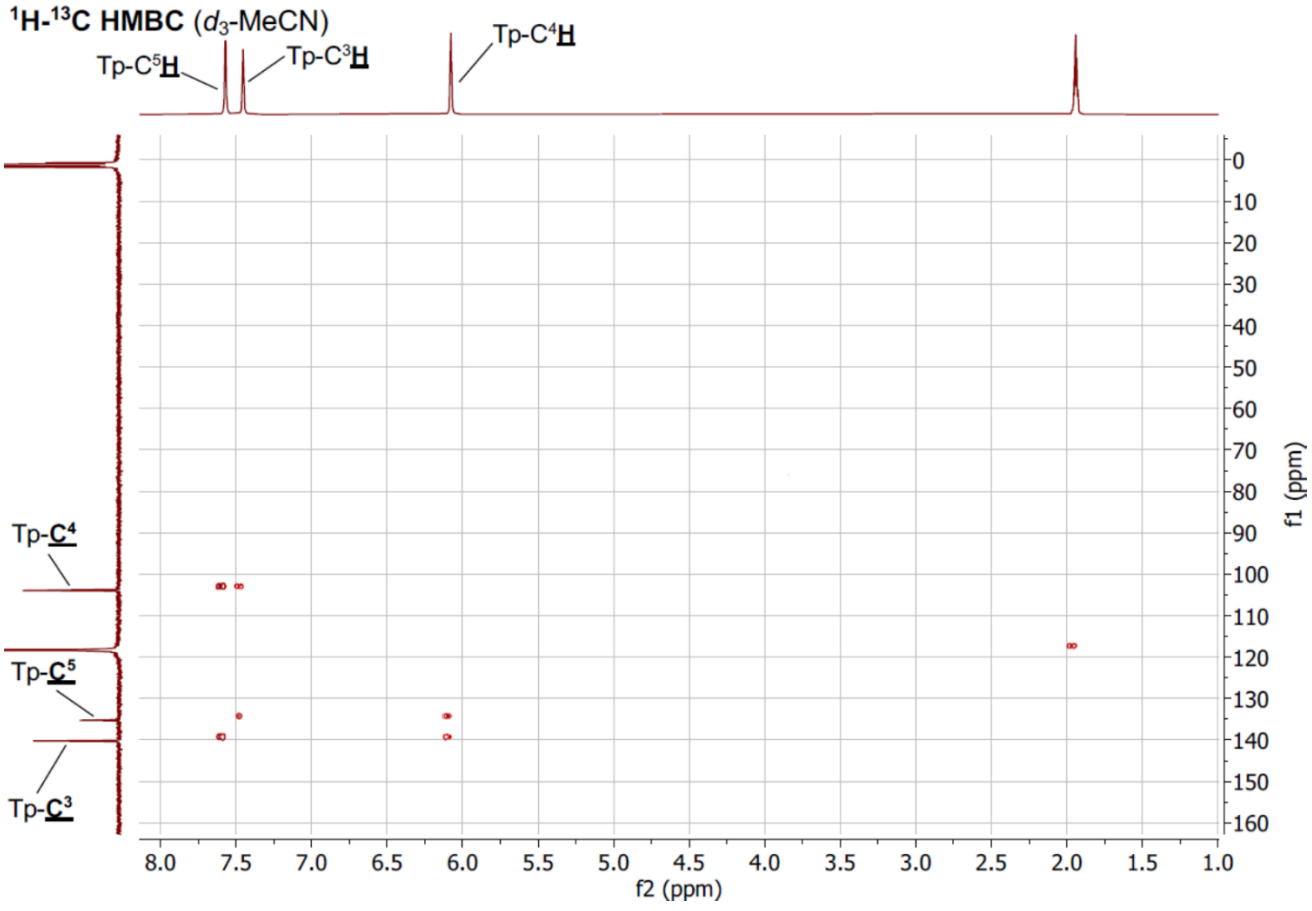

Figure S 5. ^{1}H-^{13}C HMBC NMR spectrum of K(Tp), recorded in d_3-MeCN.

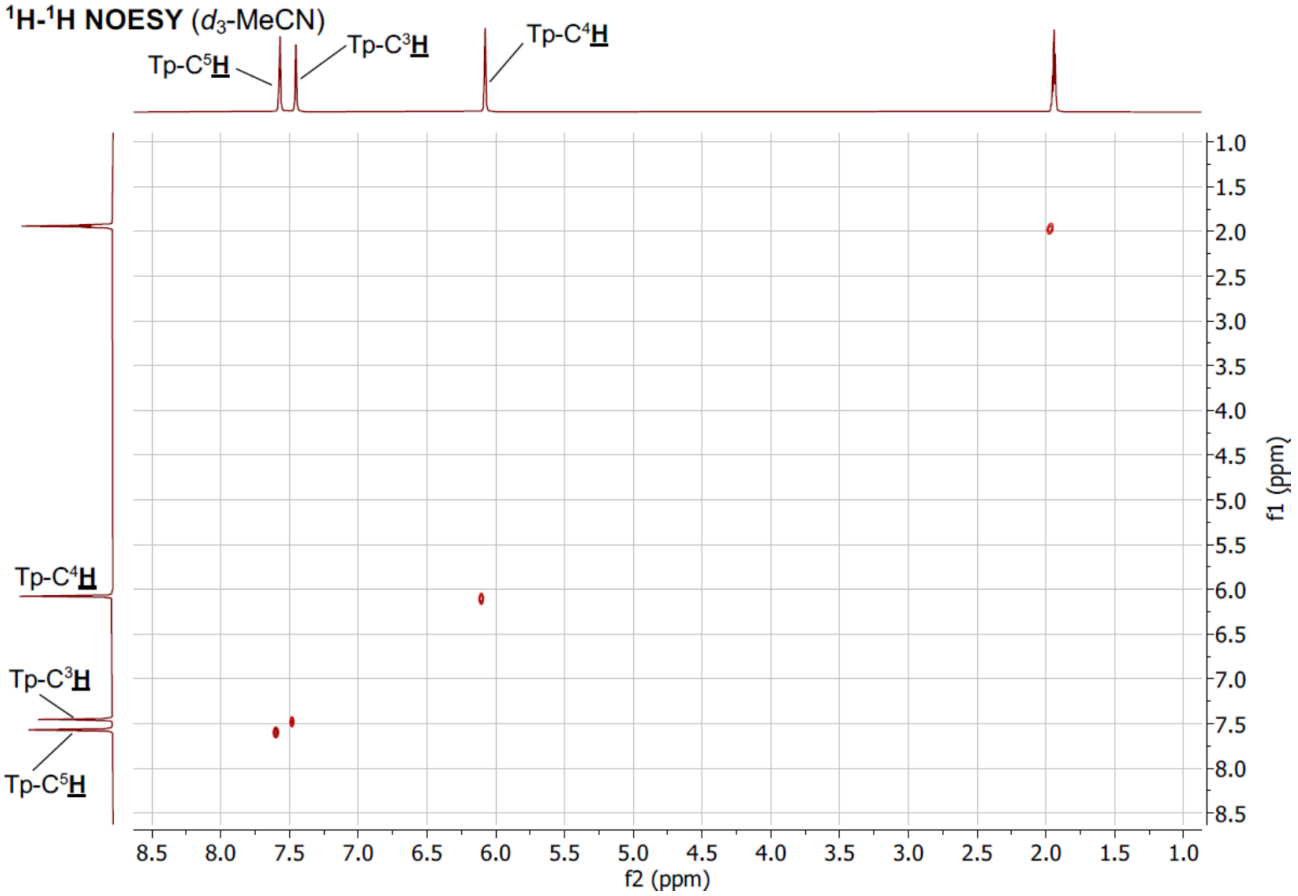

Figure S 6. ^{1}H-^{1}H NOESY NMR spectrum of K(Tp), recorded in d_3-MeCN.

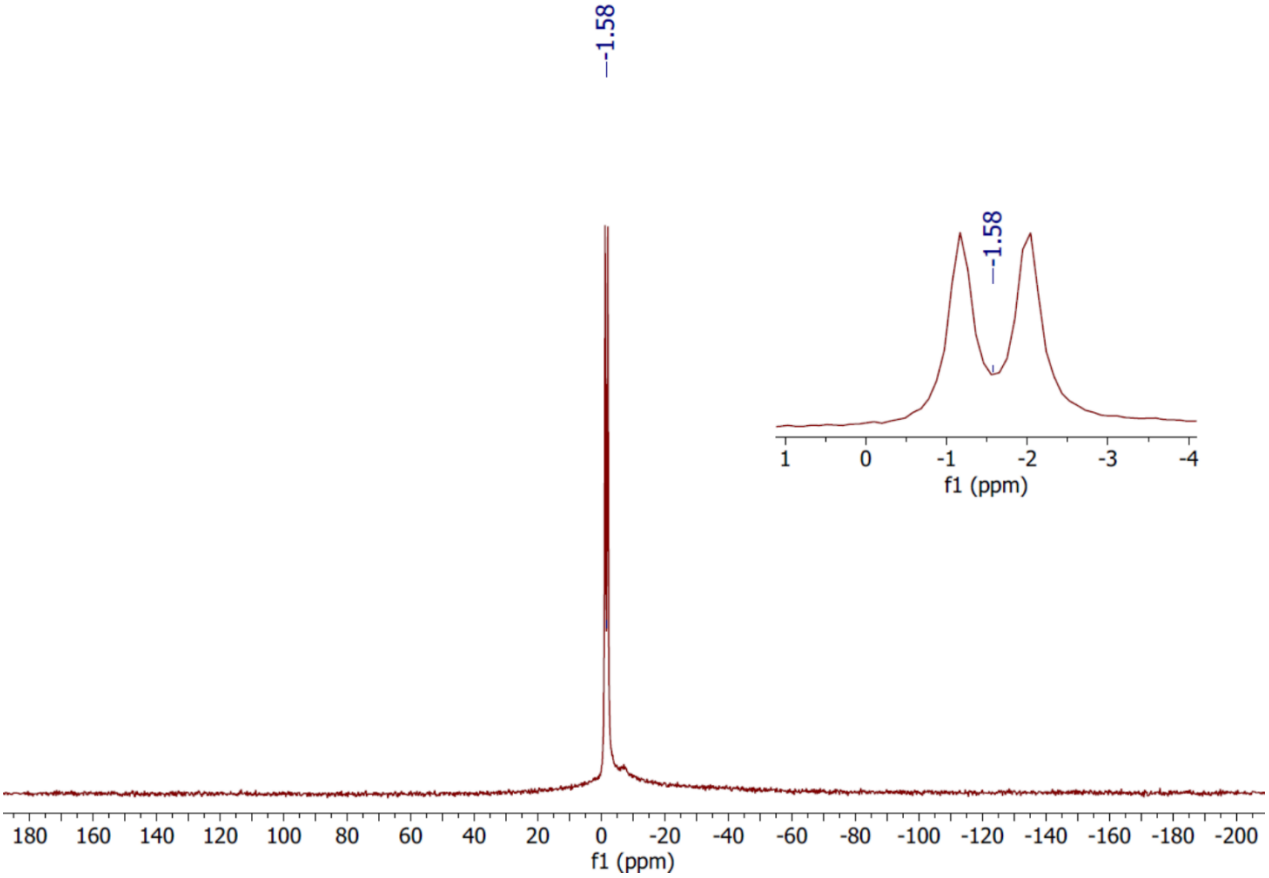

Figure S 7. ^{11}B NMR spectrum of K(Tp), recorded in d_3-MeCN.

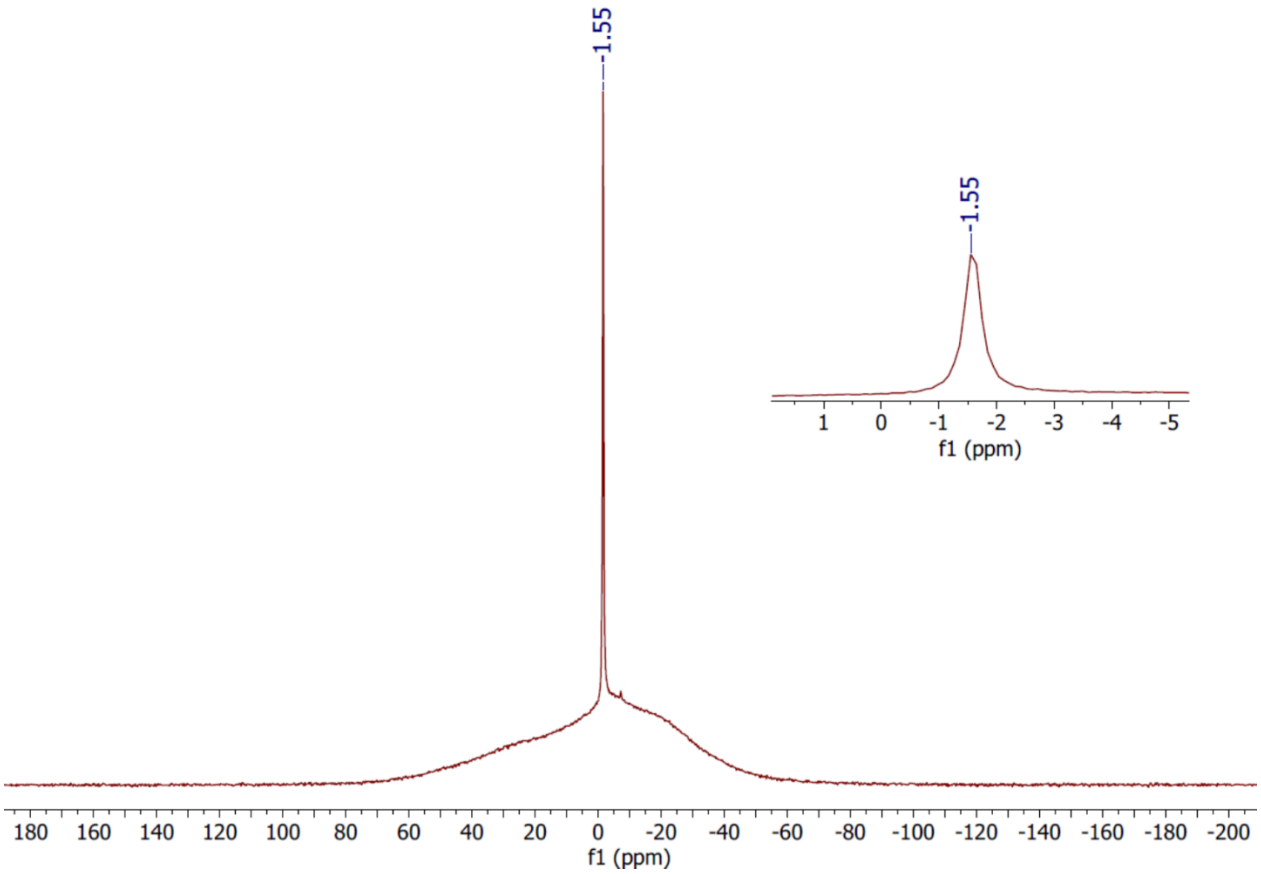

Figure S 8. $^{11}B\{^{1}H\}$ NMR spectrum of K(Tp), recorded in d_3-MeCN.

S1.2 $Ln(OTf)_3$ (Ln = Y, Eu, Gd, Yb)

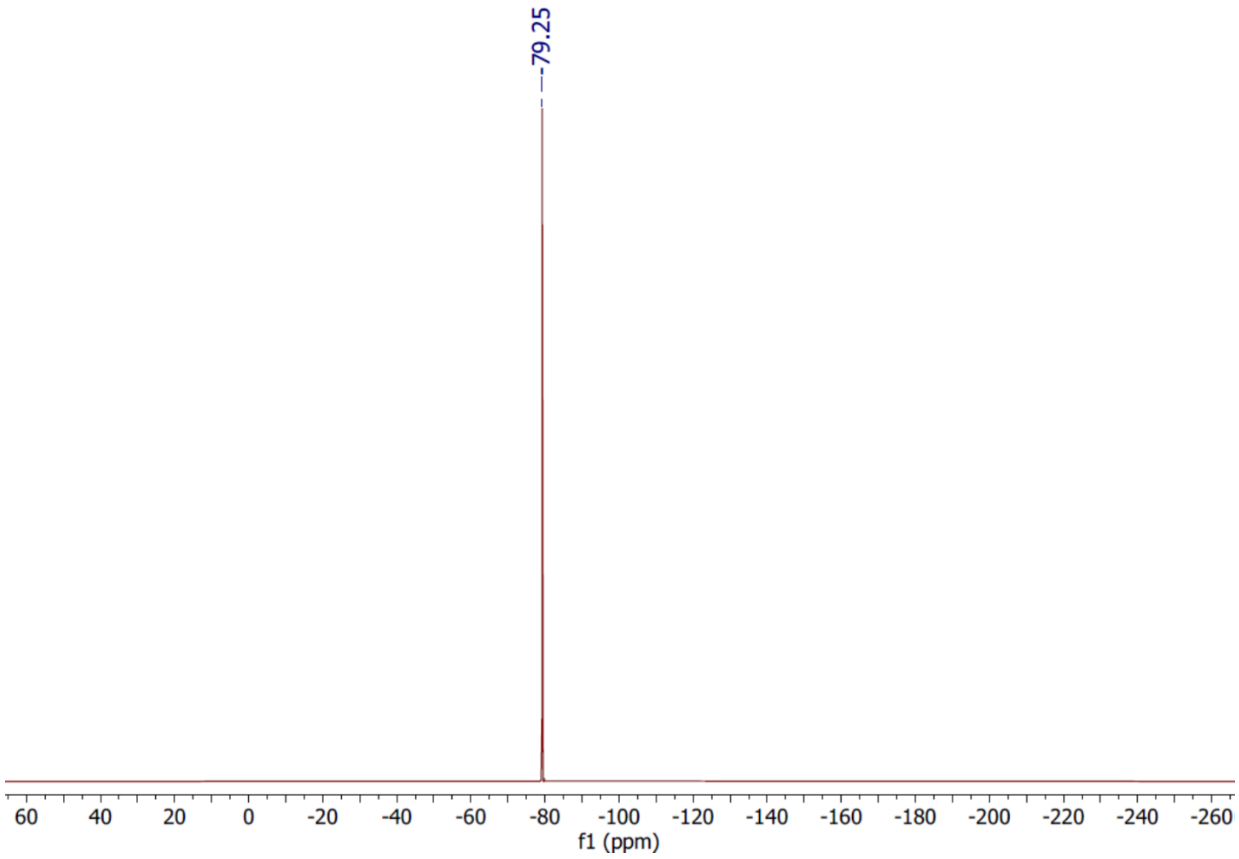

Figure S 9. ^{19}F NMR spectrum of $Y(OTf)_3$, recorded in d_3-MeCN.

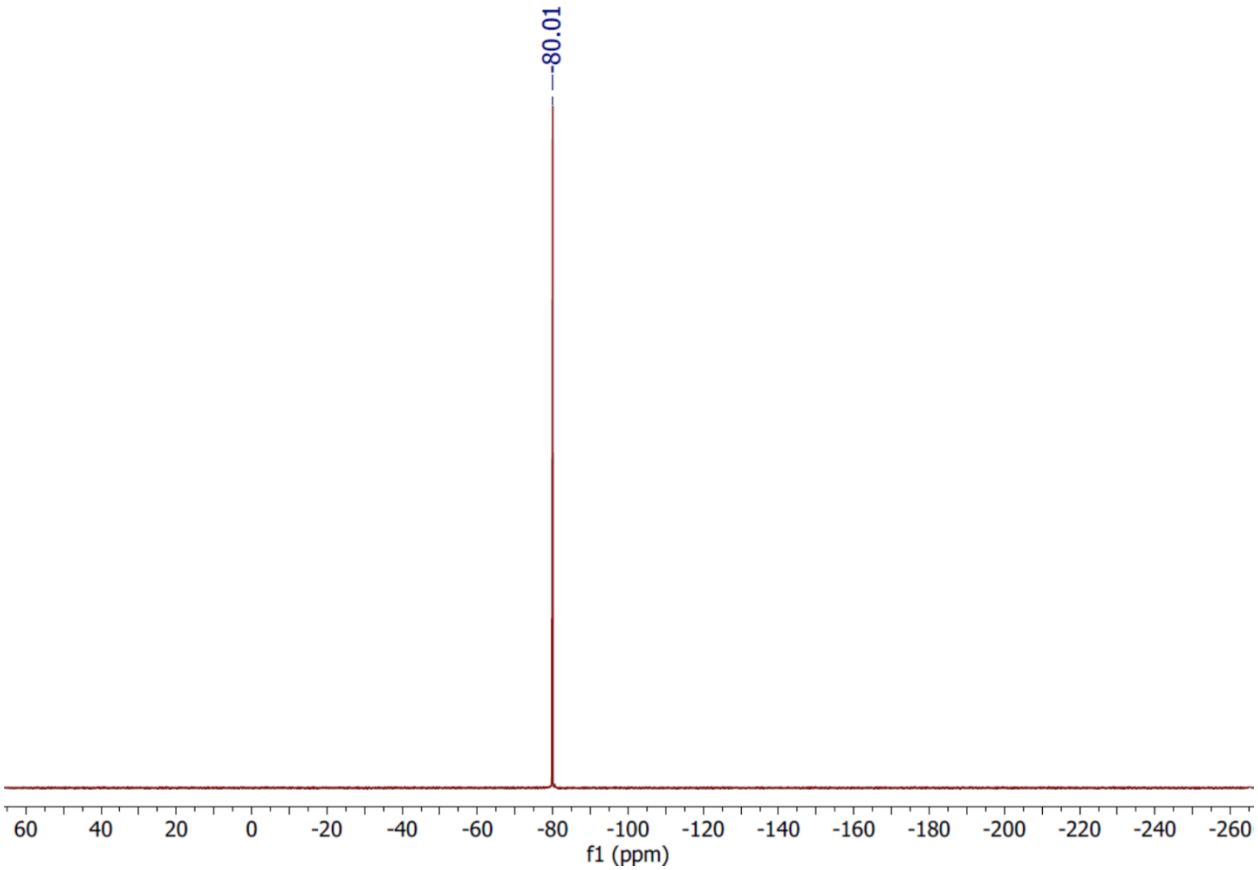

Figure S 10. ^{19}F NMR spectrum of Eu(OTf)$_3$, recorded in d_3-MeCN.

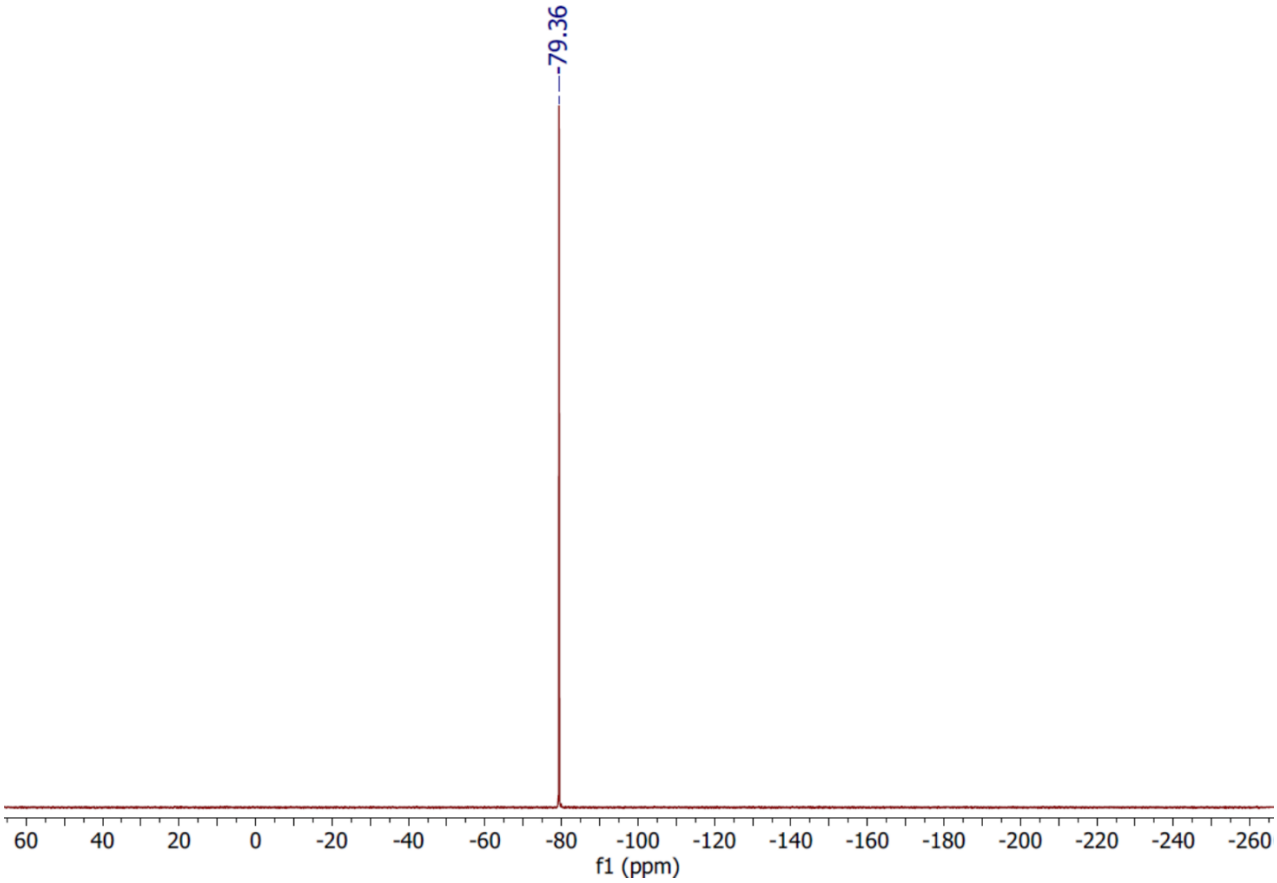

Figure S 11. ^{19}F NMR spectrum of Gd(OTf)$_3$, recorded in d_3-MeCN.

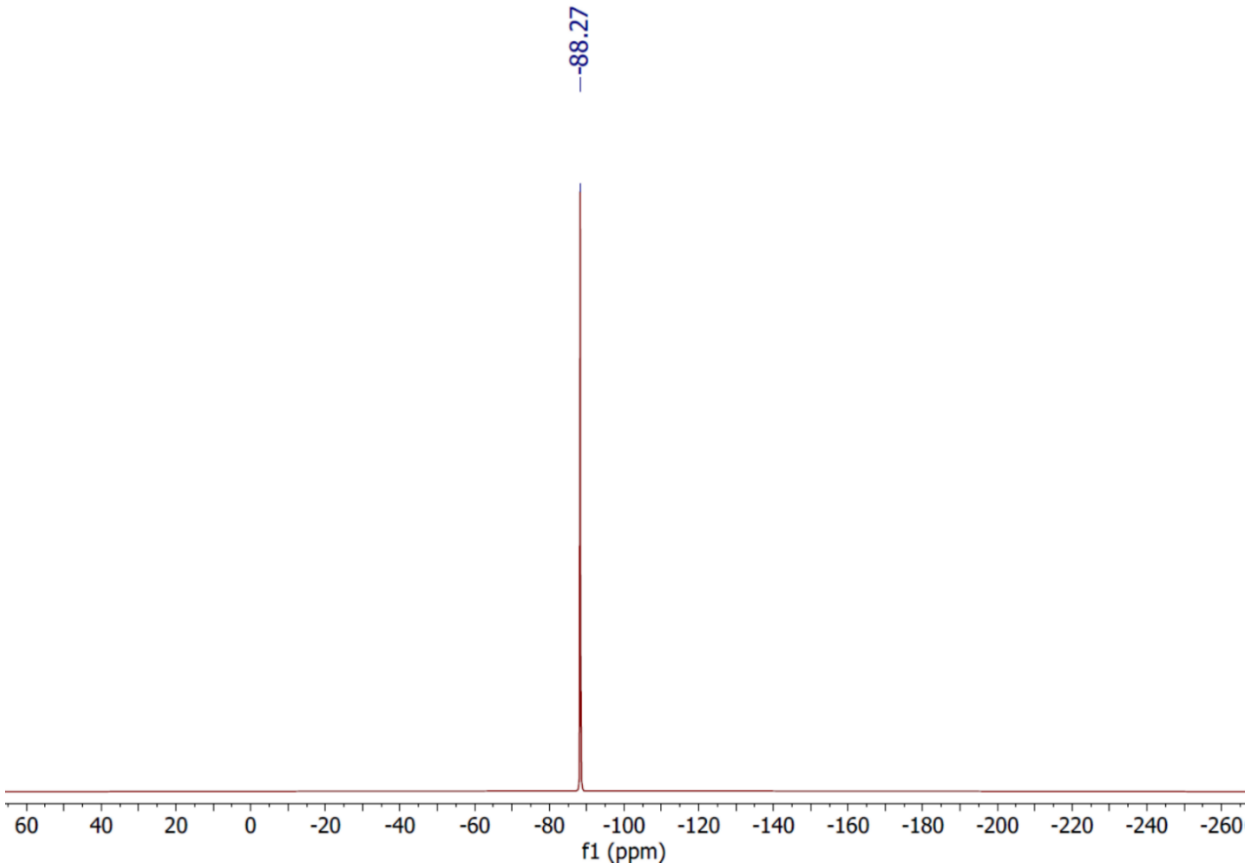

Figure S 12. ^{19}F NMR spectrum of Yb(OTf)$_3$, recorded in d_3-MeCN.

S1.3 [Ln(Tp)$_2$(OTf)] 1-Ln (Ln = Y, Eu, Gd, Yb)

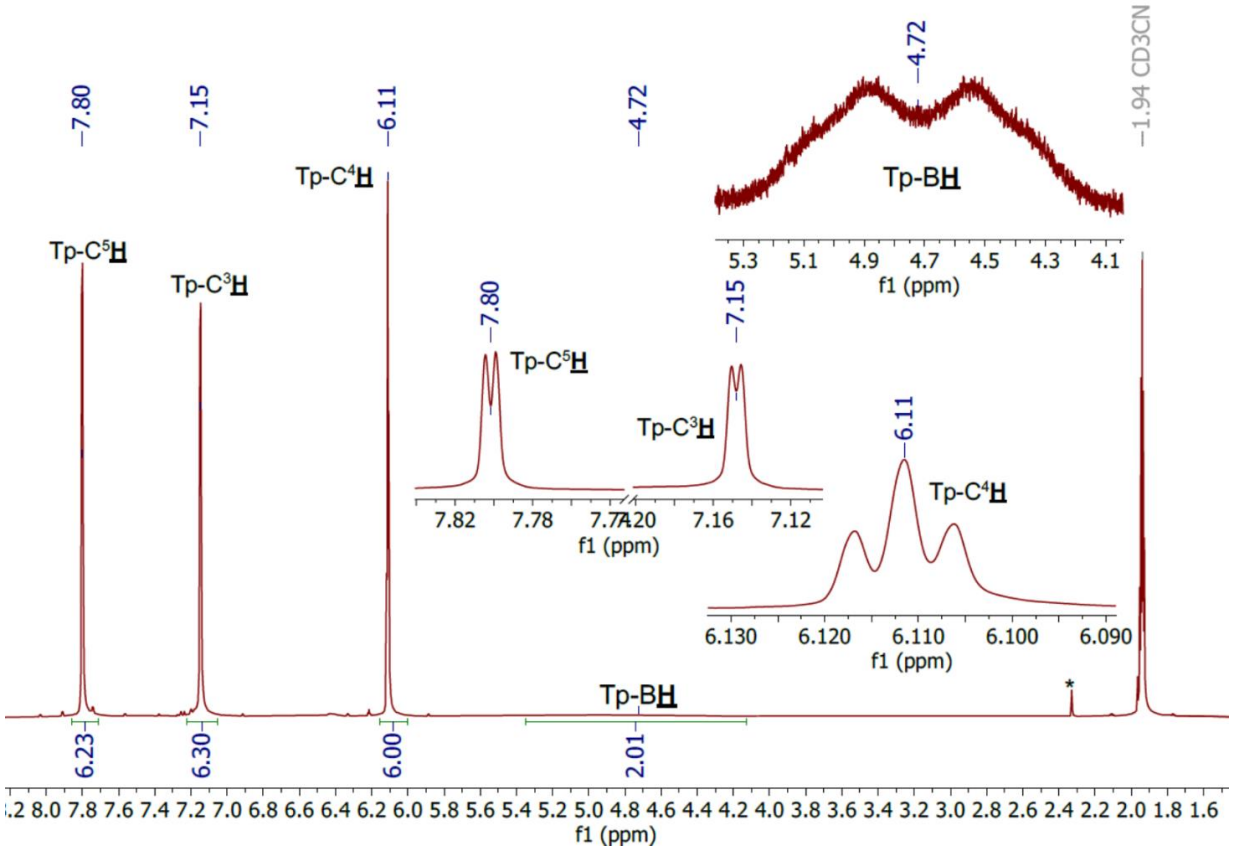

Figure S 13. ^{1}H NMR spectrum of [Y(Tp)$_2$(OTf)] **1-Y**, recorded in d_3-MeCN. Toluene is denoted by *.

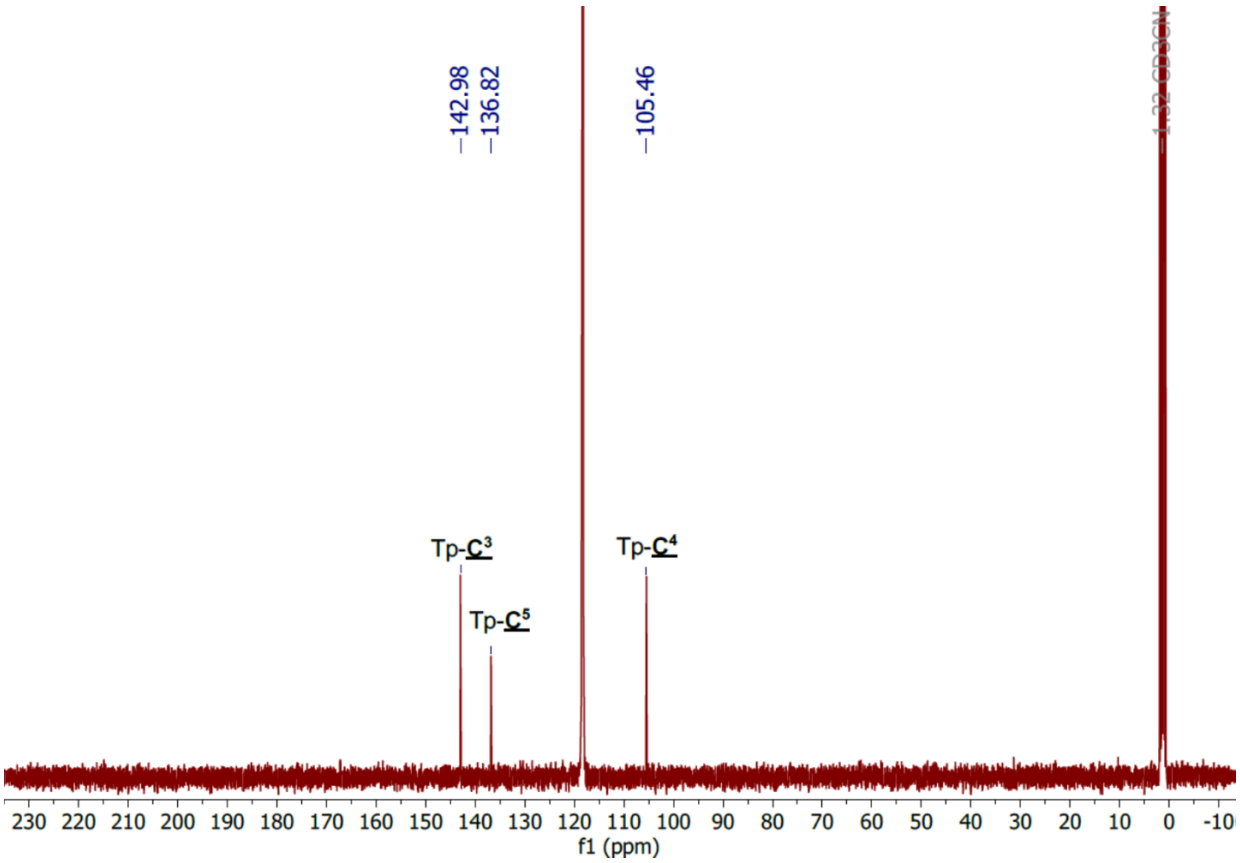

Figure S 14. $^{13}C\{^{1}H\}$ NMR spectrum of [Y(Tp)$_2$(OTf)] **1-Y**, recorded in d_3-MeCN.

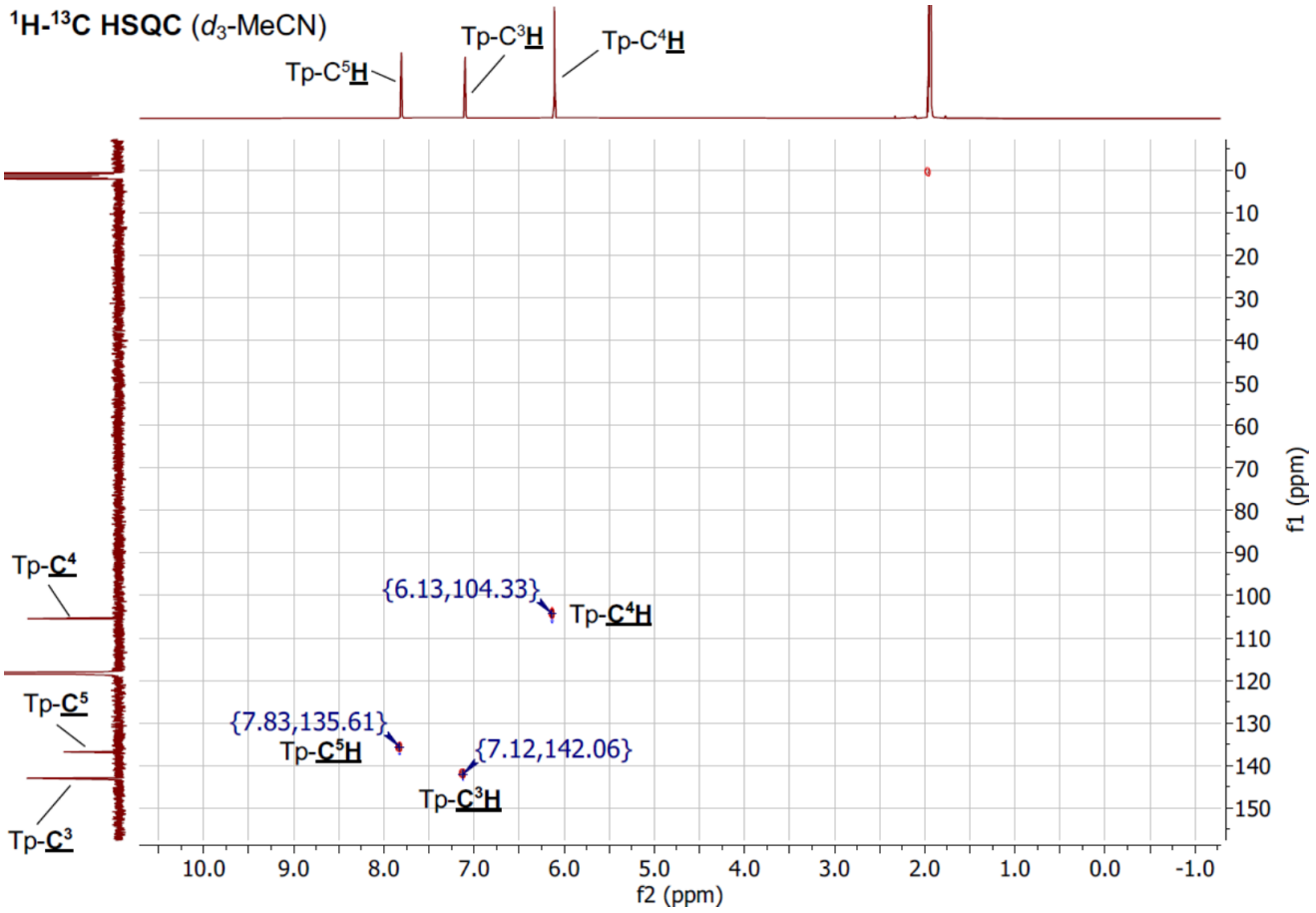

Figure S 15. ^{1}H-^{13}C HSQC NMR spectrum of [Y(Tp)$_2$(OTf)] **1-Y**, recorded in d_3-MeCN.

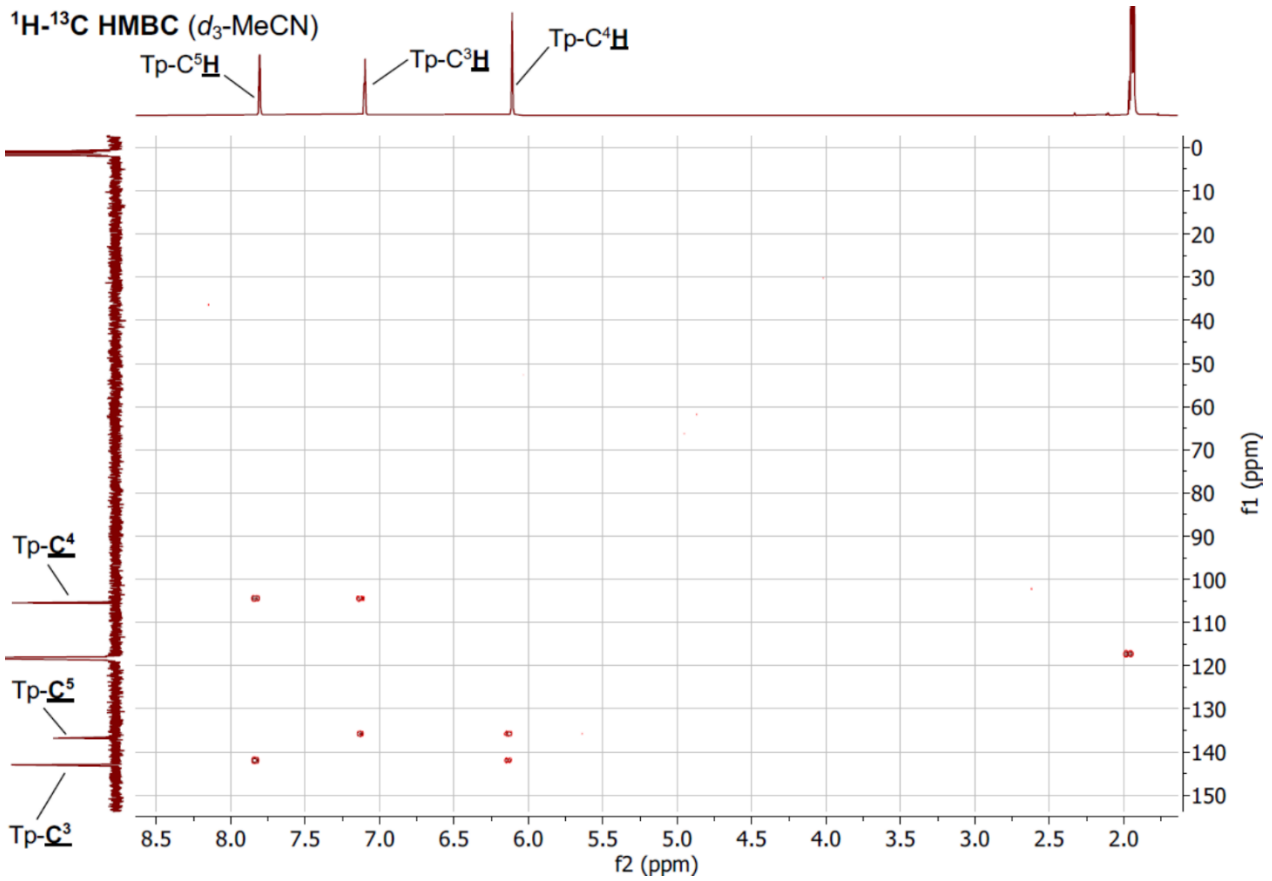

Figure S 16. ^{1}H-^{13}C HMBC NMR spectrum of [Y(Tp)$_2$(OTf)] **1-Y**, recorded in d_3-MeCN.

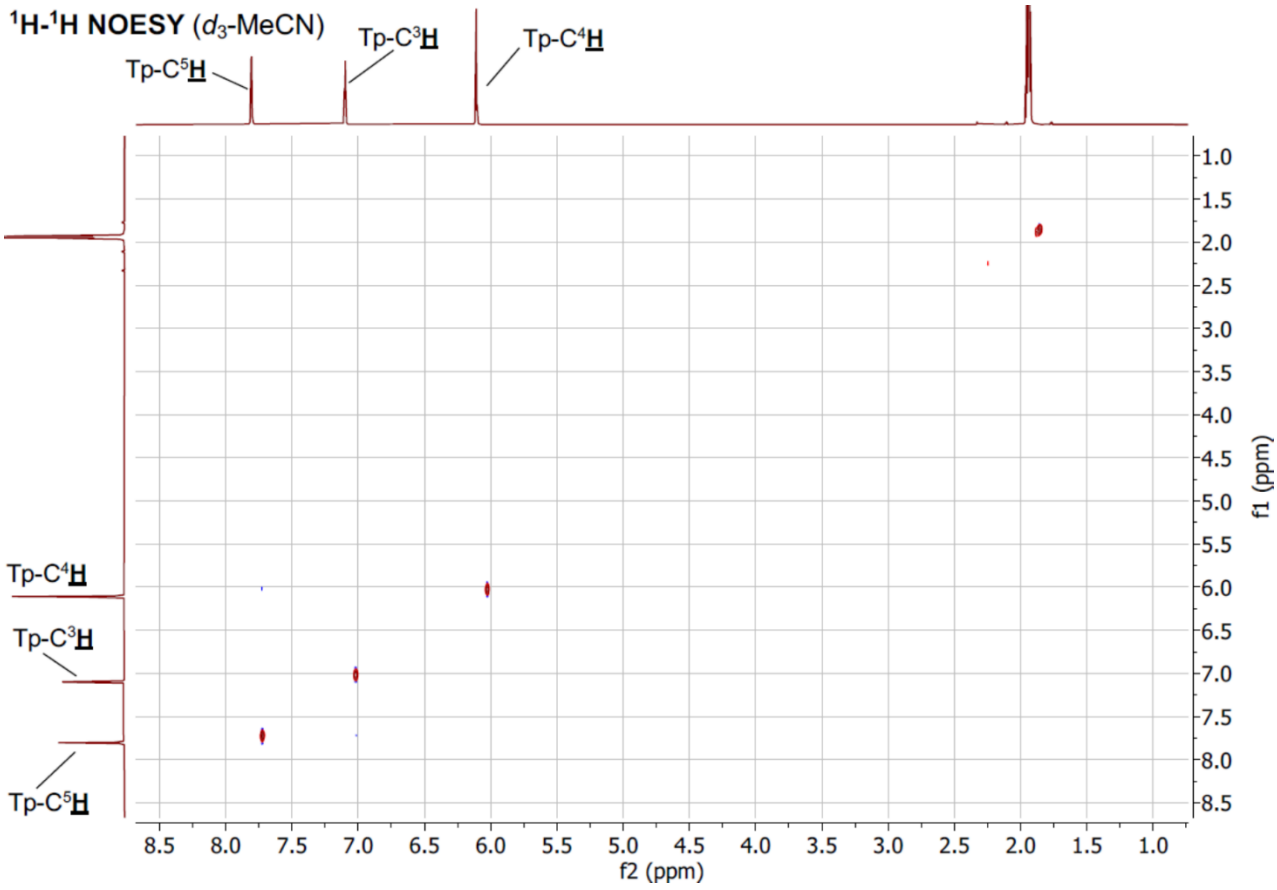

Figure S 17. ^{1}H-^{1}H NOESY NMR spectrum of [Y(Tp)$_2$(OTf)] **1-Y**, recorded in d_3-MeCN.

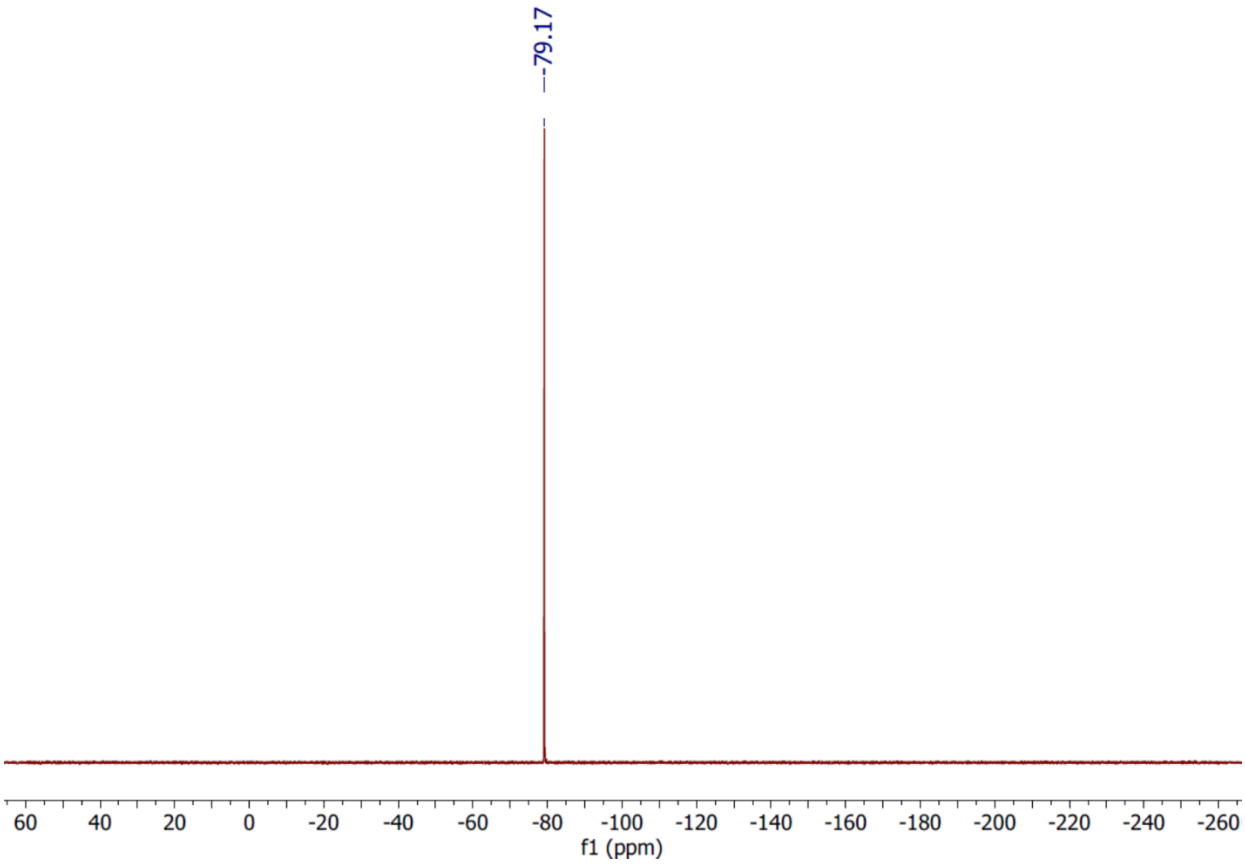

Figure S 18. ^{19}F NMR spectrum of [Y(Tp)$_2$(OTf)] **1-Y**, recorded in d_3-MeCN.

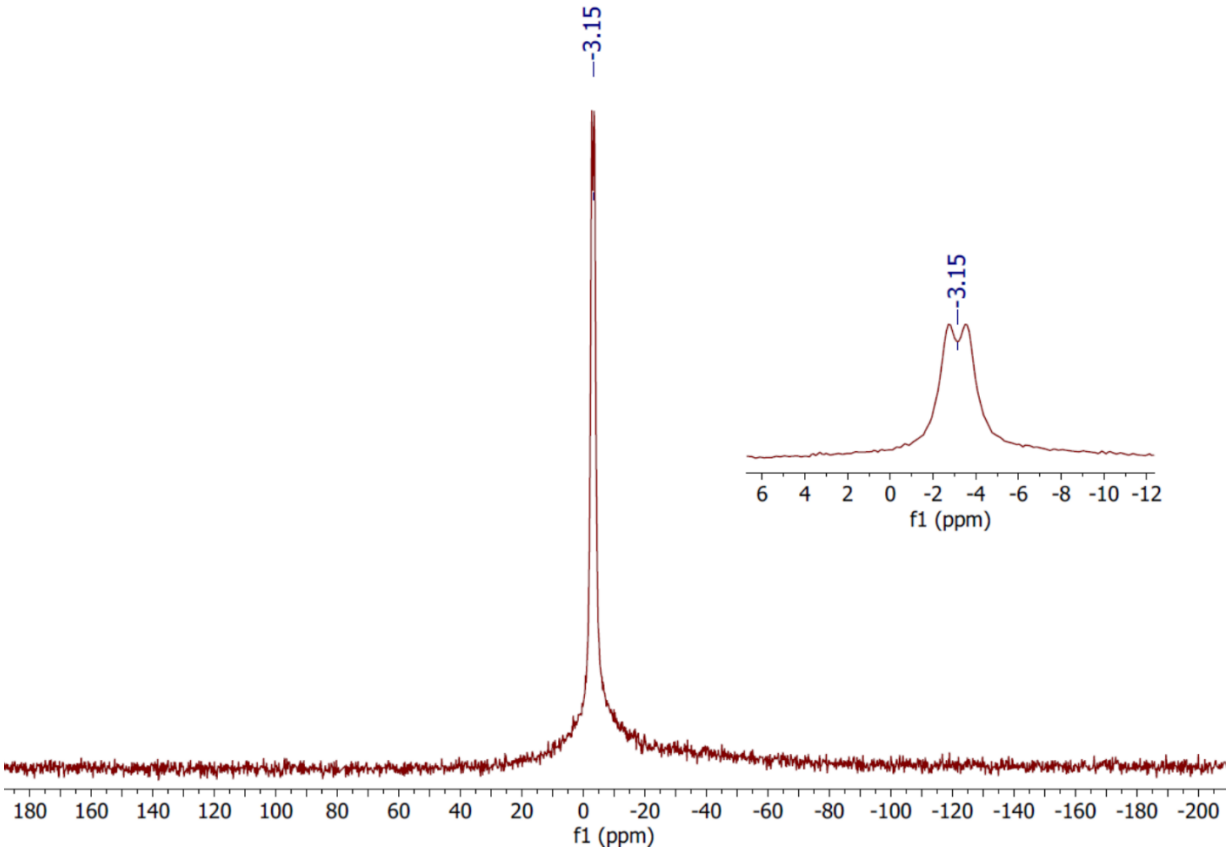

Figure S 19. ^{11}B NMR spectrum of [Y(Tp)$_2$(OTf)] **1-Y**, recorded in d_3-MeCN.

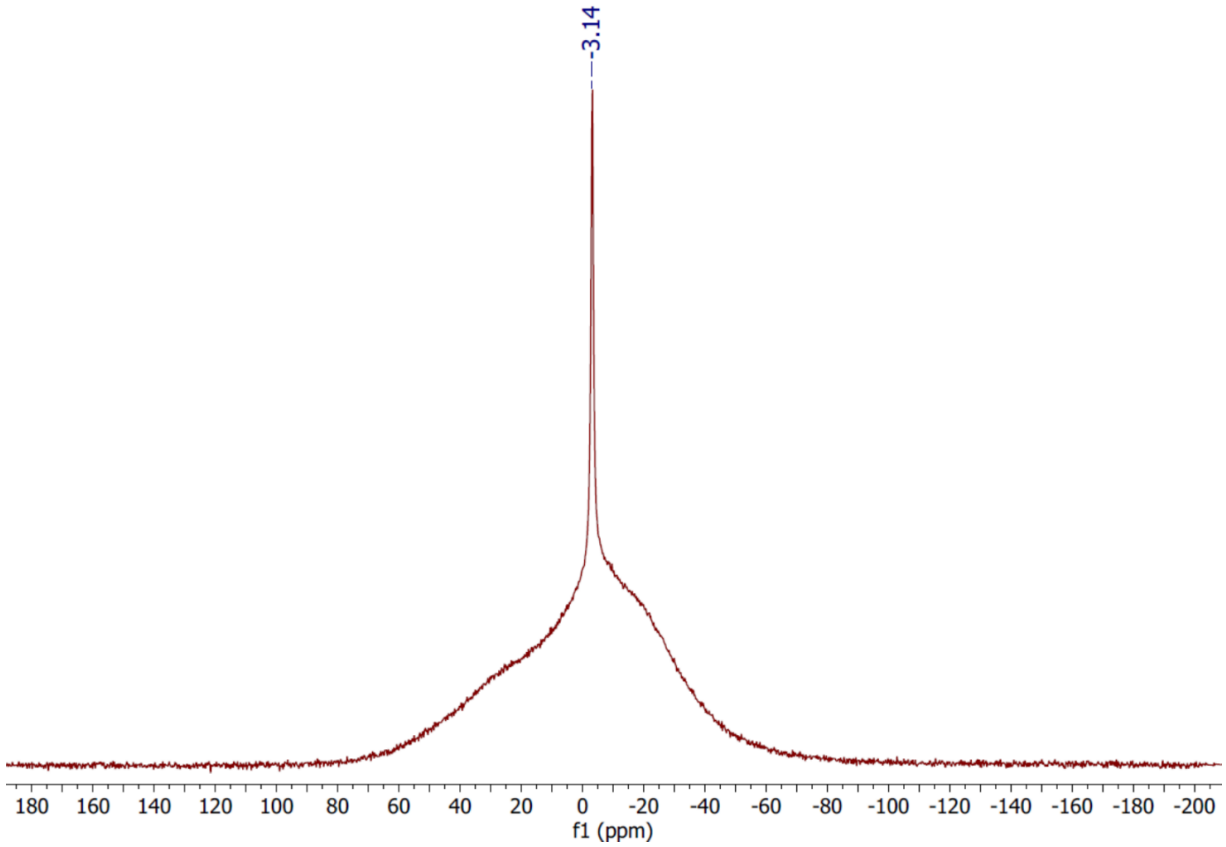

Figure S 20. $^{11}B\{^{1}H\}$ NMR spectrum of $[Y(Tp)_2(OTf)]$ **1-Y**, recorded in d_3-MeCN.

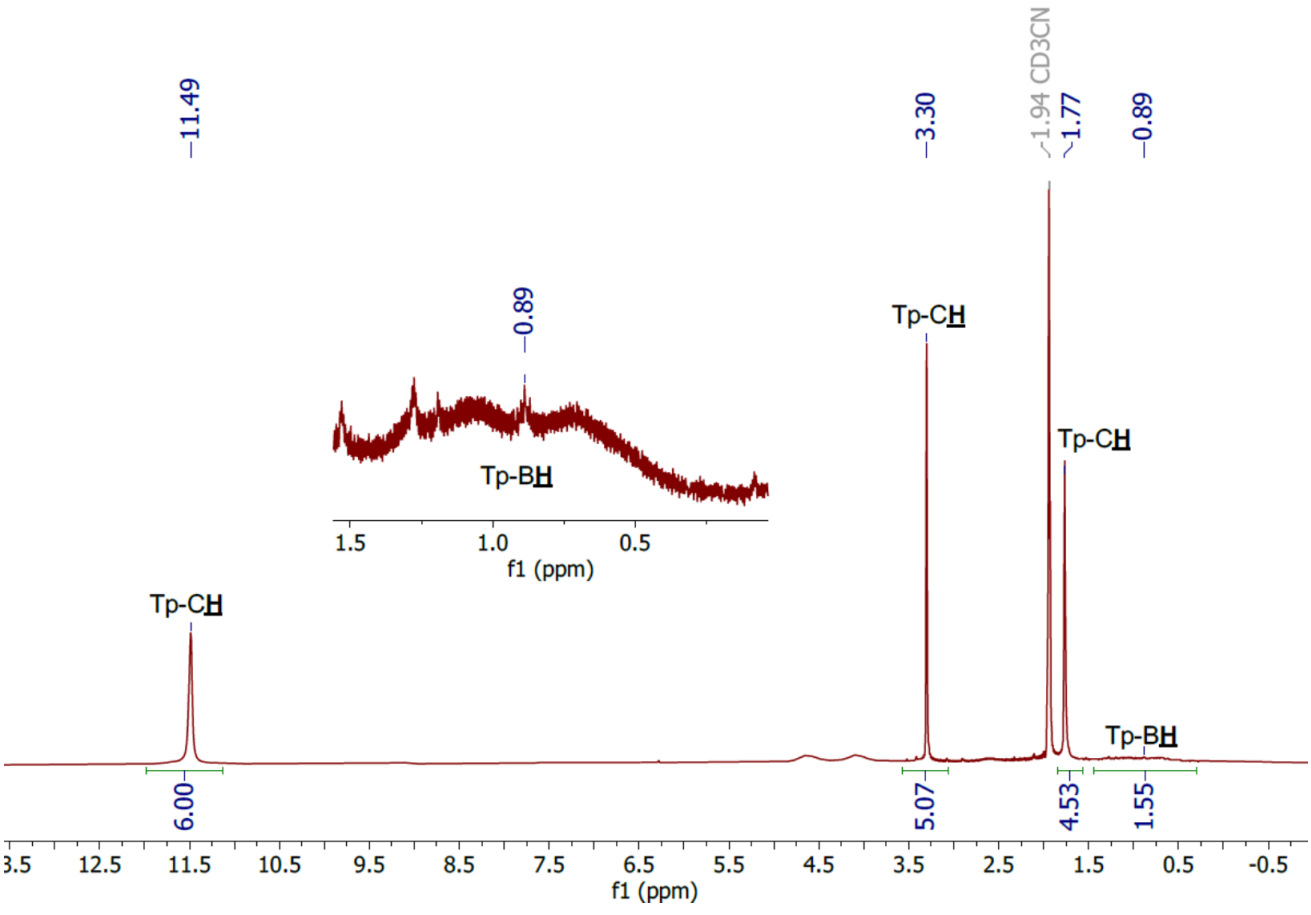

Figure S 21. ^{1}H NMR spectrum of $[Eu(Tp)_2(OTf)]$ **1-Eu**, recorded in d_3-MeCN.

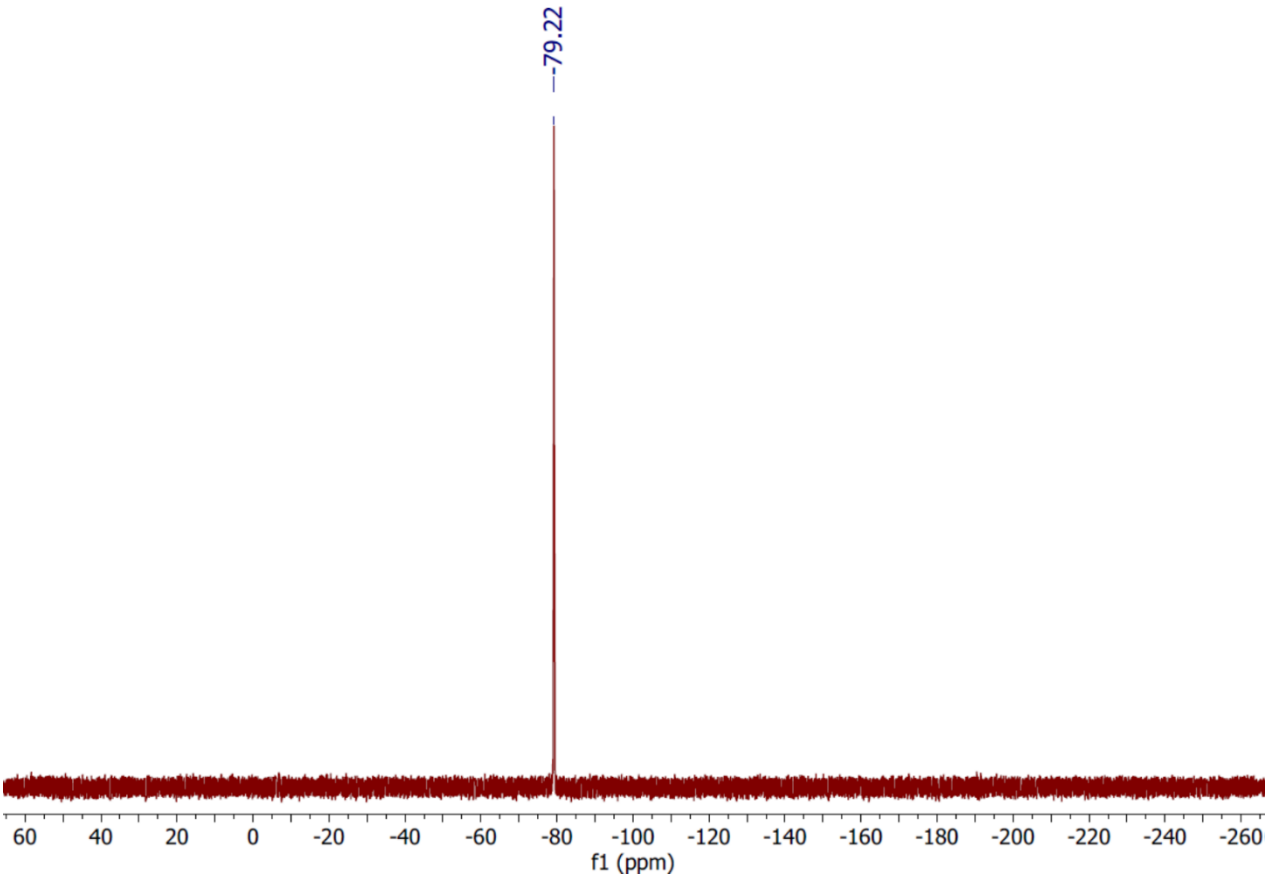

Figure S 22. ^{19}F NMR spectrum of [Eu(Tp)$_2$(OTf)] **1-Eu**, recorded in d_3-MeCN.

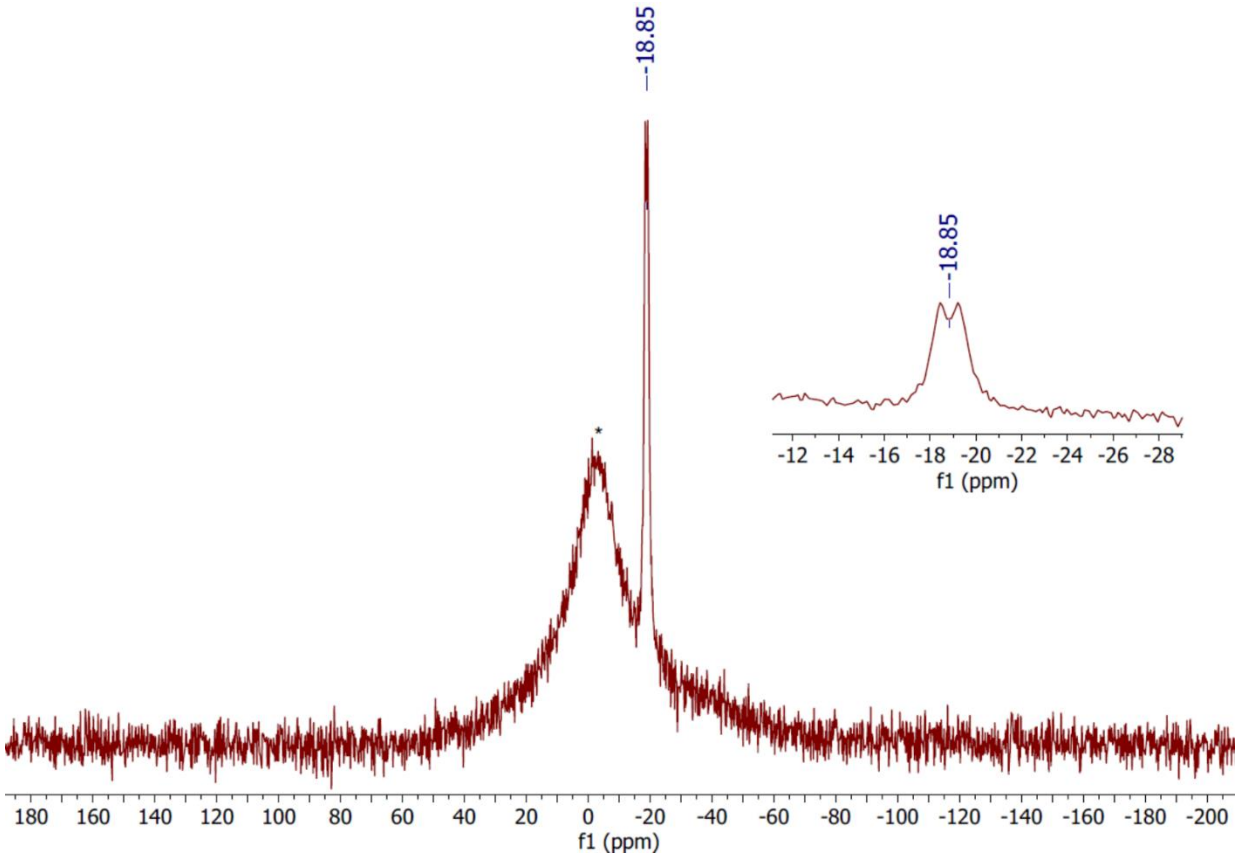

Figure S 23. ^{11}B NMR spectrum of [Eu(Tp)$_2$(OTf)] **1-Eu**, recorded in d_3-MeCN. Borosilicate glass is denoted by *.

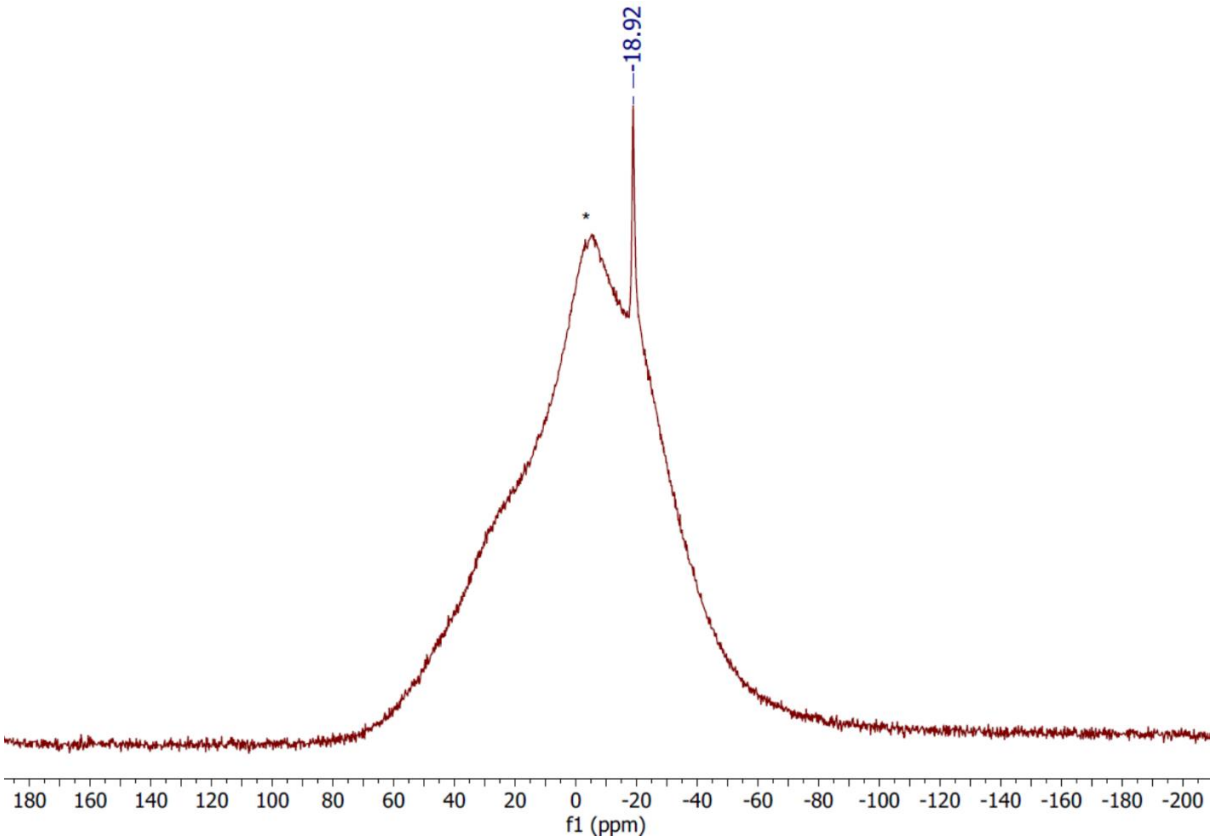

Figure S 24. $^{11}B\{^{1}H\}$ NMR spectrum of $[Eu(Tp)_2(OTf)]$ **1-Eu**, recorded in d_3-MeCN. Borosilicate glass is denoted by *.

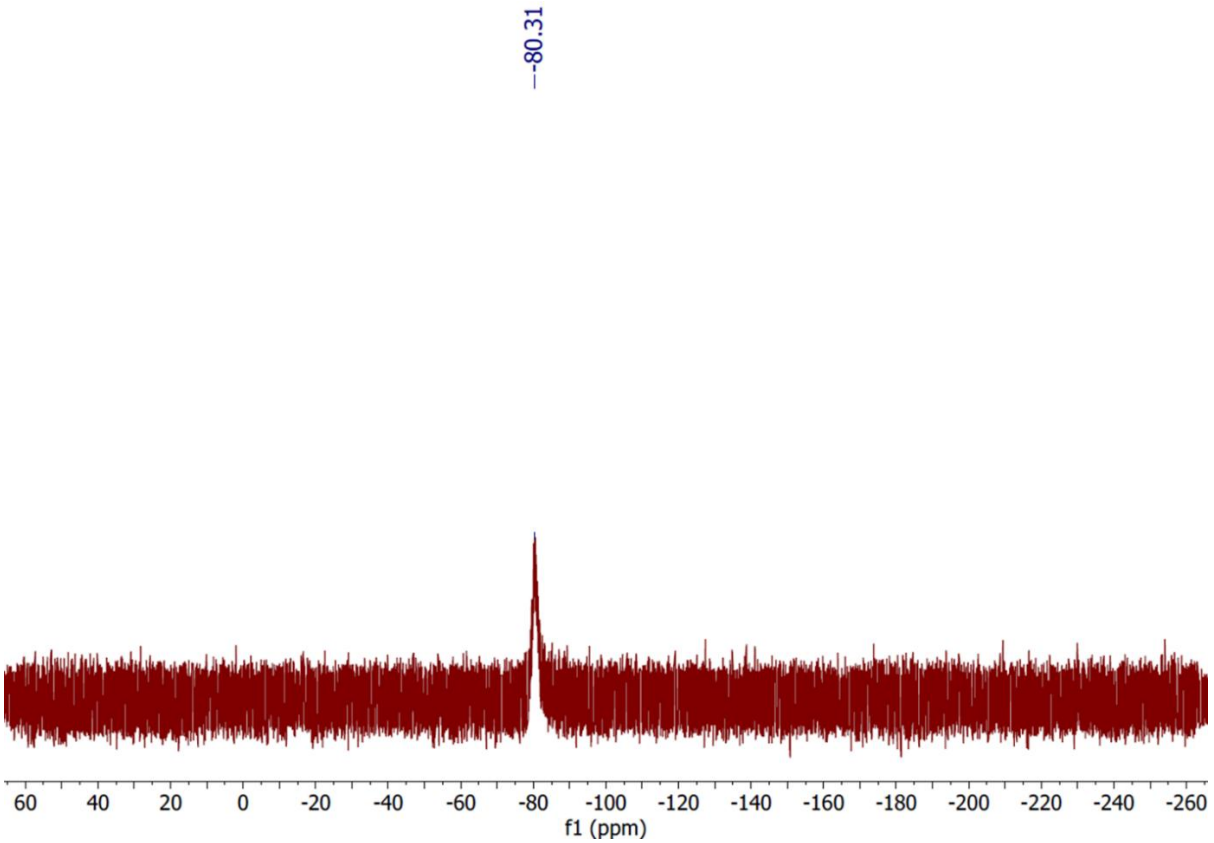

Figure S 25. ^{19}F NMR spectrum of $[Gd(Tp)_2(OTf)]$ **1-Gd**, recorded in d_3-MeCN.

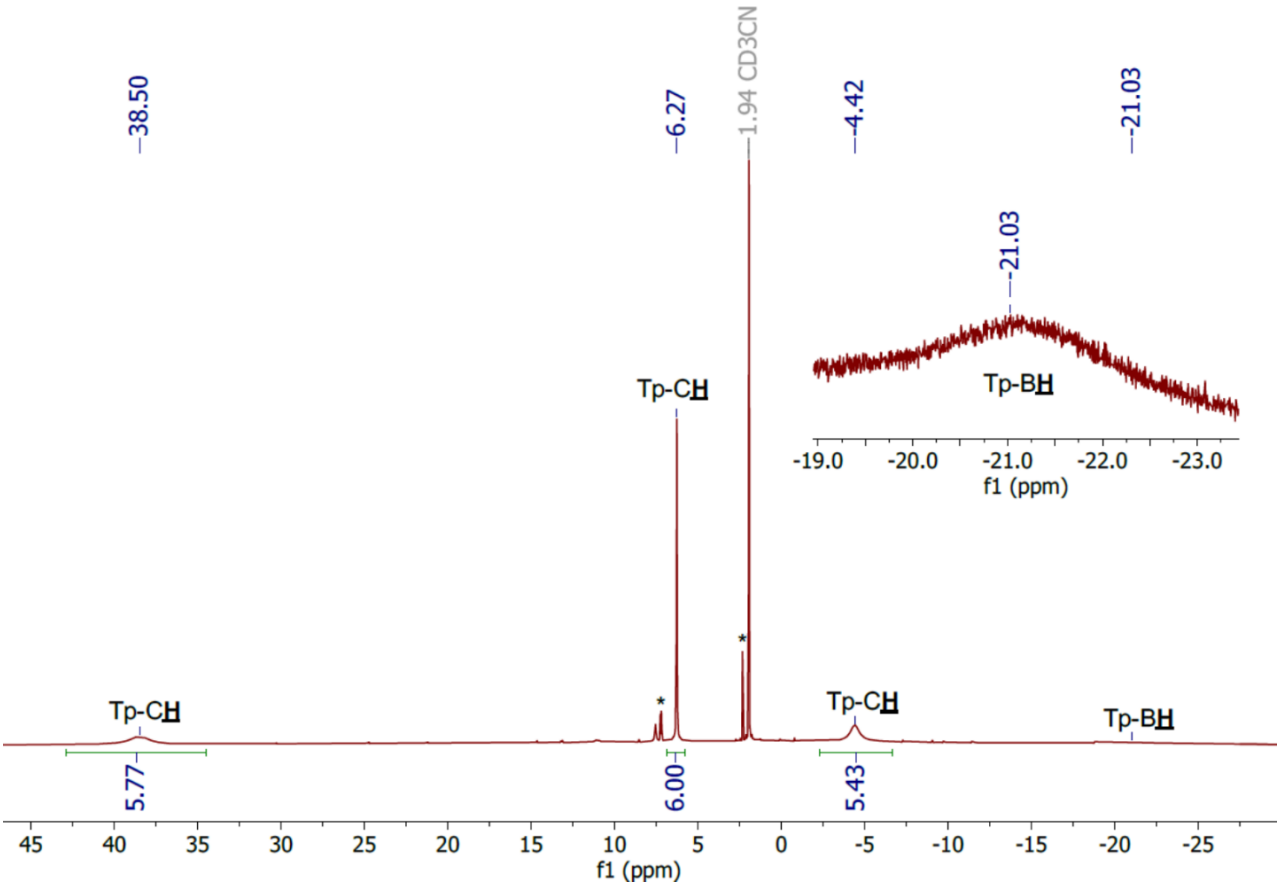

Figure S 26. ^{1}H NMR spectrum of [Yb(Tp)$_2$(OTf)] **1-Yb**, recorded in d_3-MeCN. Toluene is denoted by *.

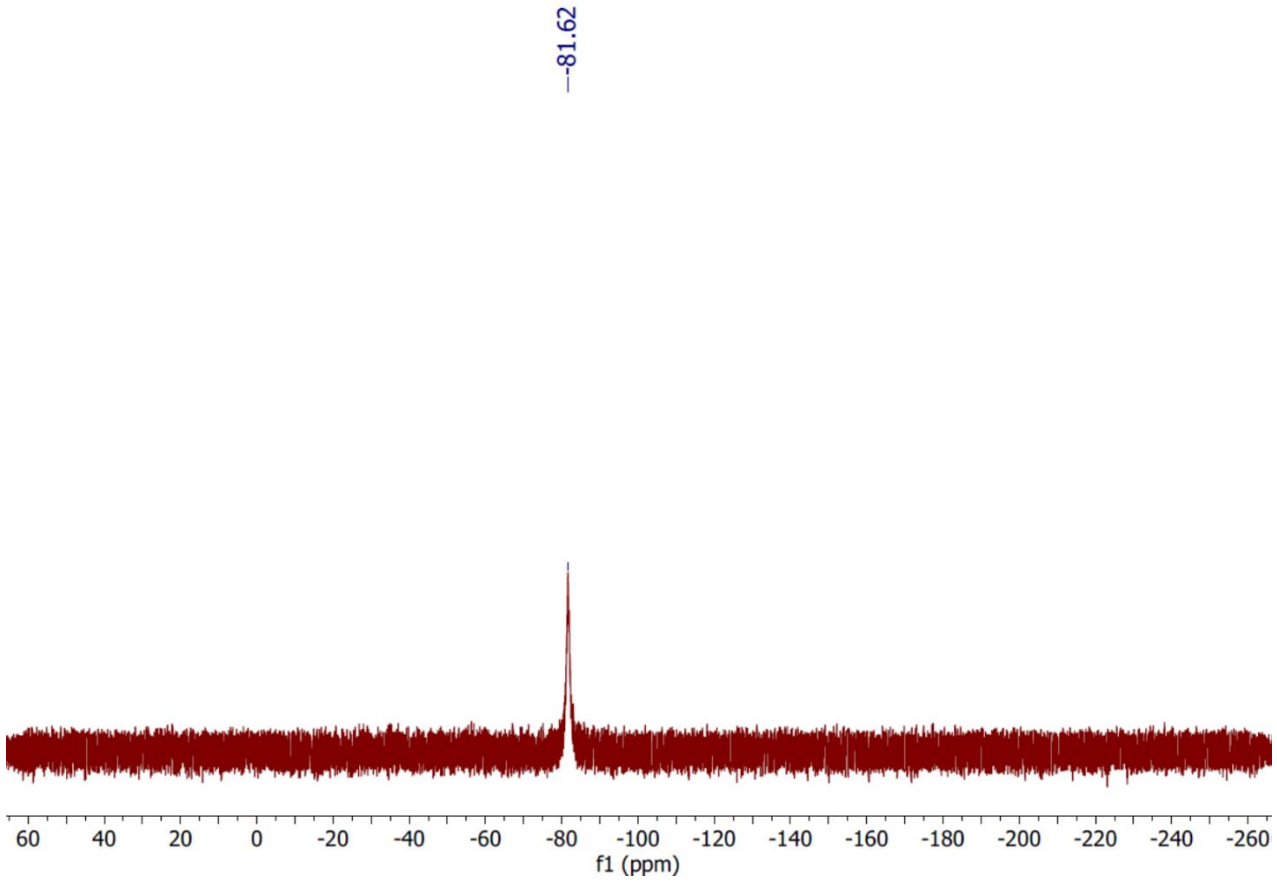

Figure S 27. ^{19}F NMR spectrum of [Yb(Tp)$_2$(OTf)] **1-Yb**, recorded in d_3-MeCN.

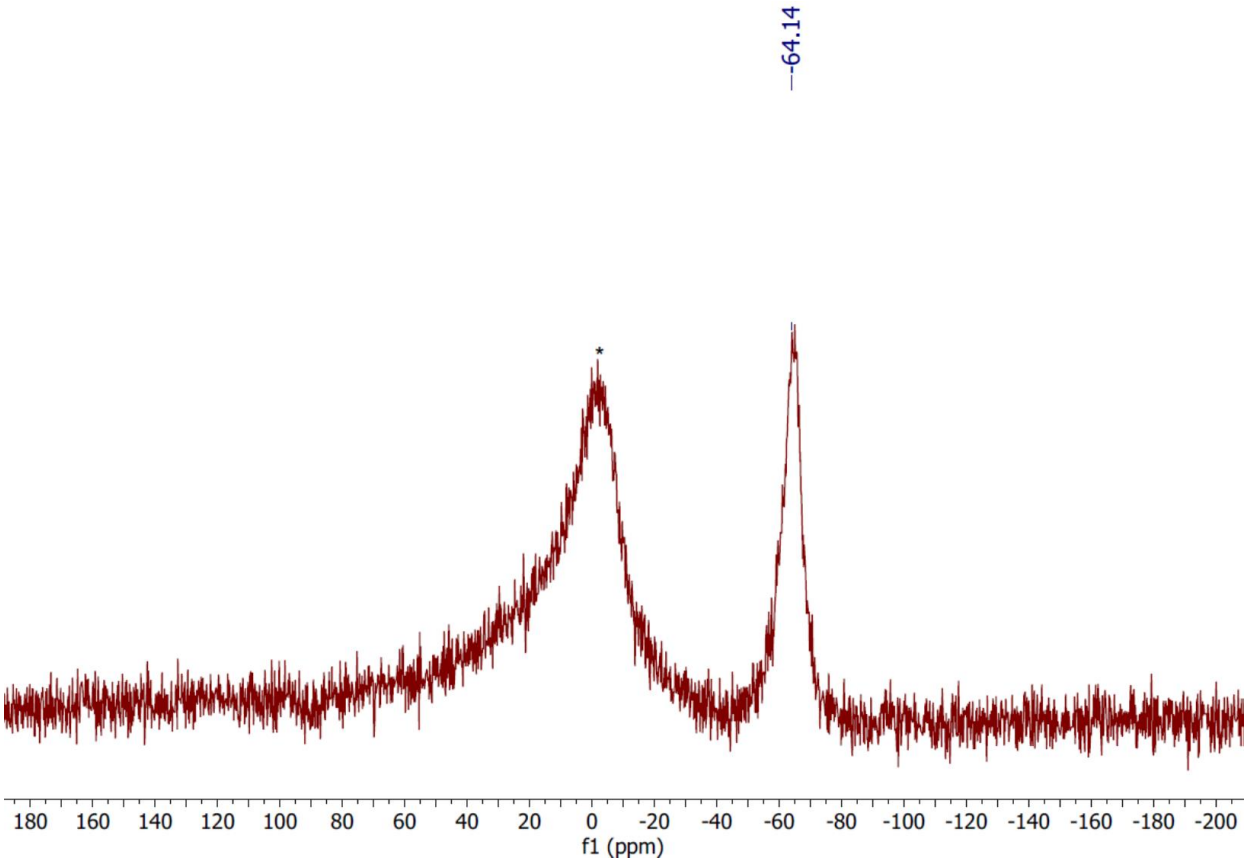

Figure S 28. ^{11}B NMR spectrum of [Yb(Tp)$_2$(OTf)] **1-Yb**, recorded in d_3-MeCN. Borosilicate glass is denoted by *.

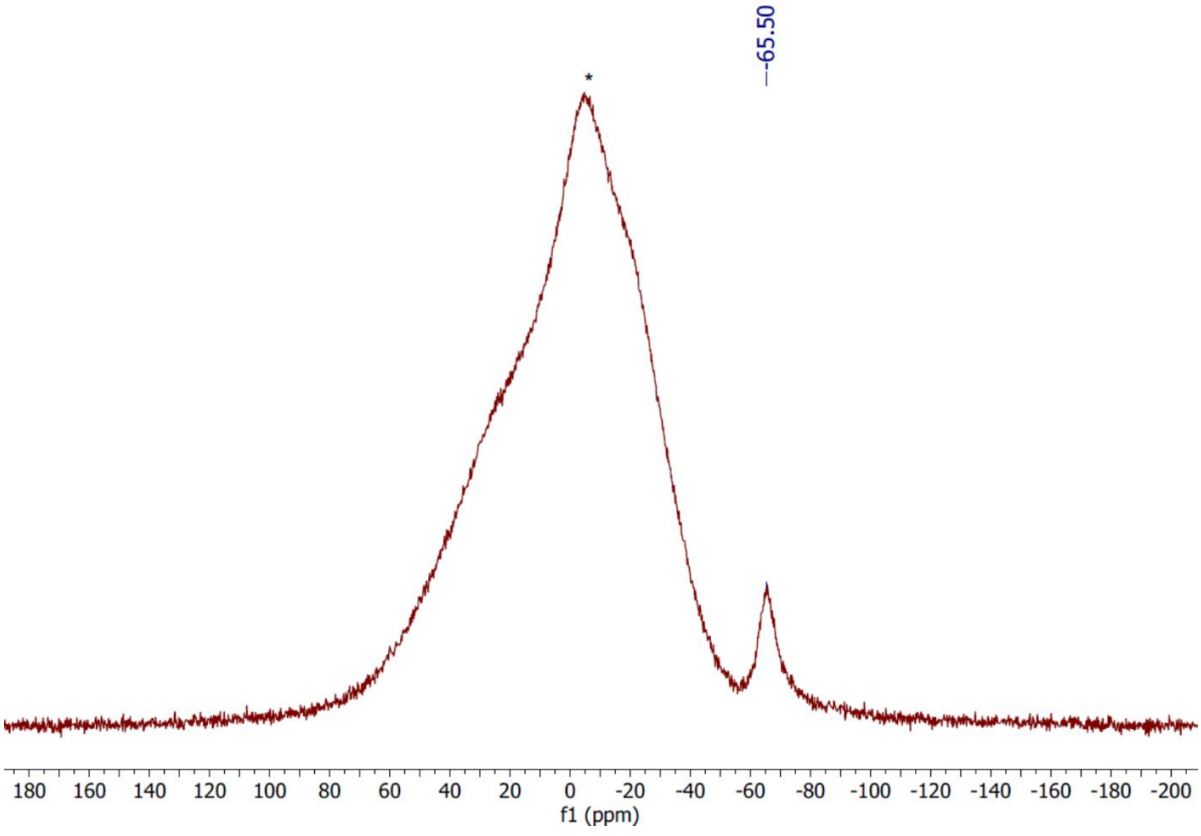

Figure S 29. ^{11}B{^{1}H} NMR spectrum of [Yb(Tp)$_2$(OTf)] **1-Yb**, recorded in d_3-MeCN. Borosilicate glass is denoted by *.

S1.4 [Ln(Tp)$_2$(hfac)] 2-Ln (Ln = Y, Eu, Yb)

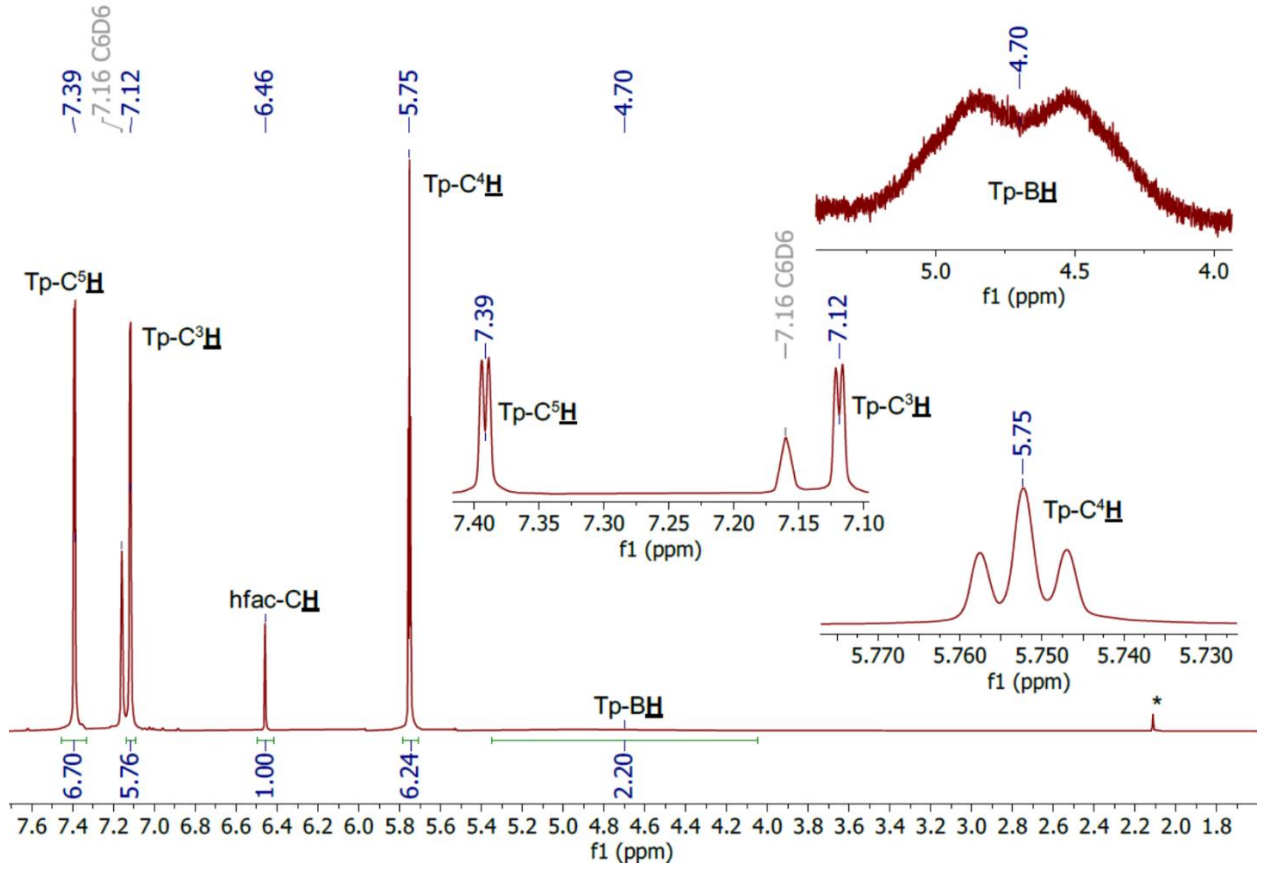

Figure S 30. ^{1}H NMR spectrum of [Y(Tp)$_2$(hfac)] **2-Y**, recorded in d_6-benzene. Toluene is denoted by *.

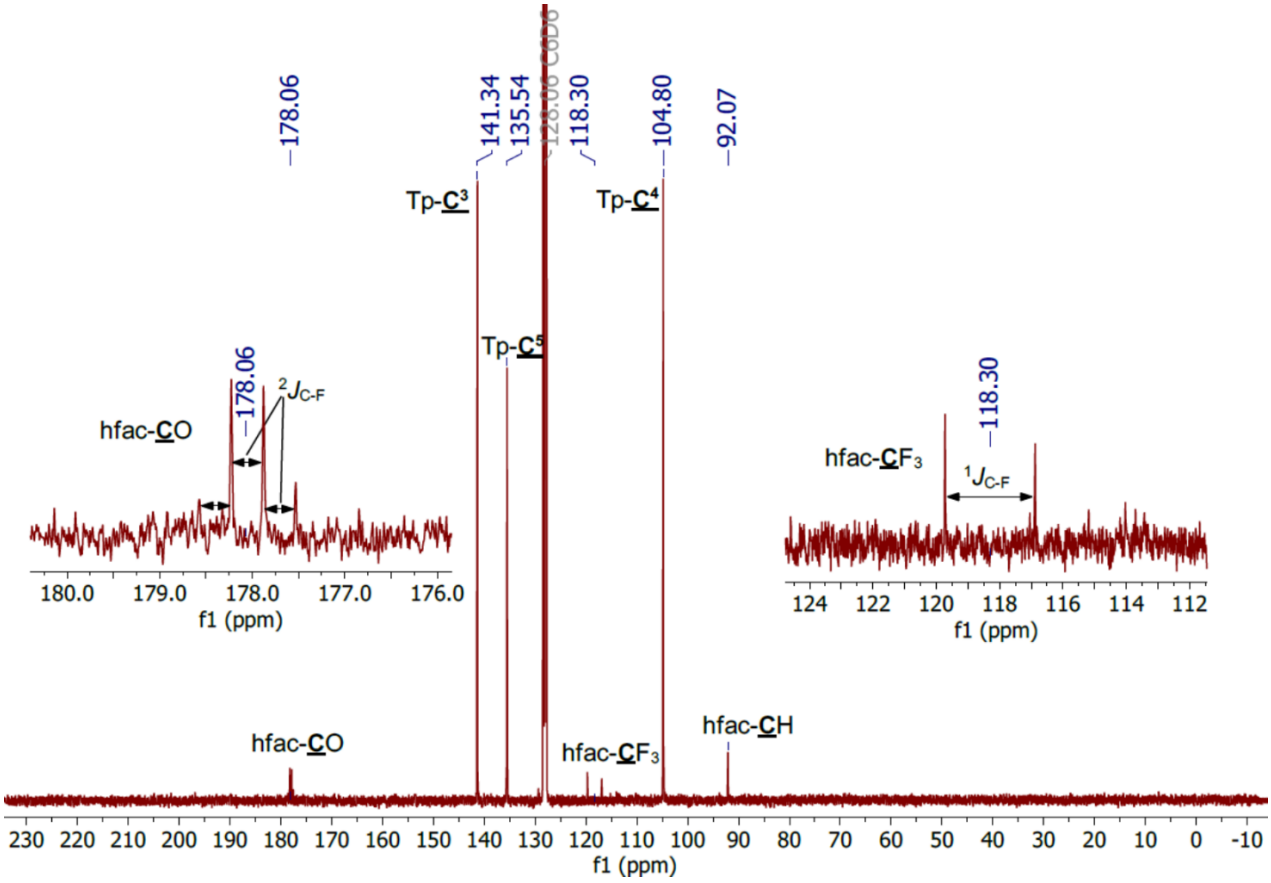

Figure S 31. ^{13}C{^{1}H} NMR spectrum of [Y(Tp)$_2$(hfac)] **2-Y**, recorded in d_6-benzene.

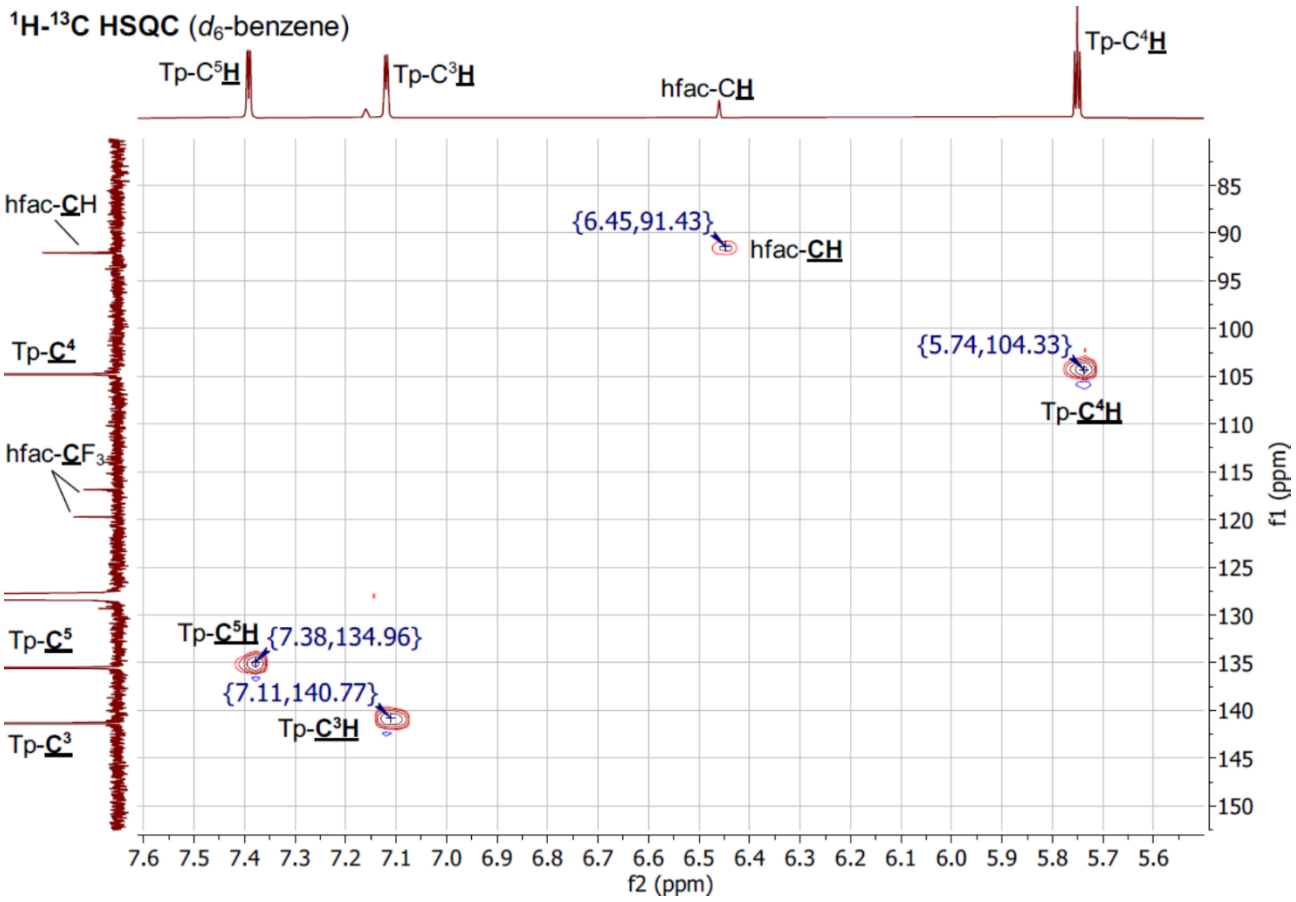

Figure S 32. ^{1}H-^{13}C HSQC NMR spectrum of [Y(Tp)$_2$(hfac)] **2-Y**, recorded in d_6-benzene.

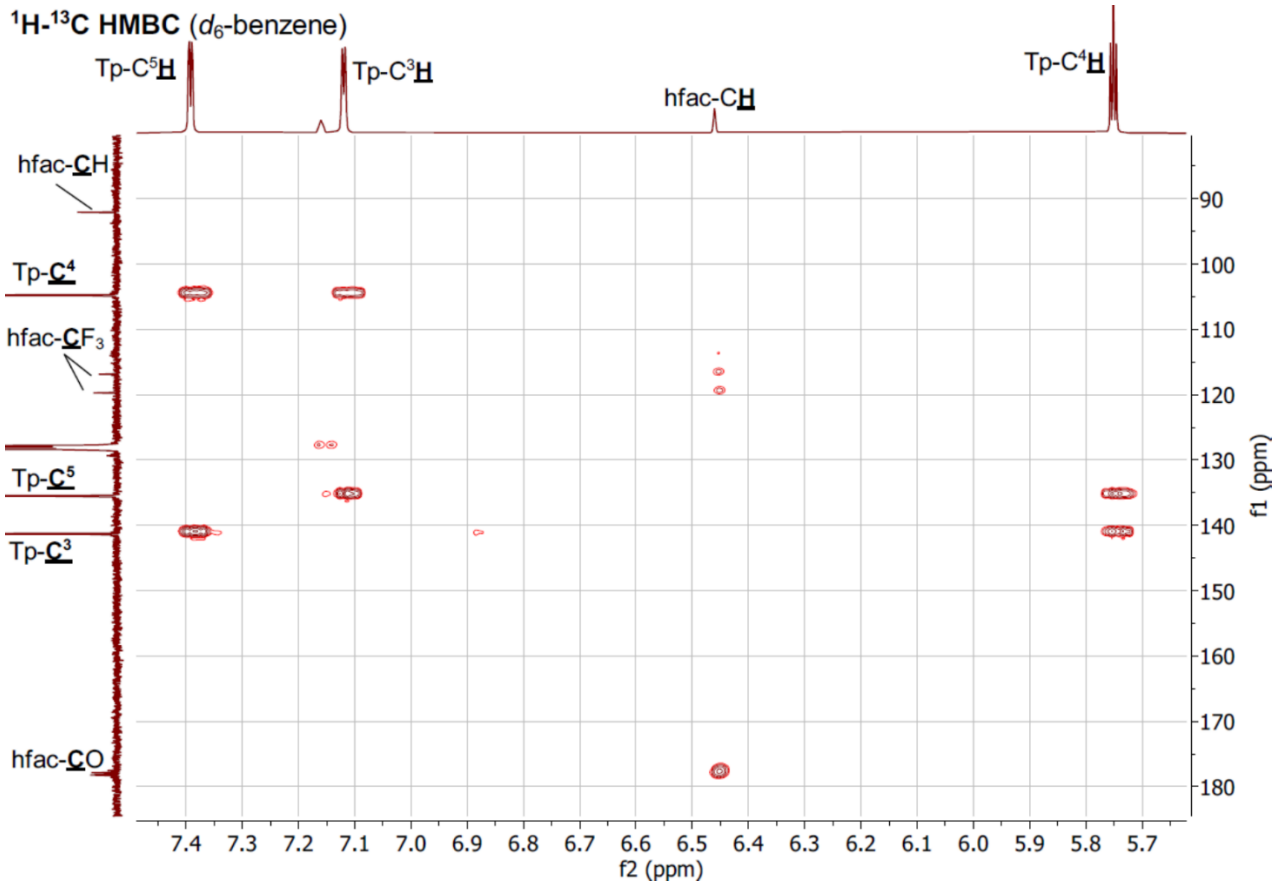

Figure S 33. ^{1}H-^{13}C HMBC NMR spectrum of [Y(Tp)$_2$(hfac)] **2-Y**, recorded in d_6-benzene.

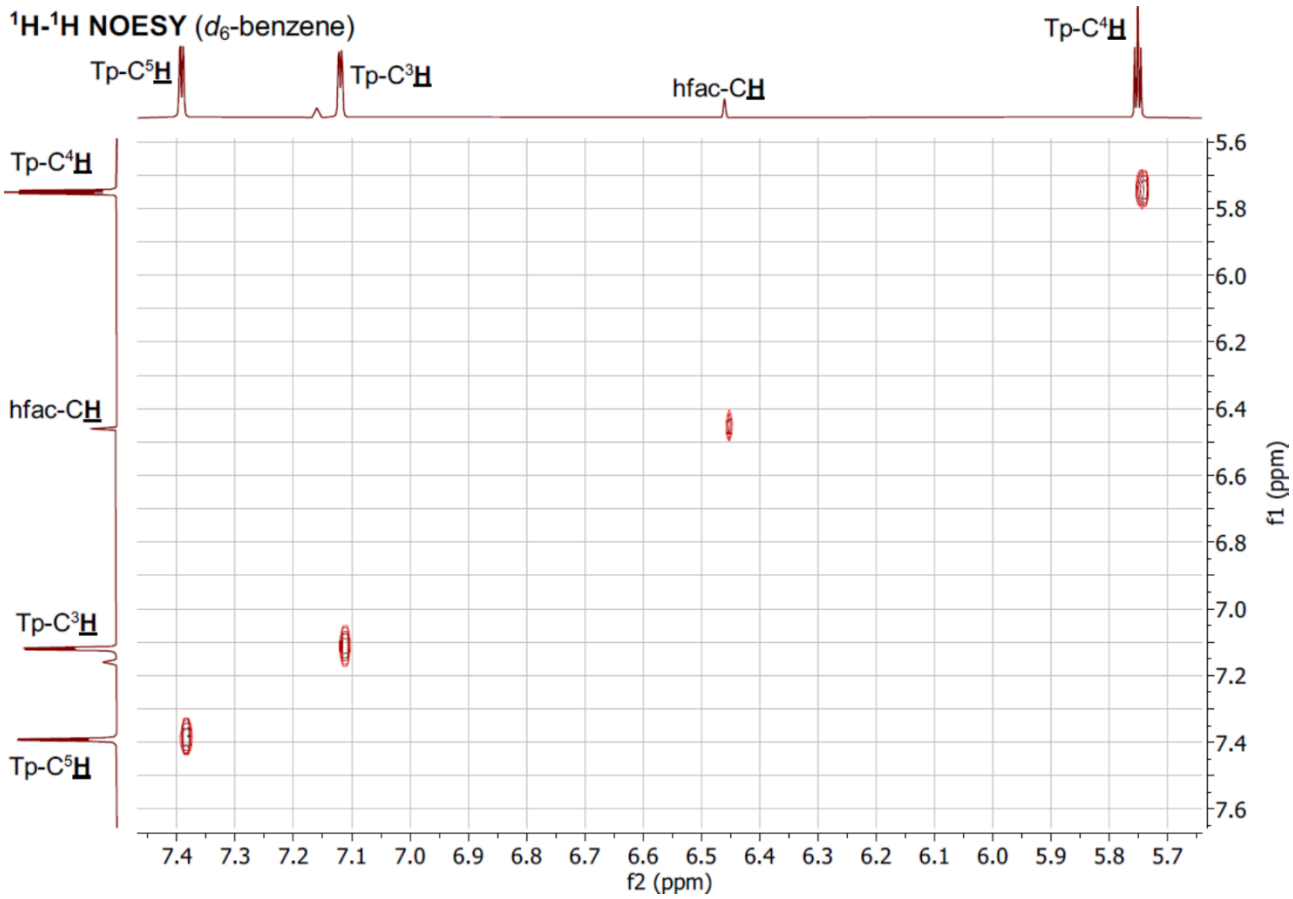

Figure S 34. ^{1}H-^{1}H NOESY NMR spectrum of [Y(Tp)$_2$(hfac)] **2-Y**, recorded in d_6-benzene.

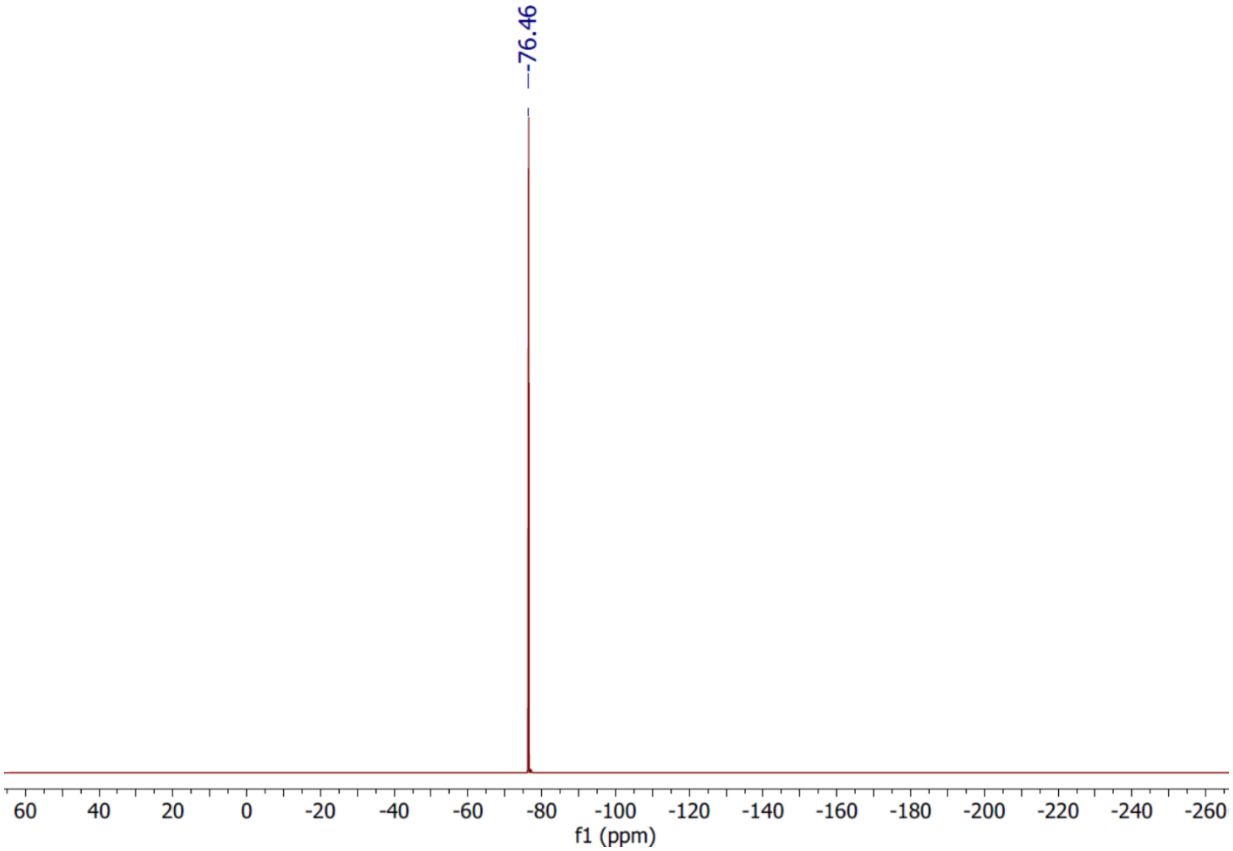

Figure S 35. ^{19}F NMR spectrum of [Y(Tp)$_2$(hfac)] **2-Y**, recorded in d_6-benzene.

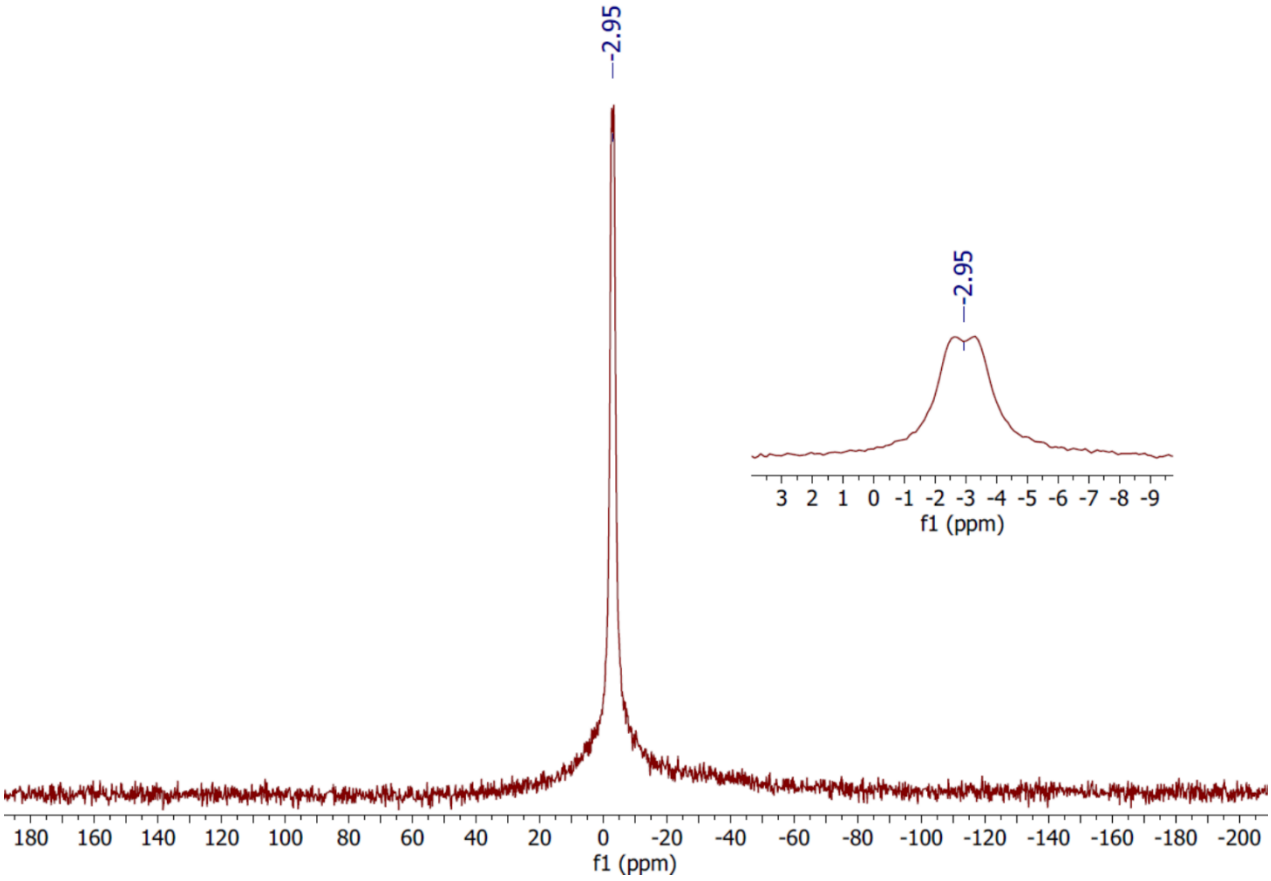

Figure S 36. ^{11}B NMR spectrum of [Y(Tp)$_2$(hfac)] **2-Y**, recorded in d_6-benzene.

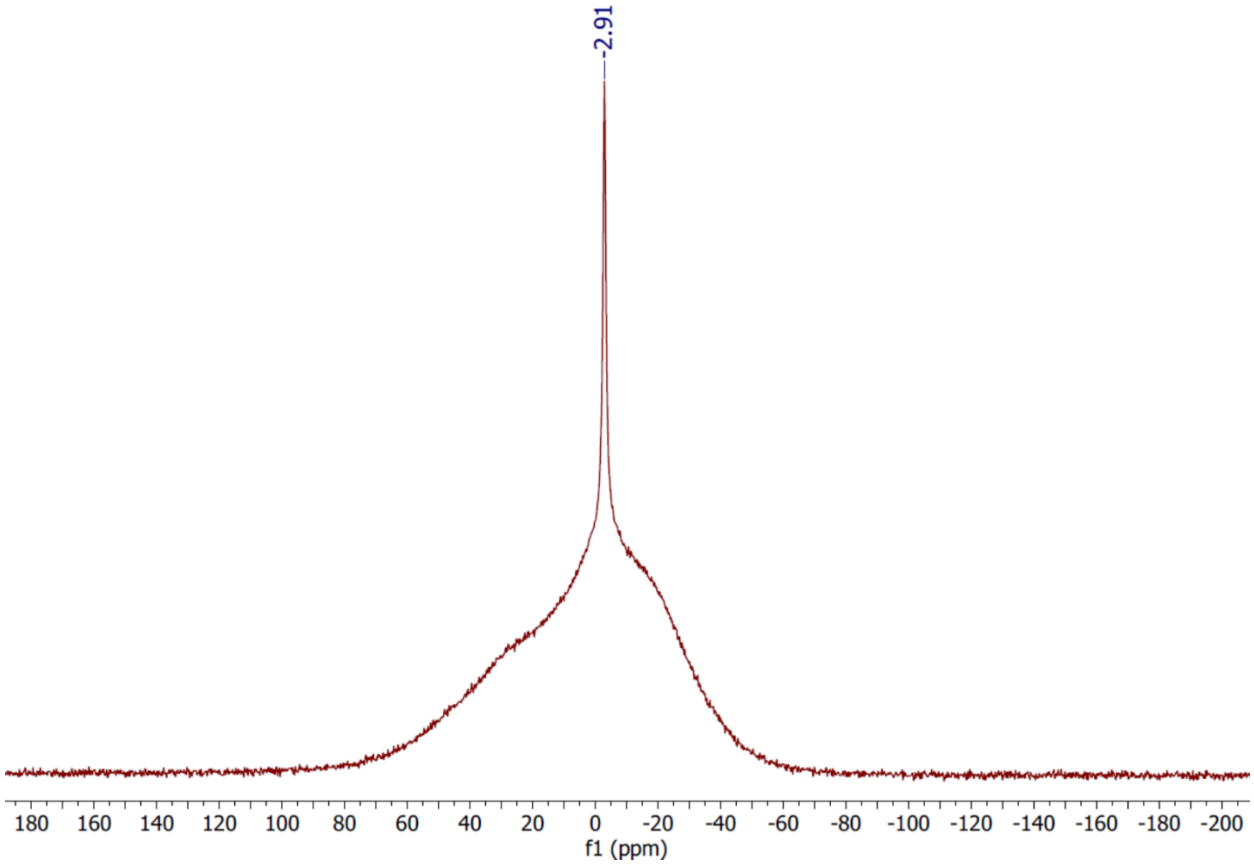

Figure S 37. ^{11}B{^{1}H} NMR spectrum of [Y(Tp)$_2$(hfac)] **2-Y**, recorded in d_6-benzene.

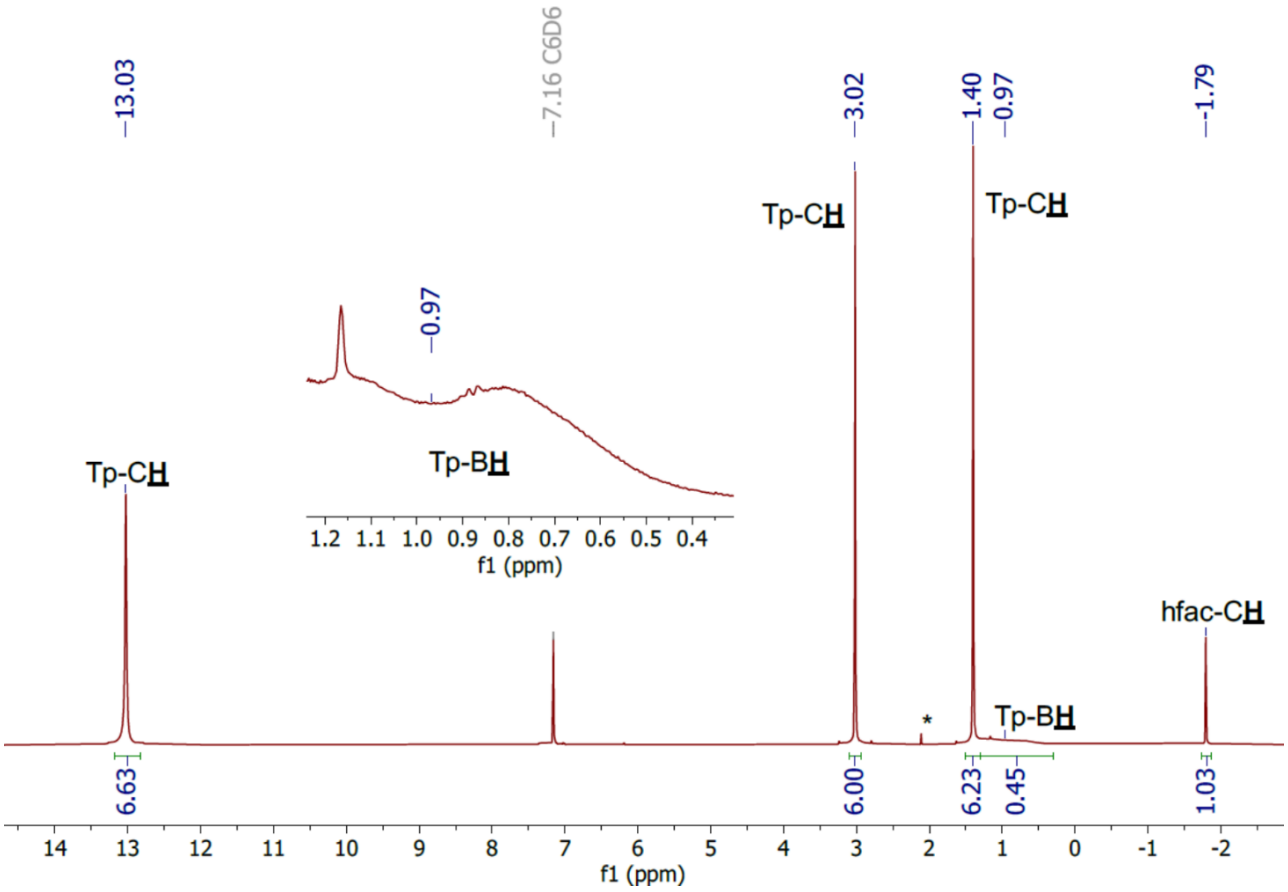

Figure S 38. ^{1}H NMR spectrum of [Eu(Tp)$_2$(hfac)] **2-Eu**, recorded in d_6-benzene. Toluene is denoted by *.

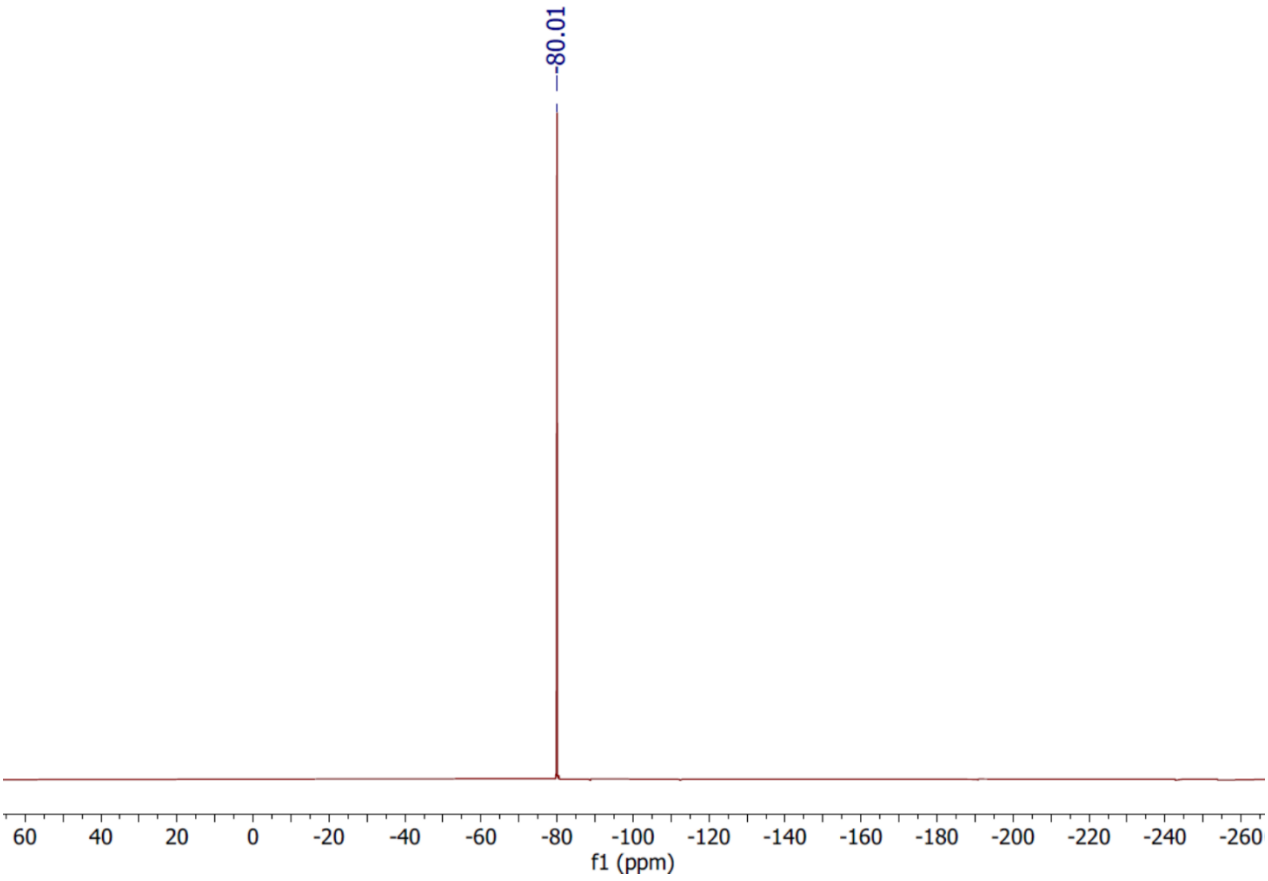

Figure S 39. ^{19}F NMR spectrum of [Eu(Tp)$_2$(hfac)] **2-Eu**, recorded in d_6-benzene.

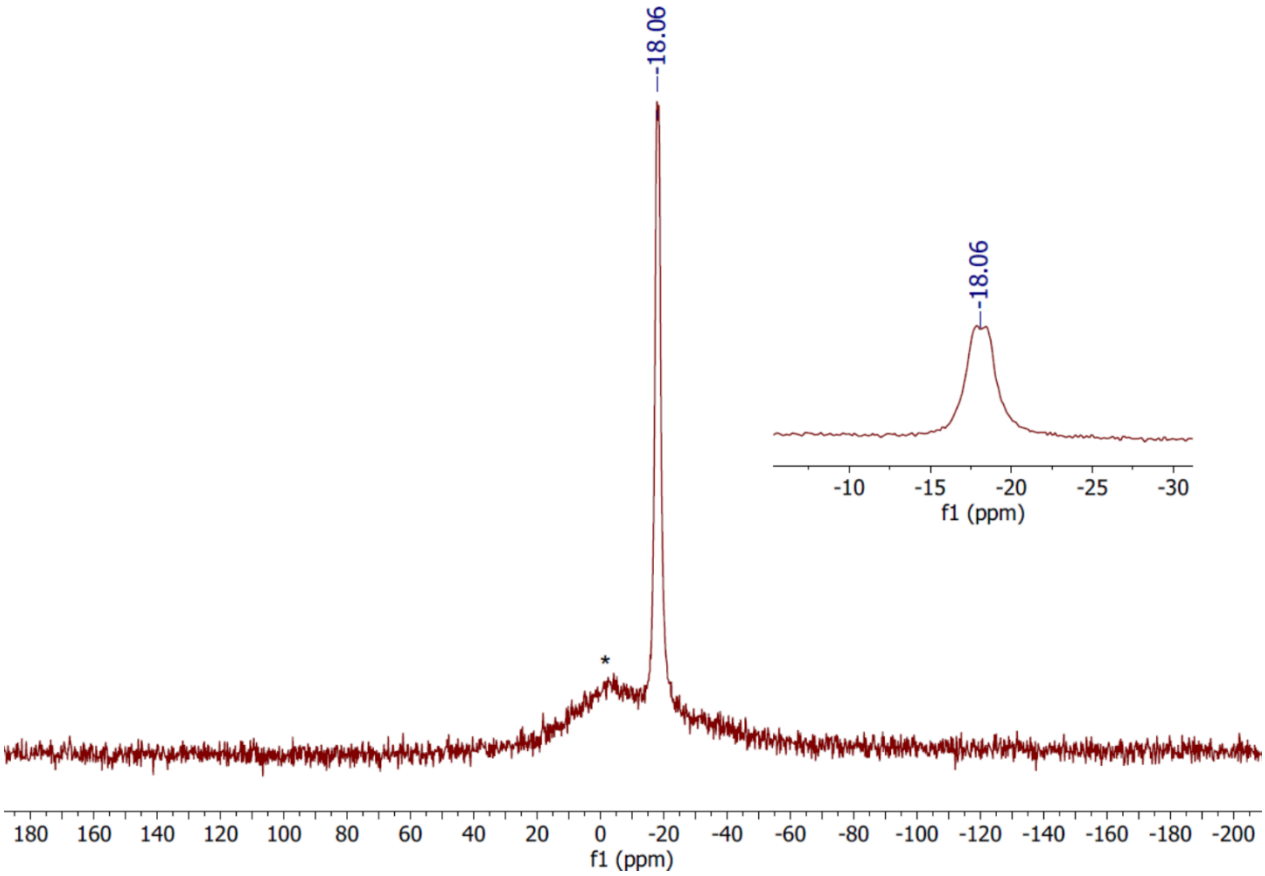

Figure S 40. ^{11}B NMR spectrum of [Eu(Tp)$_2$(hfac)] **2-Eu**, recorded in d_6-benzene. Borosilicate glass is denoted by *.

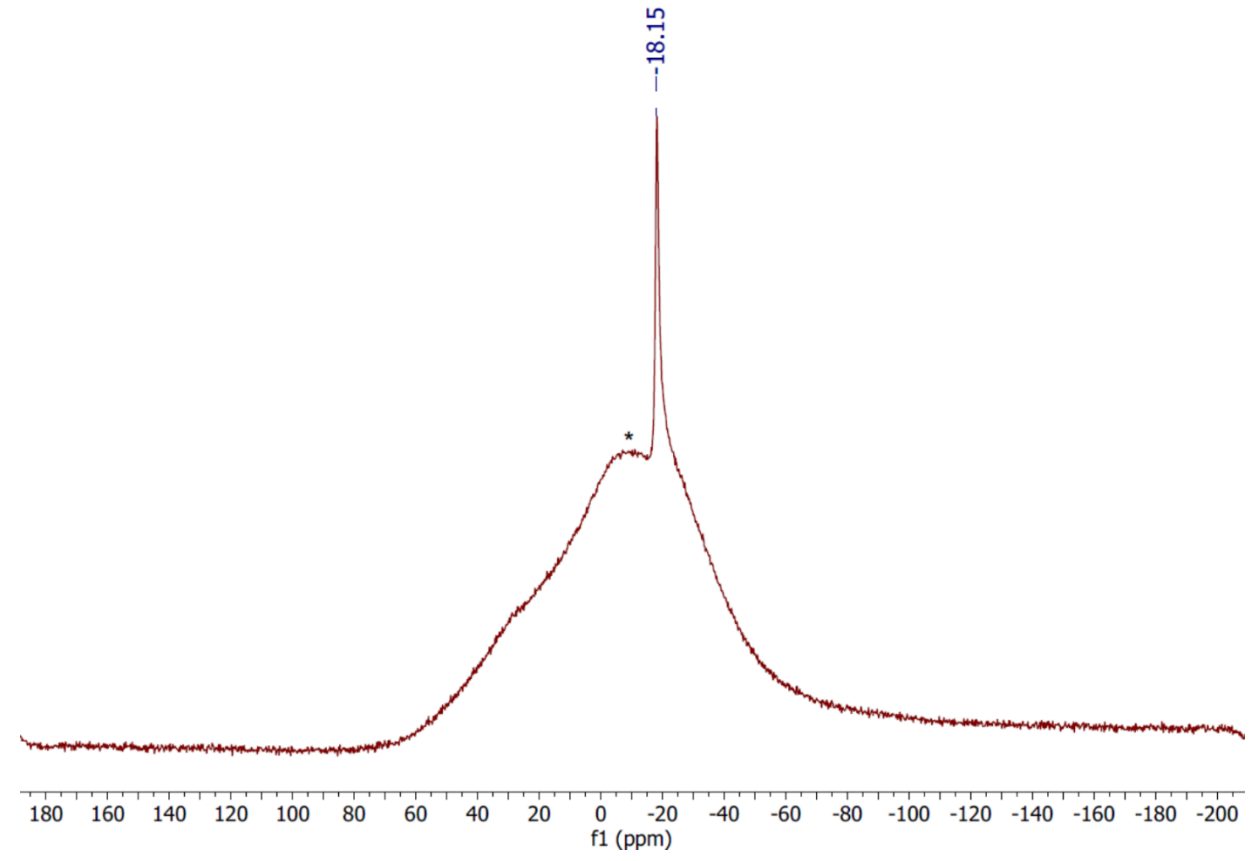

Figure S 41. ^{11}B{^{1}H} NMR spectrum of [Eu(Tp)$_2$(hfac)] **2-Eu**, recorded in d_6-benzene. Borosilicate glass is denoted by *.

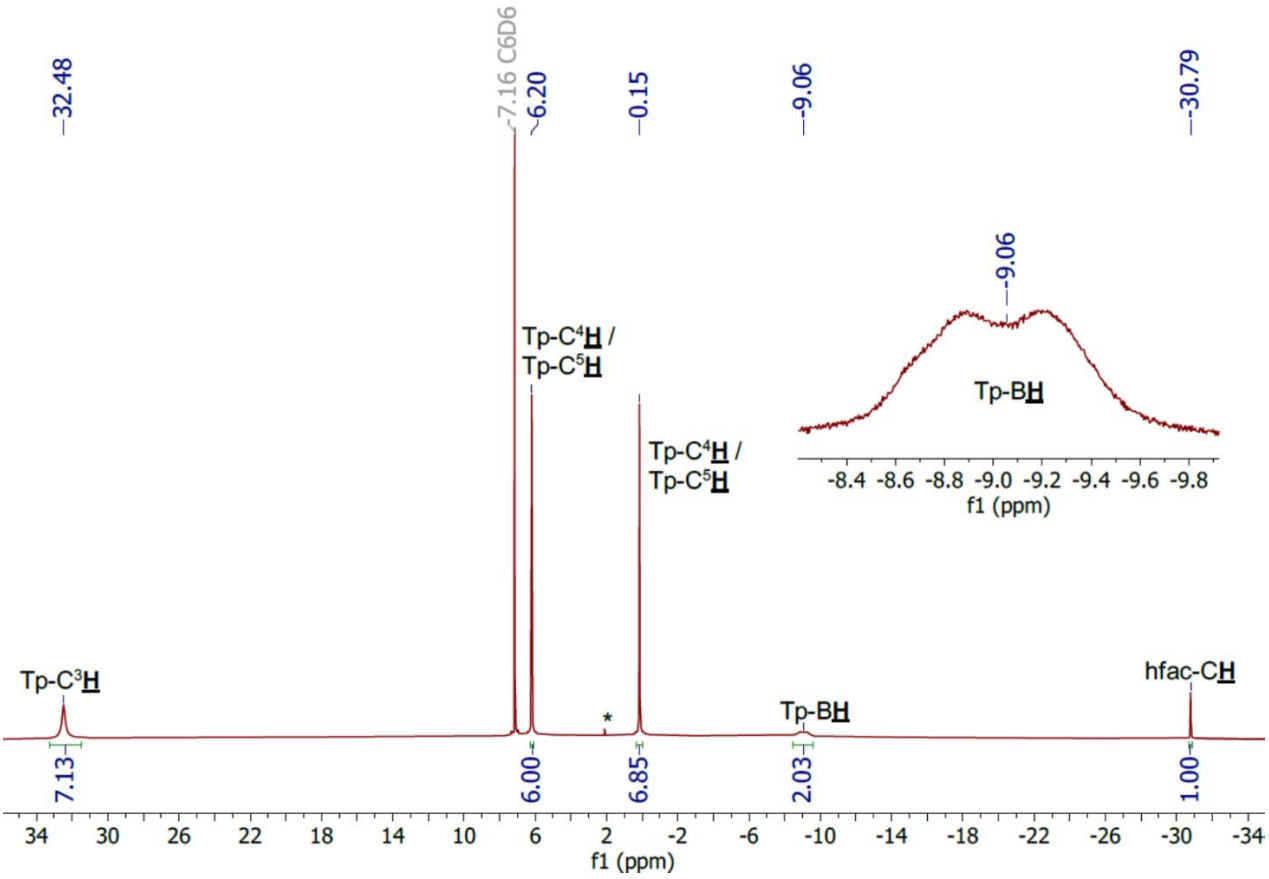

Figure S 42. ^{1}H NMR spectrum of [Yb(Tp)$_2$(hfac)] **2-Yb**, recorded in d_6-benzene. Toluene is denoted by *.

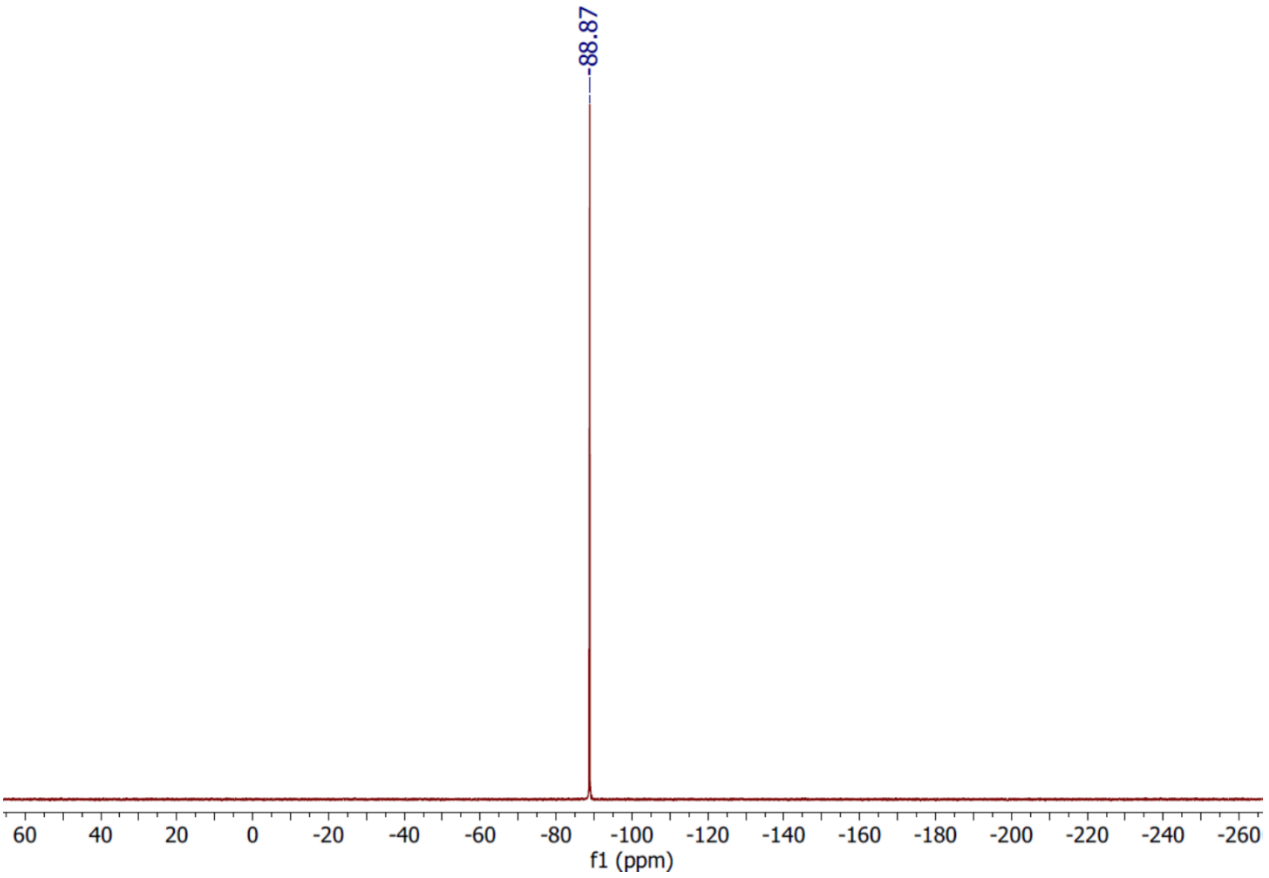

Figure S 43. ^{19}F NMR spectrum of [Yb(Tp)$_2$(hfac)] **2-Yb**, recorded in d_6-benzene.

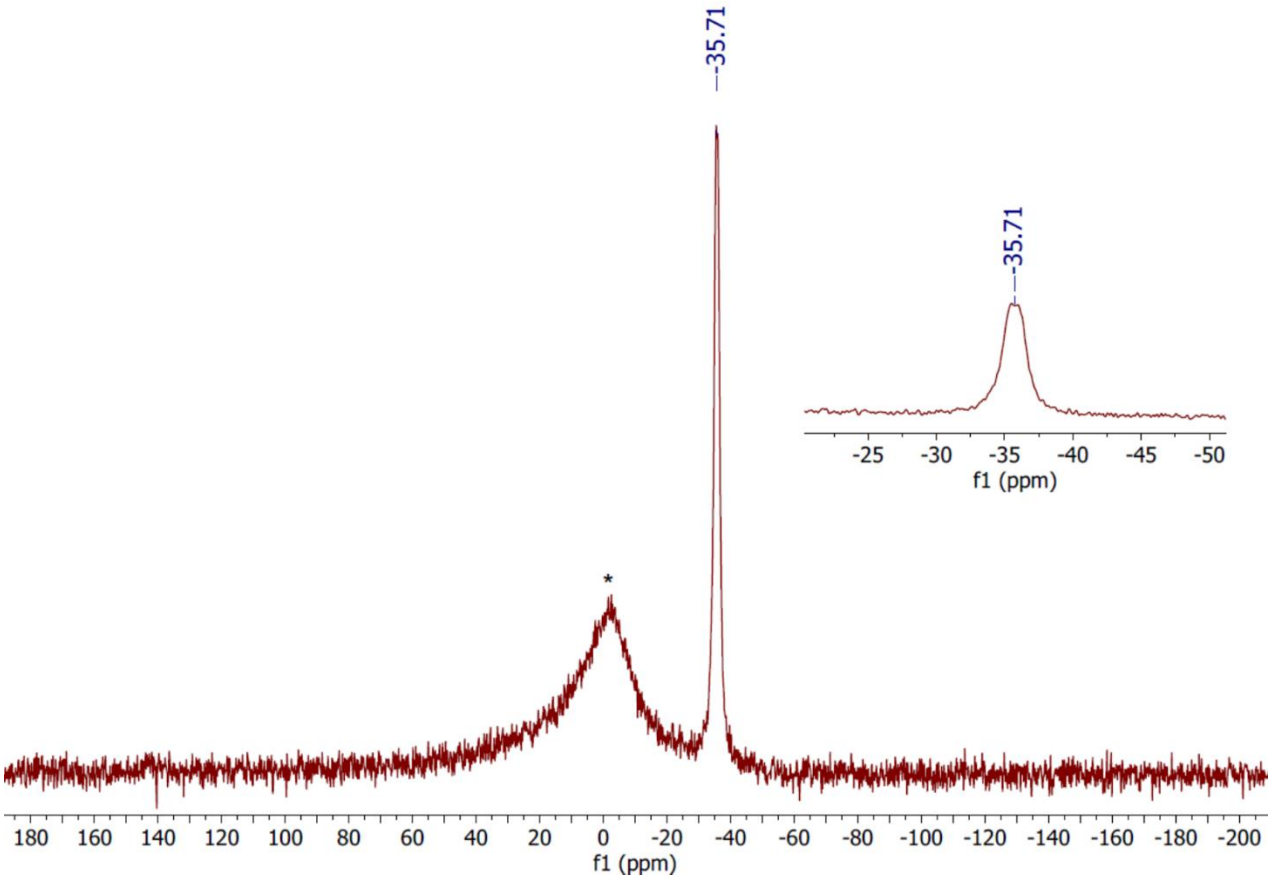

Figure S 44. ^{11}B NMR spectrum of [Yb(Tp)$_2$(hfac)] **2-Yb**, recorded in d_6-benzene. Borosilicate glass is denoted by *.

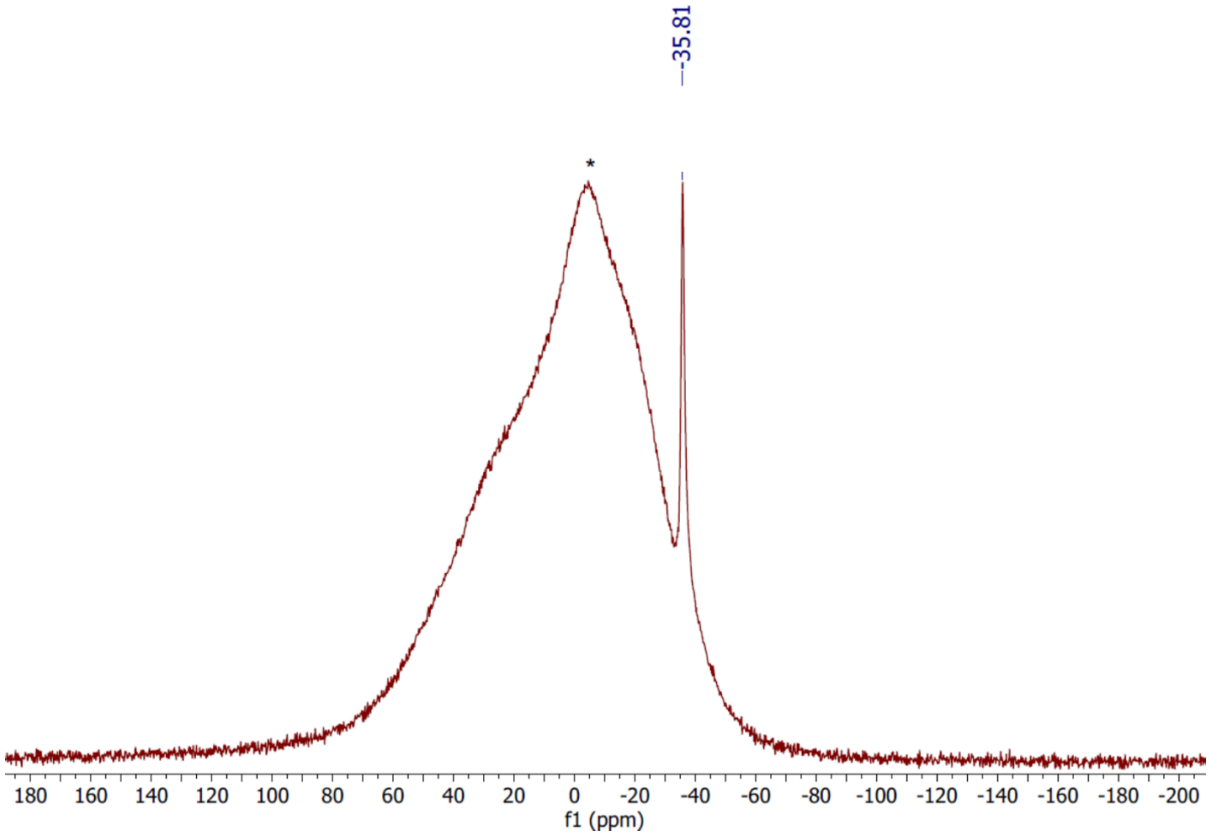

Figure S 45. ^{11}B{^{1}H} NMR spectrum of [Yb(Tp)$_2$(hfac)] **2-Yb**, recorded in d_6-benzene. Borosilicate glass is denoted by *.

S1.5 [Ln(Tp)$_2$(N'')] 3-Ln (Ln = Y, Yb)

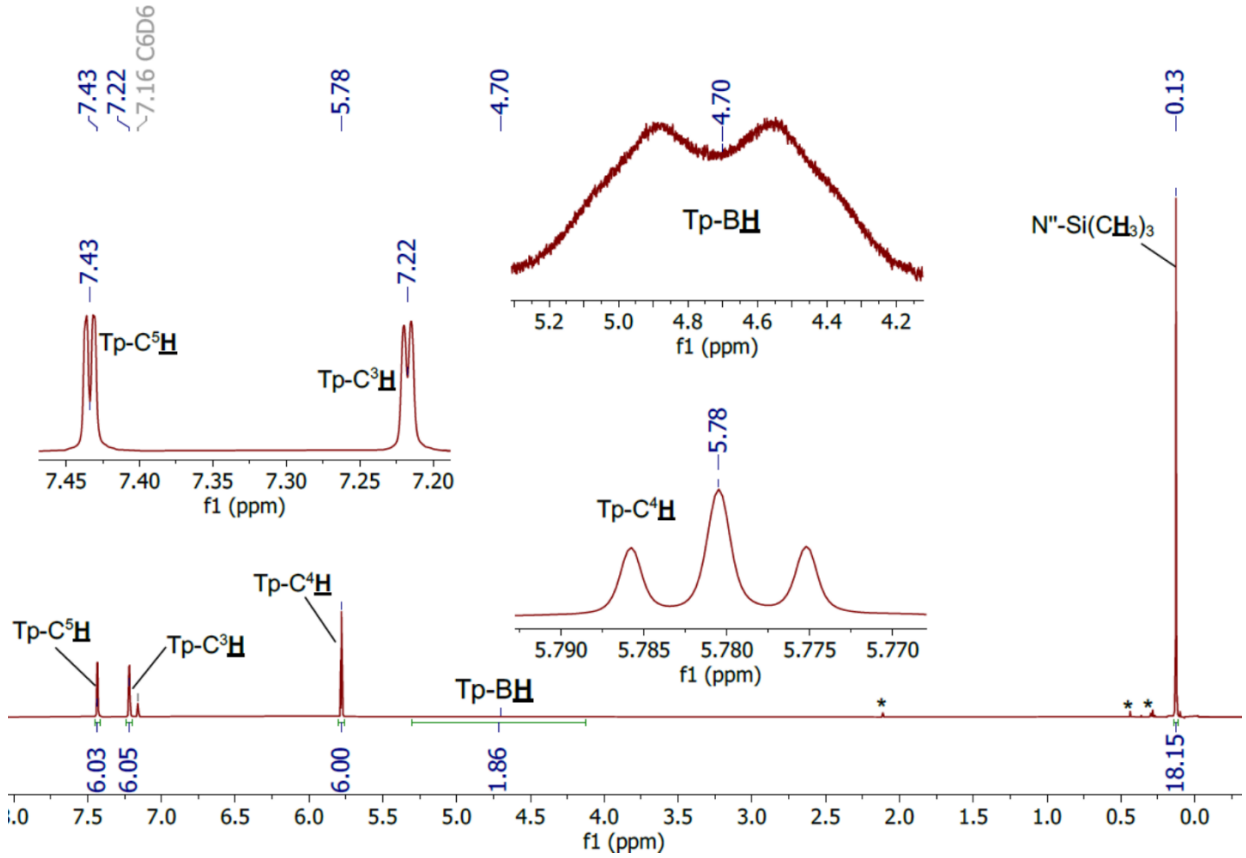

Figure S 46. ^{1}H NMR of [Y(Tp)$_2$(N'')] **3-Y**, recorded in d_6-benzene. Toluene and minor impurities are denoted with *.

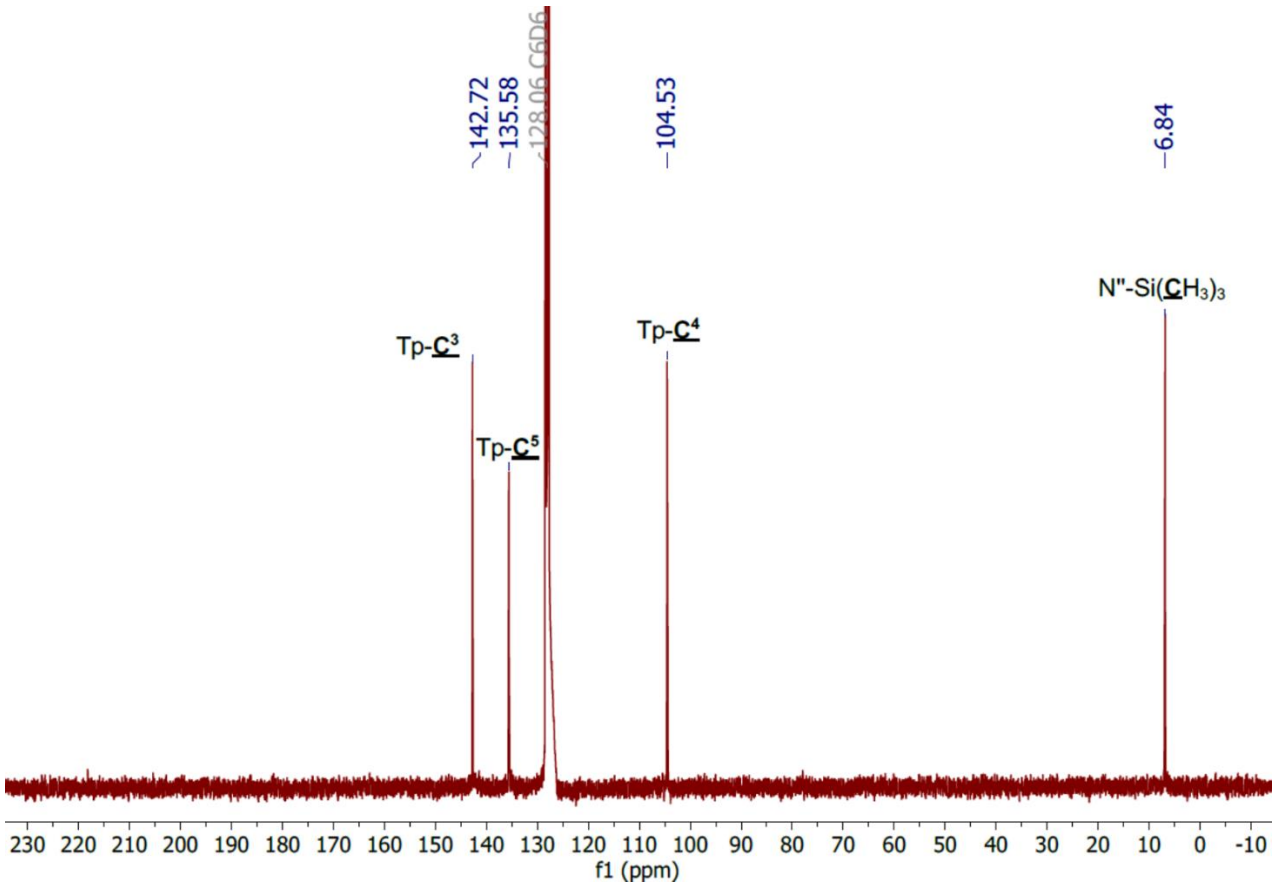

Figure S 47. ^{13}C{^{1}H} NMR of [Y(Tp)$_2$(N'')] **3-Y**, recorded in d_6-benzene.

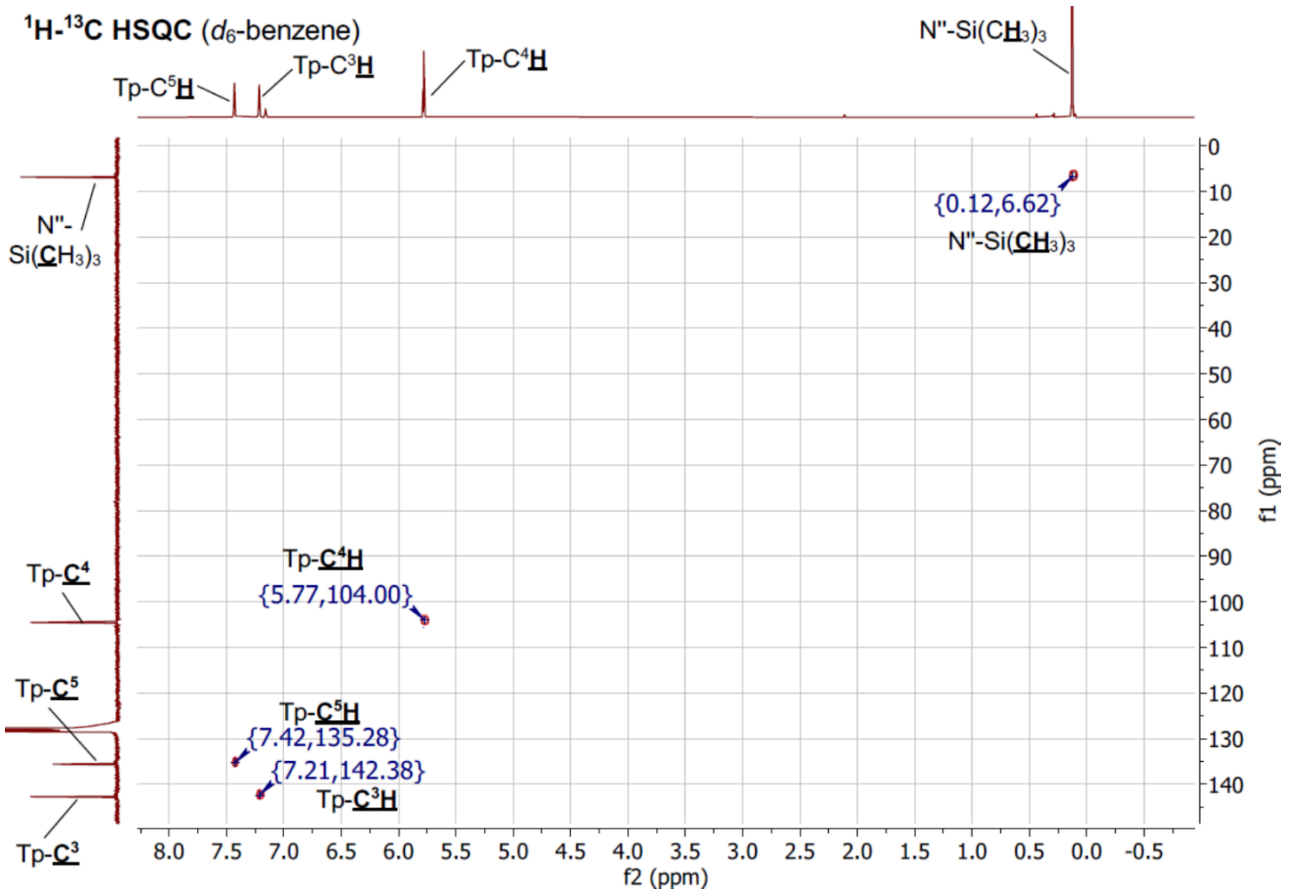

Figure S 48. ^{1}H-^{13}C HSQC NMR spectrum of [Y(Tp)$_2$(N")] **3-Y**, recorded in d_6-benzene.

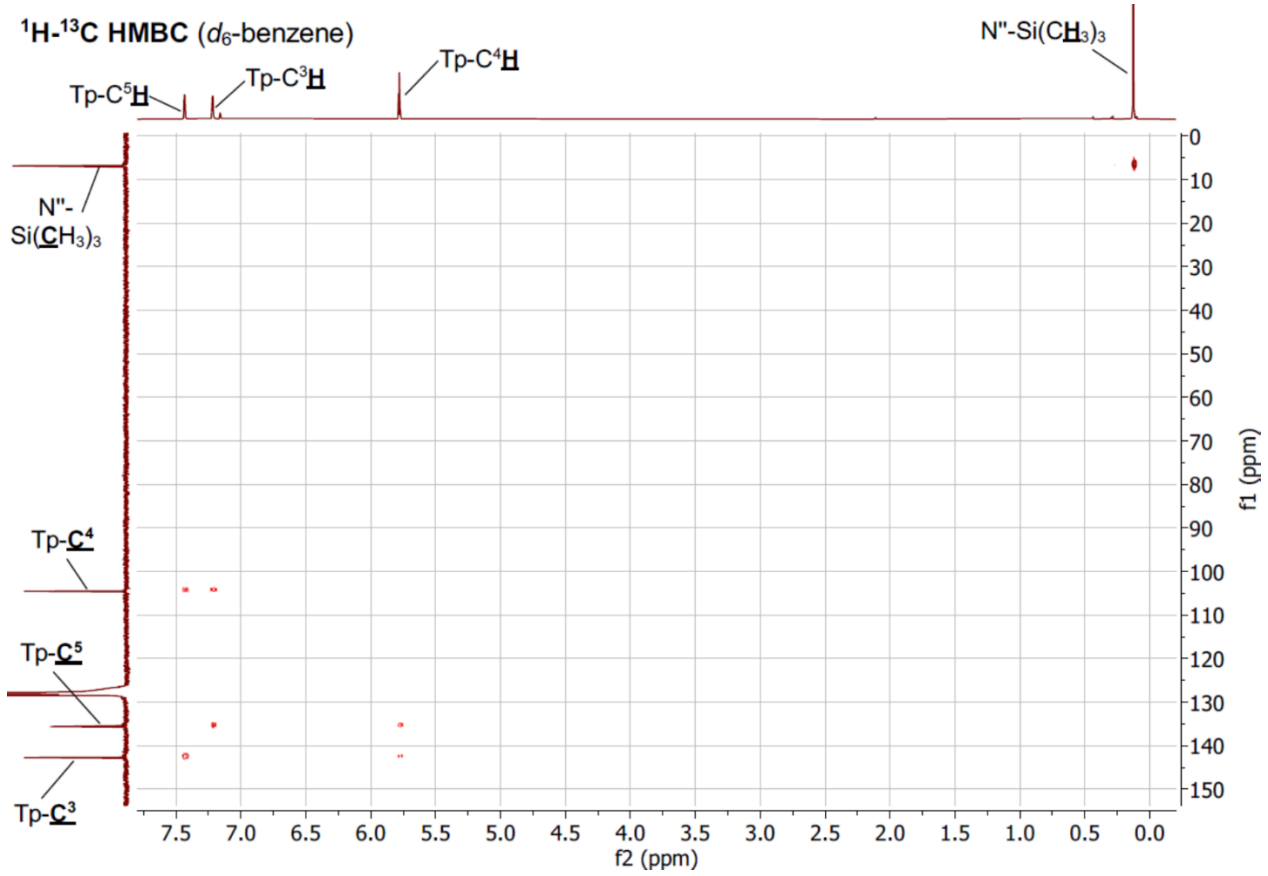

Figure S 49. ^{1}H-^{13}C HMBC NMR spectrum of [Y(Tp)$_2$(N")] **3-Y**, recorded in d_6-benzene.

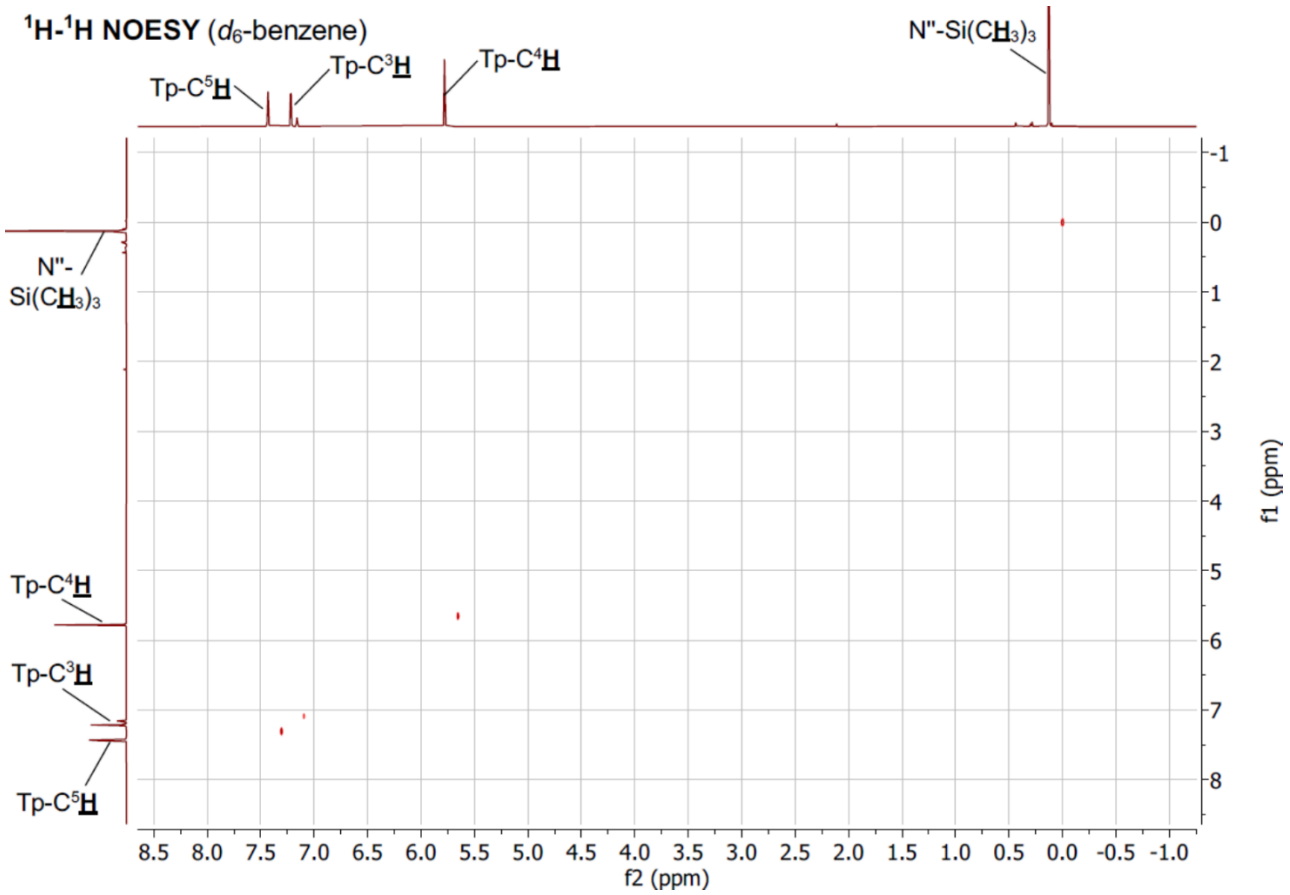

Figure S 50. ^{1}H-^{1}H NOESY NMR spectrum of [Y(Tp)$_2$(N")] **3-Y**, recorded in d_6-benzene.

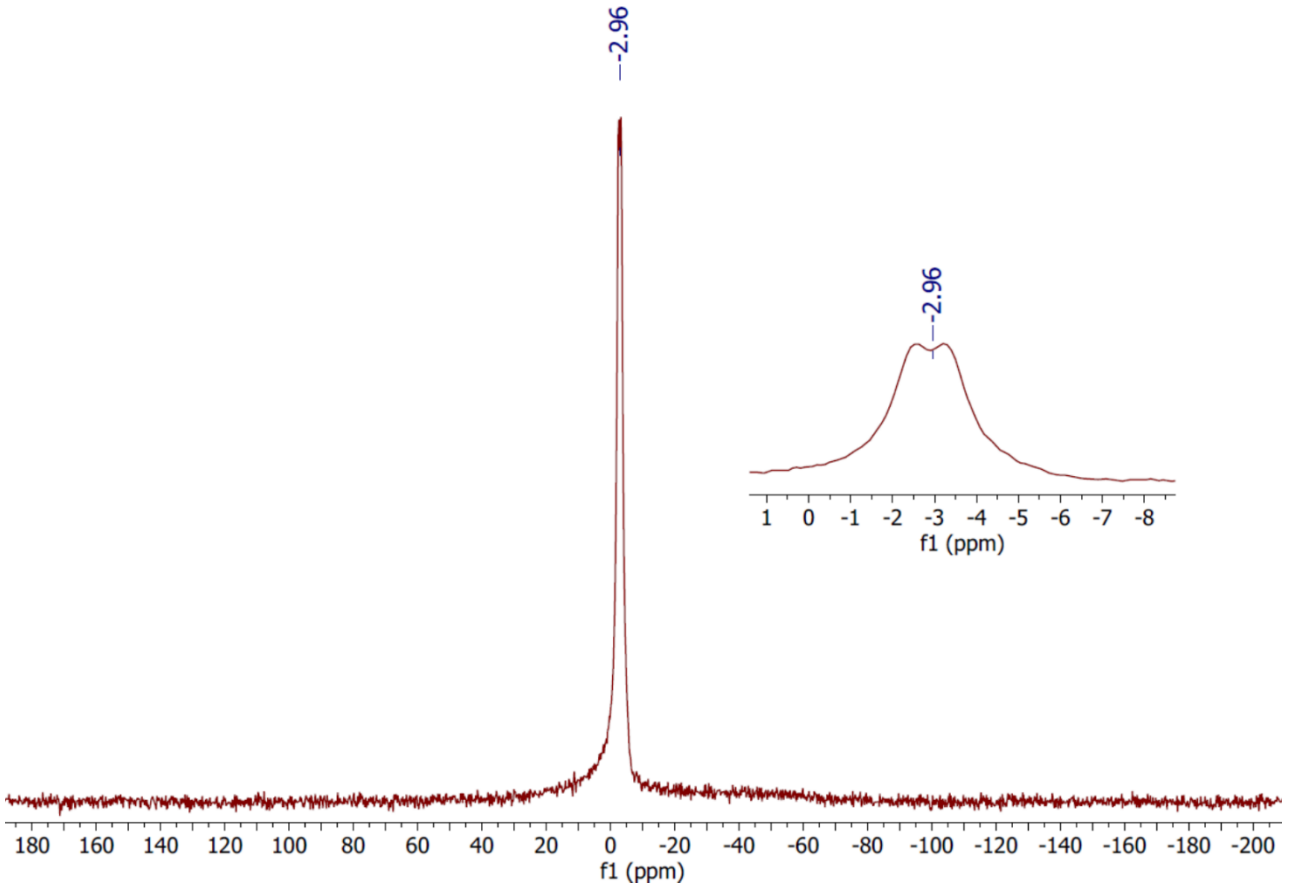

Figure S 51. ^{11}B NMR of [Y(Tp)$_2$(N")] **3-Y**, recorded in d_6-benzene.

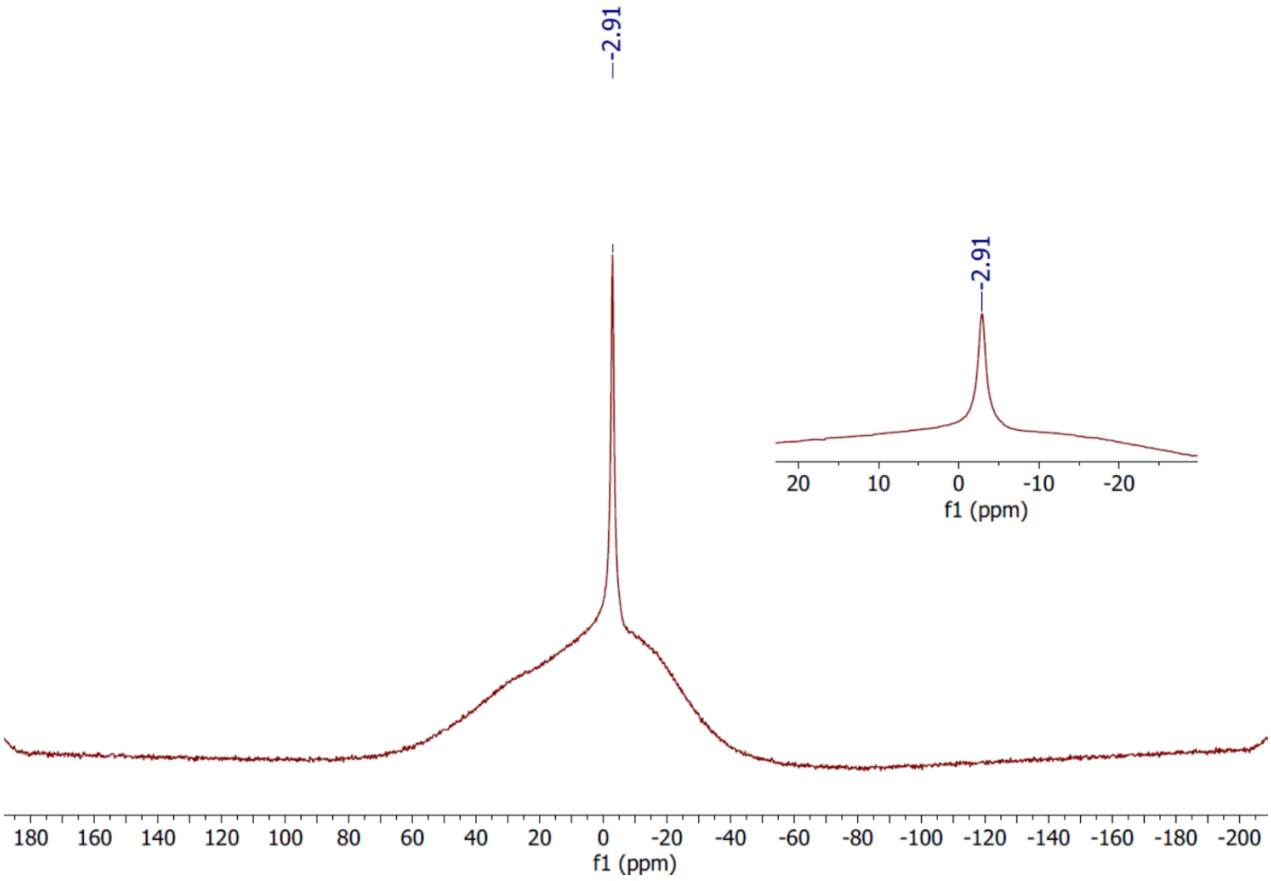

Figure S 52. $^{11}B\{^{1}H\}$ NMR of $[Y(Tp)_2(N'')]$ **3-Y**, recorded in d_6-benzene.

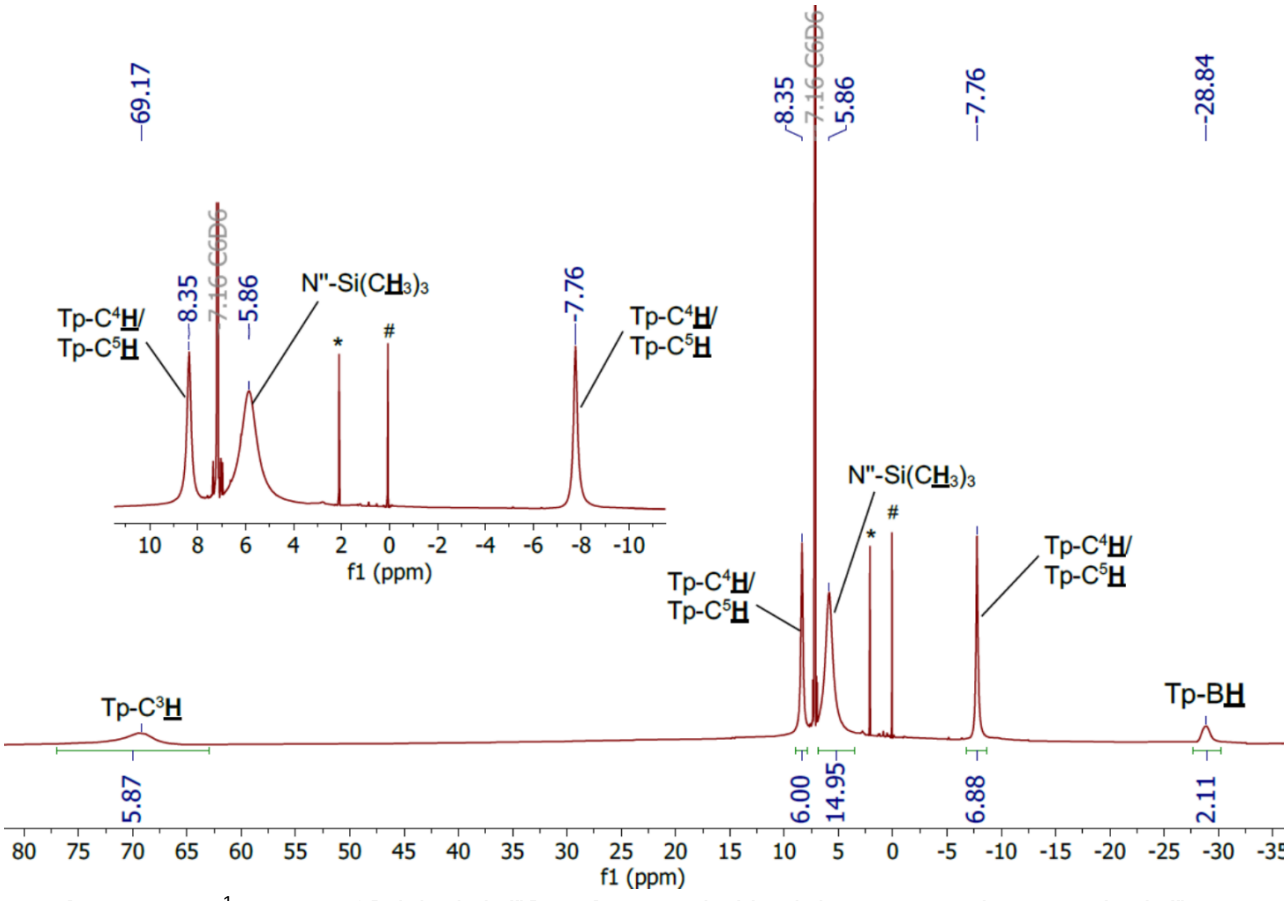

Figure S 53. ^{1}H NMR of $[Yb(Tp)_2(N'')]$ **3-Yb**, recorded in d_6-benzene. Toluene and H(N") are denoted with * and $^{\#}$, respectively.

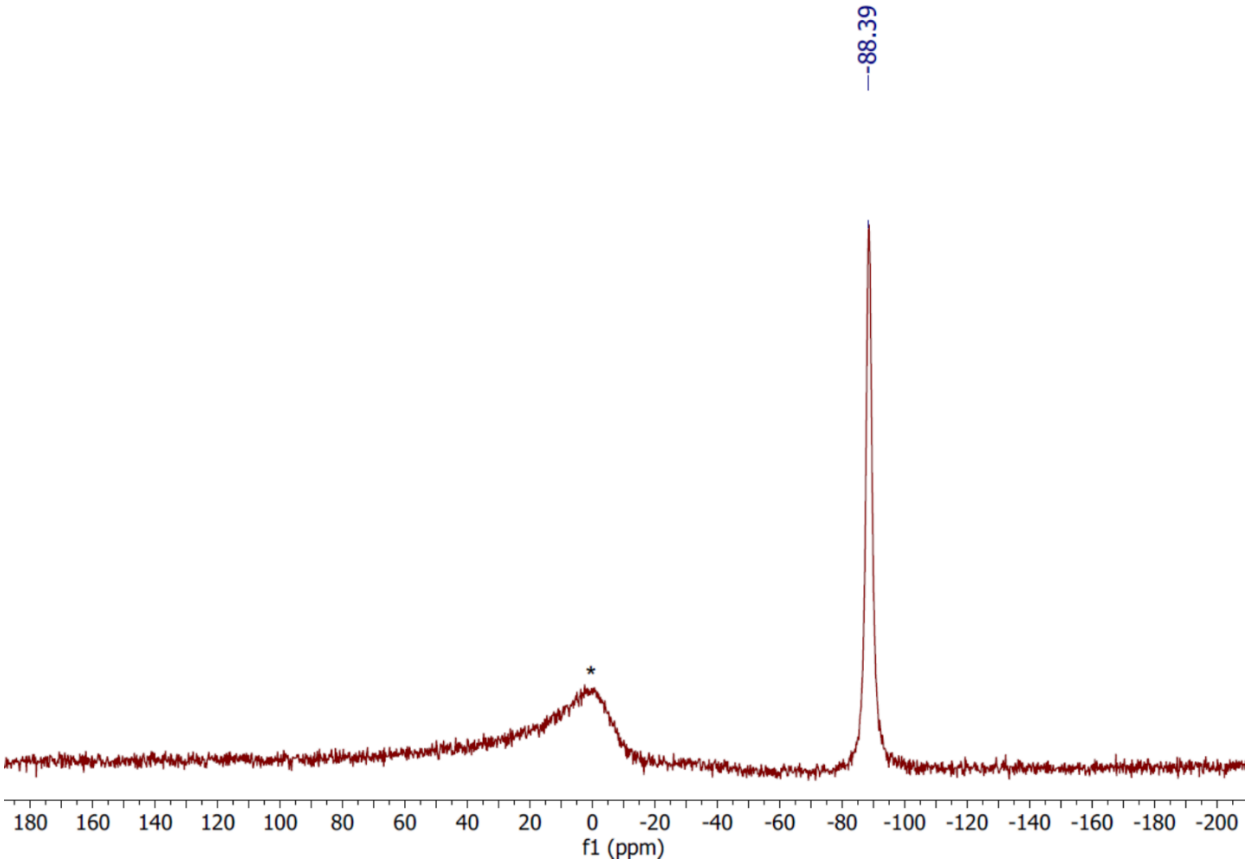

Figure S 54. ^{11}B NMR of [Yb(Tp)$_2$(N")] **3-Yb**, recorded in d_6-benzene. Borosilicate glass is denoted by *.

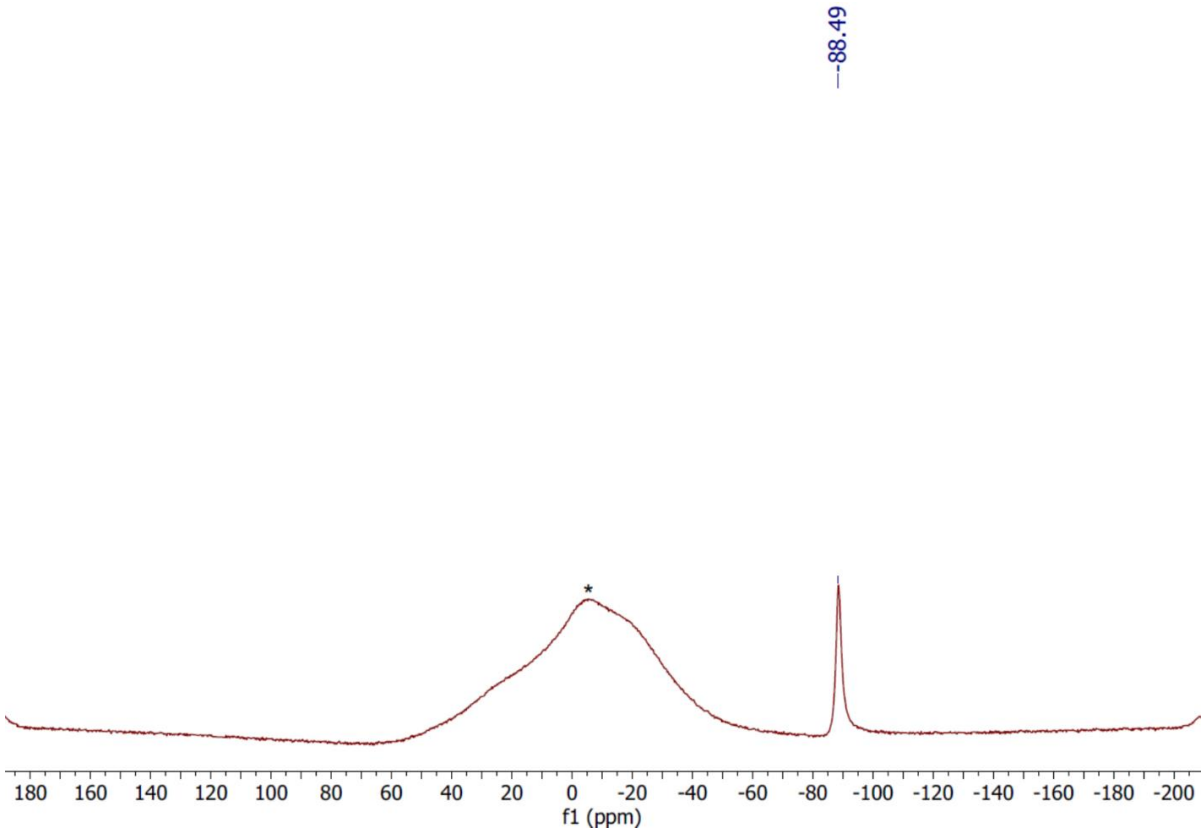

Figure S 55. ^{11}B NMR{^{1}H} of [Yb(Tp)$_2$(N")] **3-Yb**, recorded in d_6-benzene. Borosilicate glass is denoted by *.

S1.6 [{Y(Tp)$_2$(μ-OH)}$_2$] 4-Y

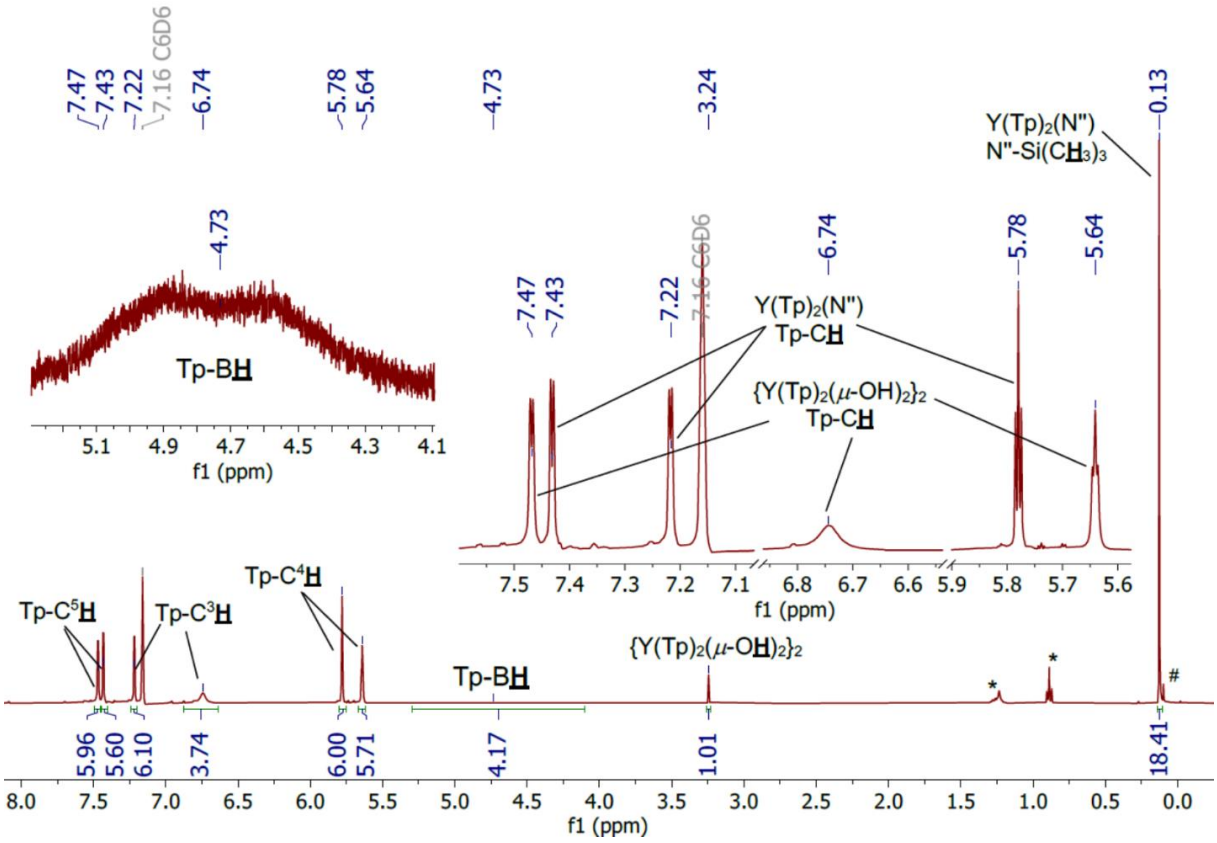

Figure S 56. ^{1}H NMR of a mixture of crystals of **3-Y** and [{Y(Tp)$_2$(μ-OH)$_2$}$_2$] **4-Y**, recorded in d_6-benzene. Hexane of crystallisation is denoted with * and H(N") is denoted with $^{\#}$.

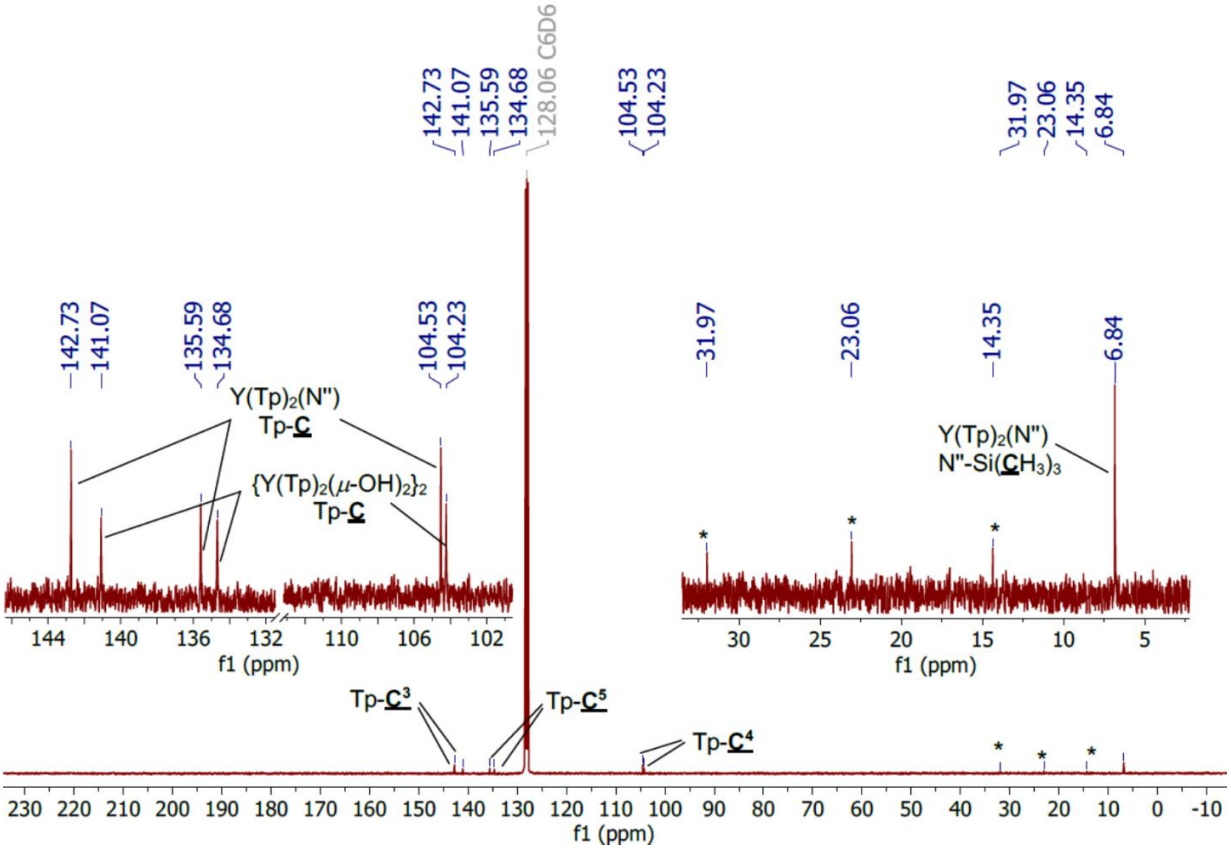

Figure S 57. ^{13}C{^{1}H} NMR of a mixture of crystals of **3-Y** and [{Y(Tp)$_2$(μ-OH)$_2$}$_2$] **4-Y**, recorded in d_6-benzene. Hexane of crystallisation is denoted with *.

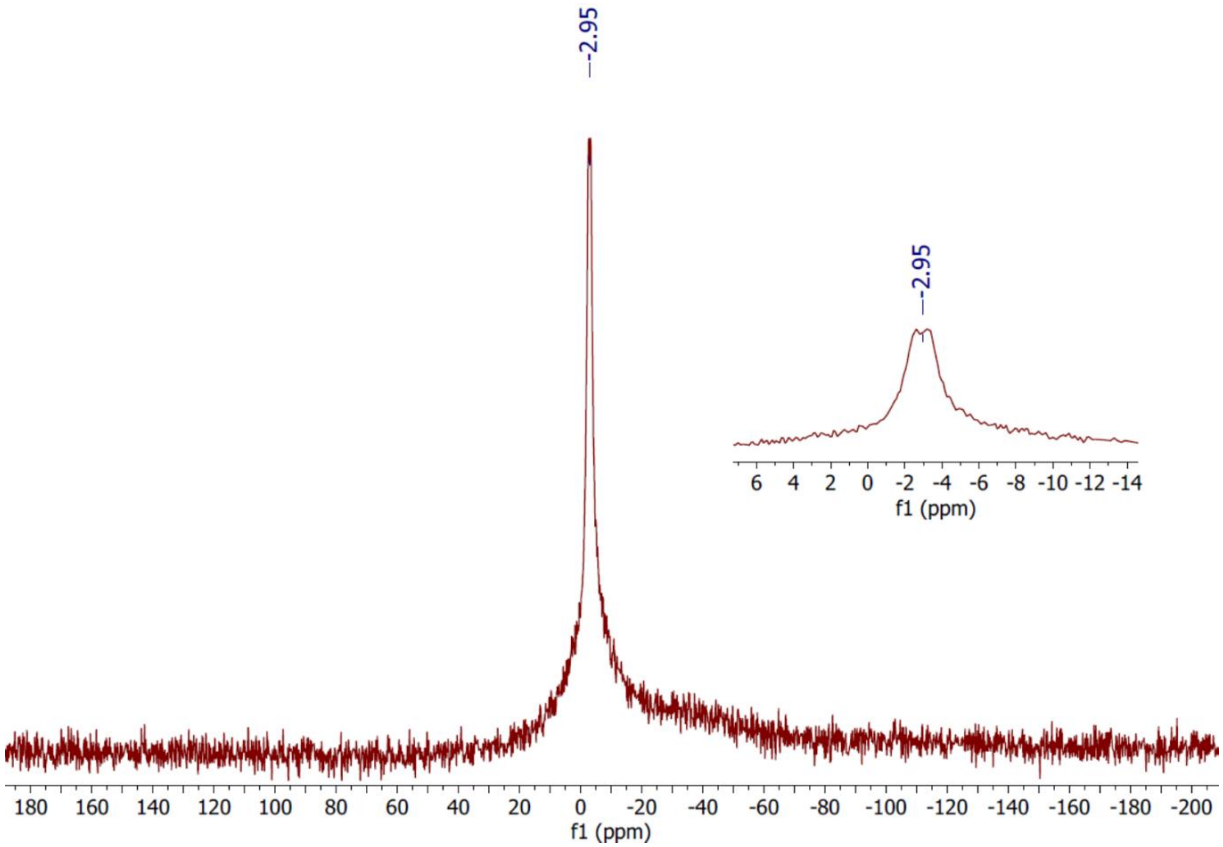

Figure S 58. $^{11}B\{^{1}H\}$ NMR of a mixture of crystals of **3-Y** and $[\{Y(Tp)_2(\mu\text{-}OH)_2\}_2]$ **4-Y**, recorded in d_6-benzene.

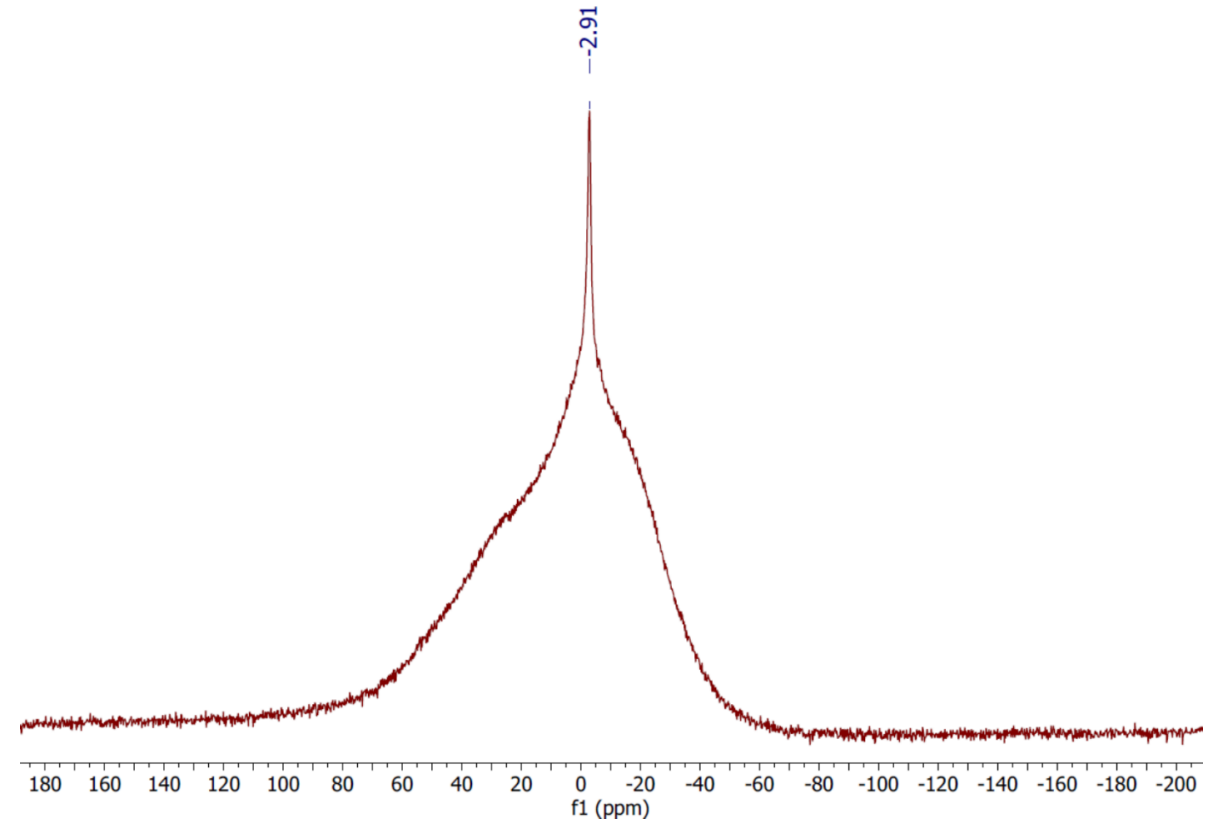

Figure S 59. $^{11}B\{^{1}H\}$ NMR of a mixture of crystals of **3-Y** and $[\{Y(Tp)_2(\mu\text{-}OH)_2\}_2]$ **4-Y**, recorded in d_6-benzene.

S1.7 [Ln(Tp)$_2$(OAr)] 5-Ln (Ln = Y, Yb)

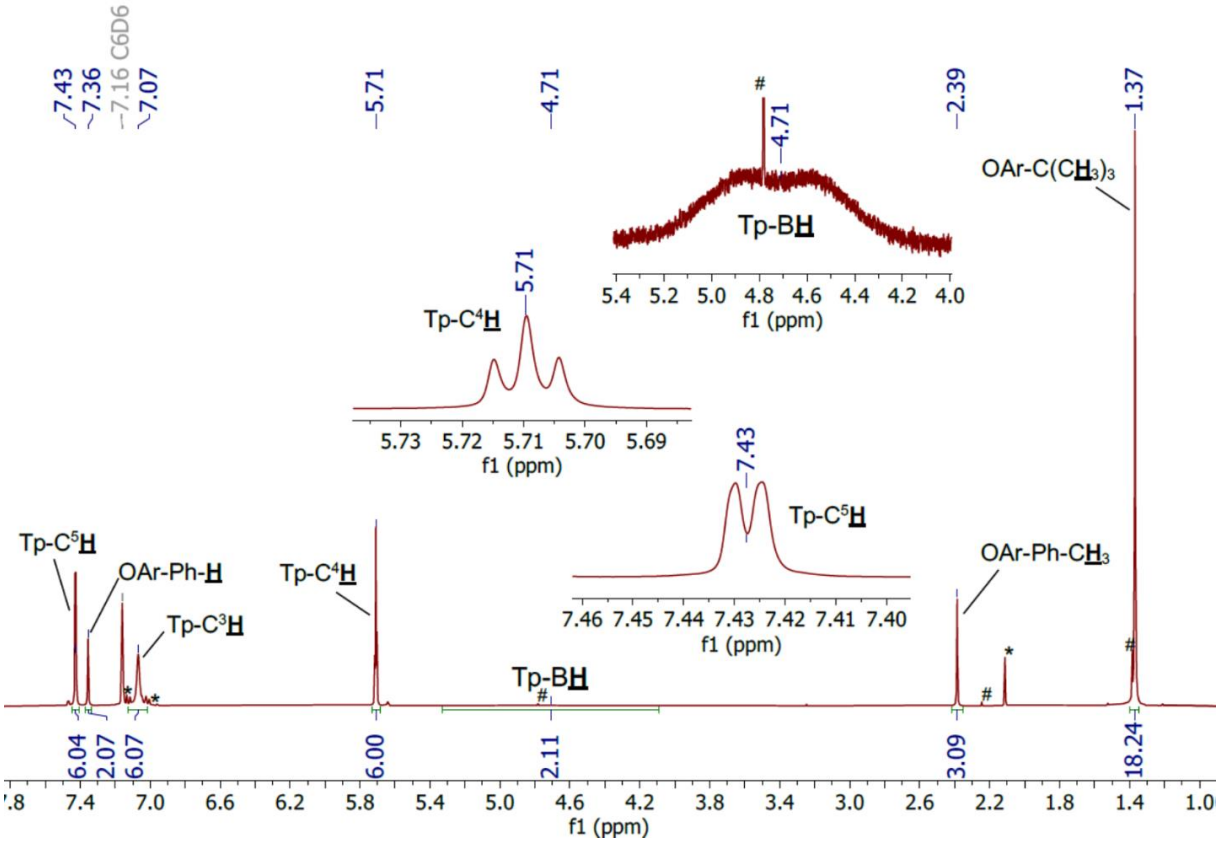

Figure S 60. ^{1}H NMR of [Y(Tp)$_2$(OAr)] **5-Y**, recorded in d_6-benzene. Toluene of crystallisation is denoted with * and H(OAr) from adventitious decomposition of **5-Y** to H(OAr) is denoted with #.

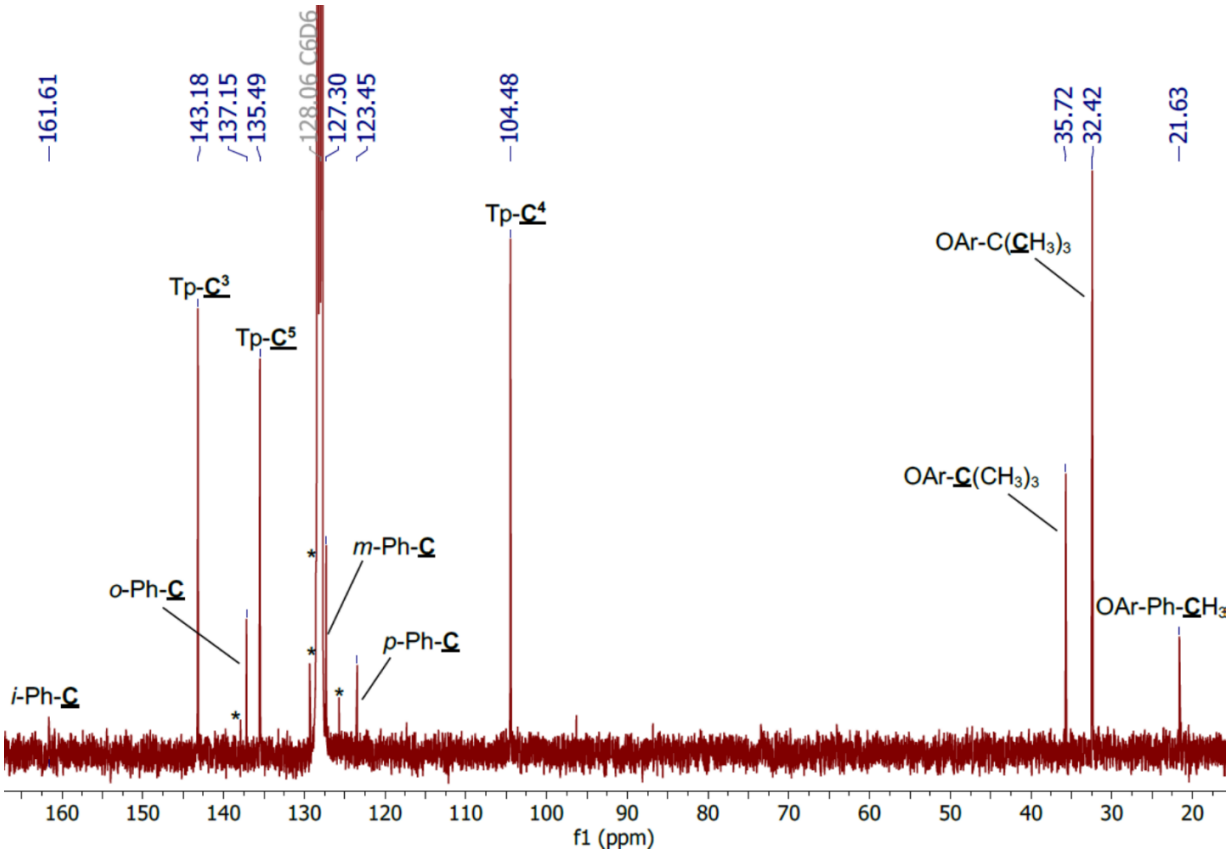

Figure S 61. ^{13}C{^{1}H} NMR of [Y(Tp)$_2$(OAr)] **5-Y**, recorded in d_6-benzene. Toluene of crystallisation is denoted with *.

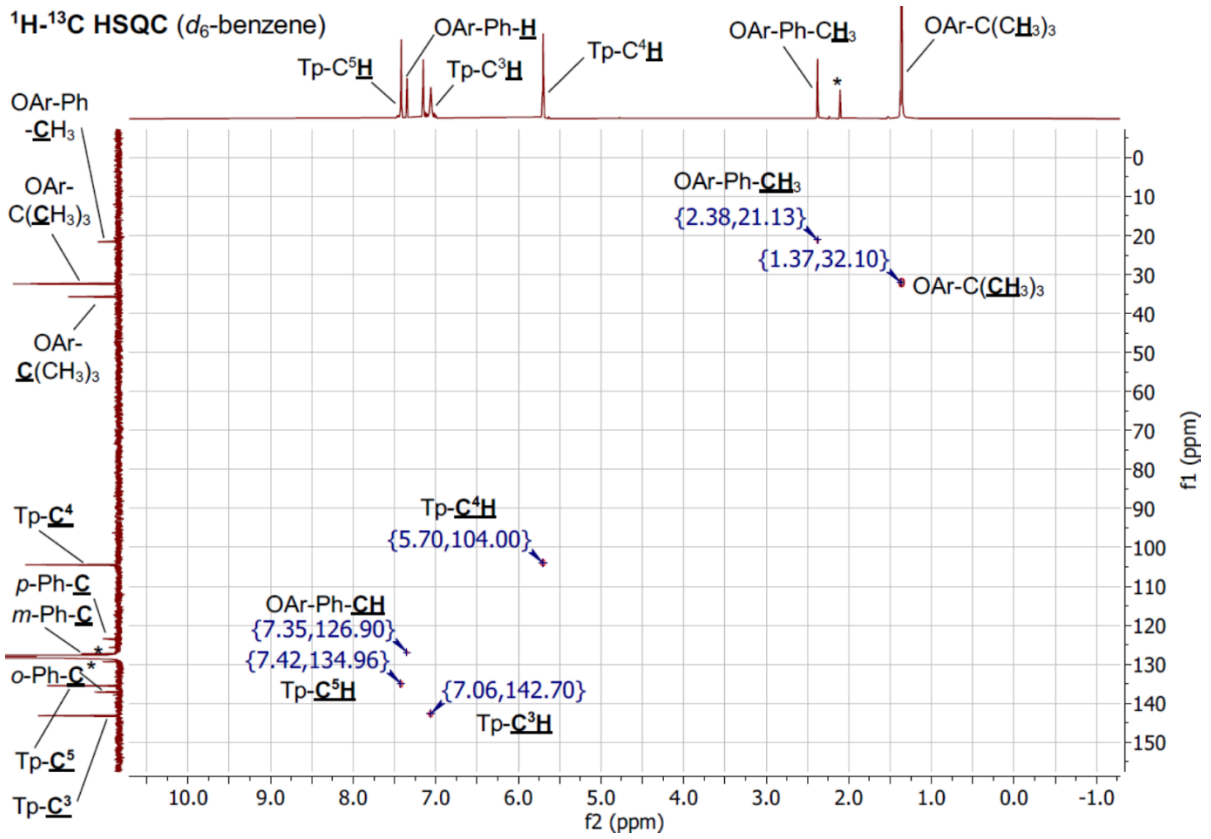

Figure S 62. ^{1}H-^{13}C HSQC NMR spectrum of [Y(Tp)$_2$(OAr)] **5-Y**, recorded in d_6-benzene.

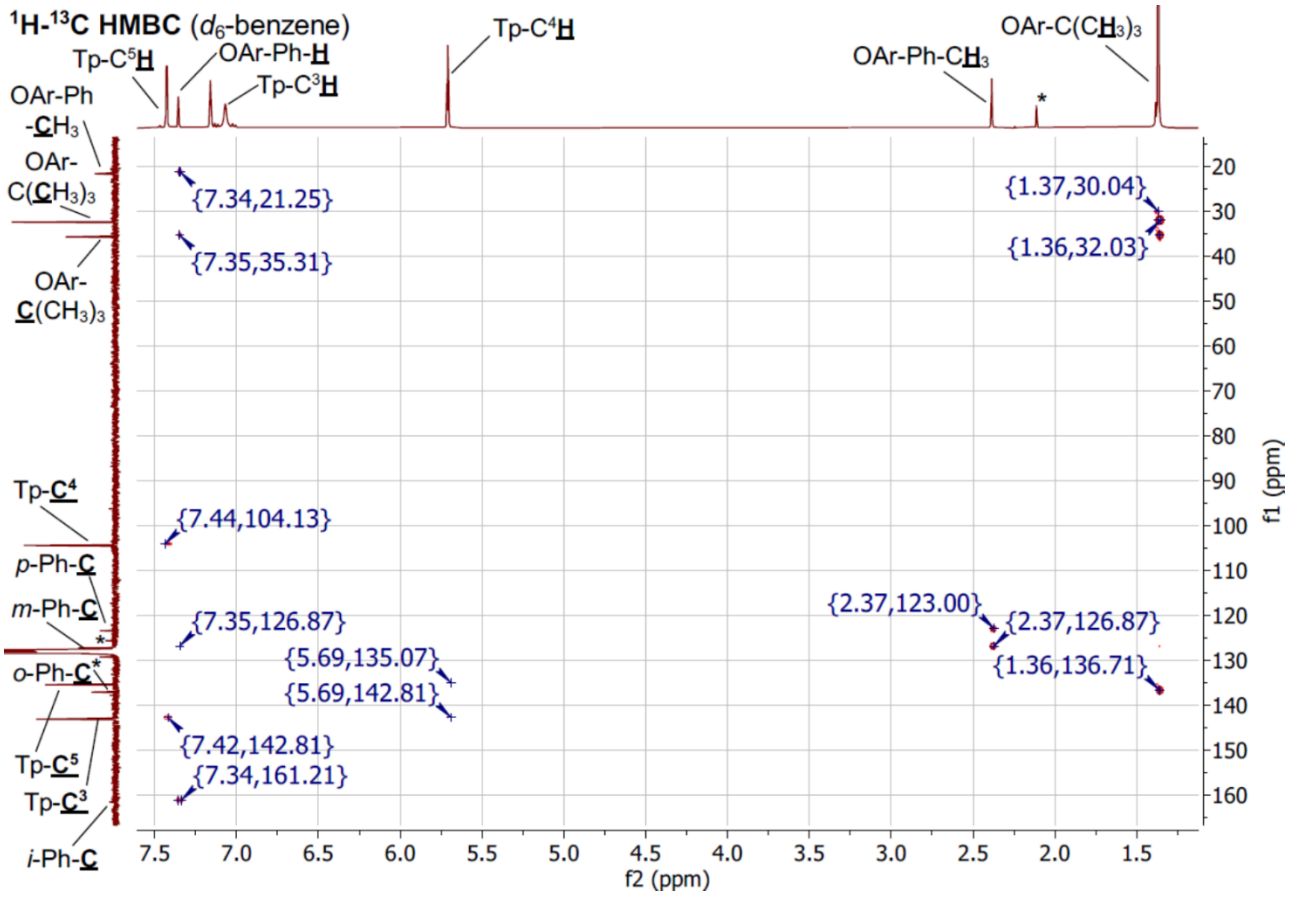

Figure S 63. ^{1}H-^{13}C HMBC NMR spectrum of [Y(Tp)$_2$(OAr)] **5-Y**, recorded in d_6-benzene.

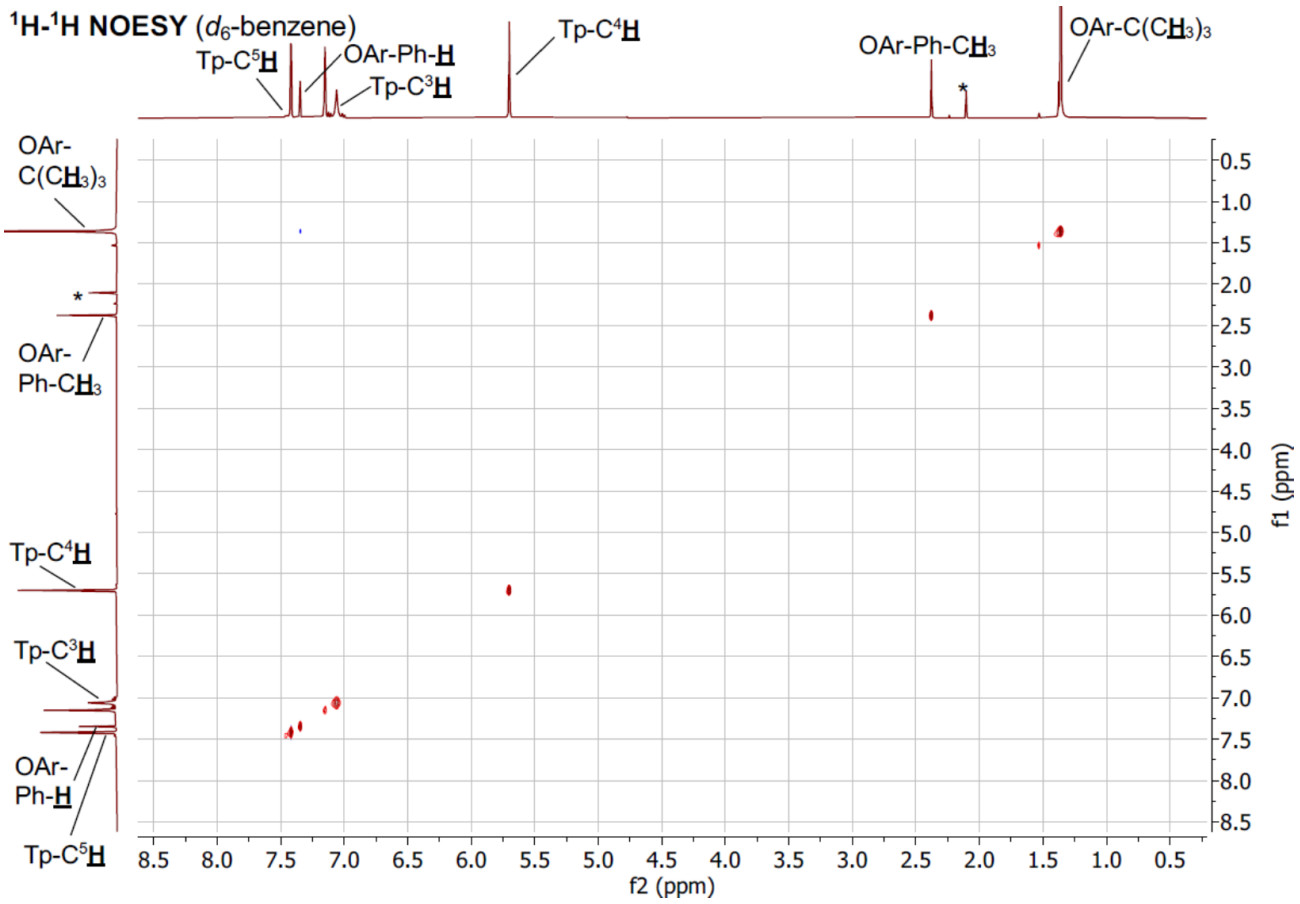

Figure S 64. ^{1}H-^{1}H NOESY NMR spectrum of [Y(Tp)$_2$(OAr)] **5-Y**, recorded in d_6-benzene.

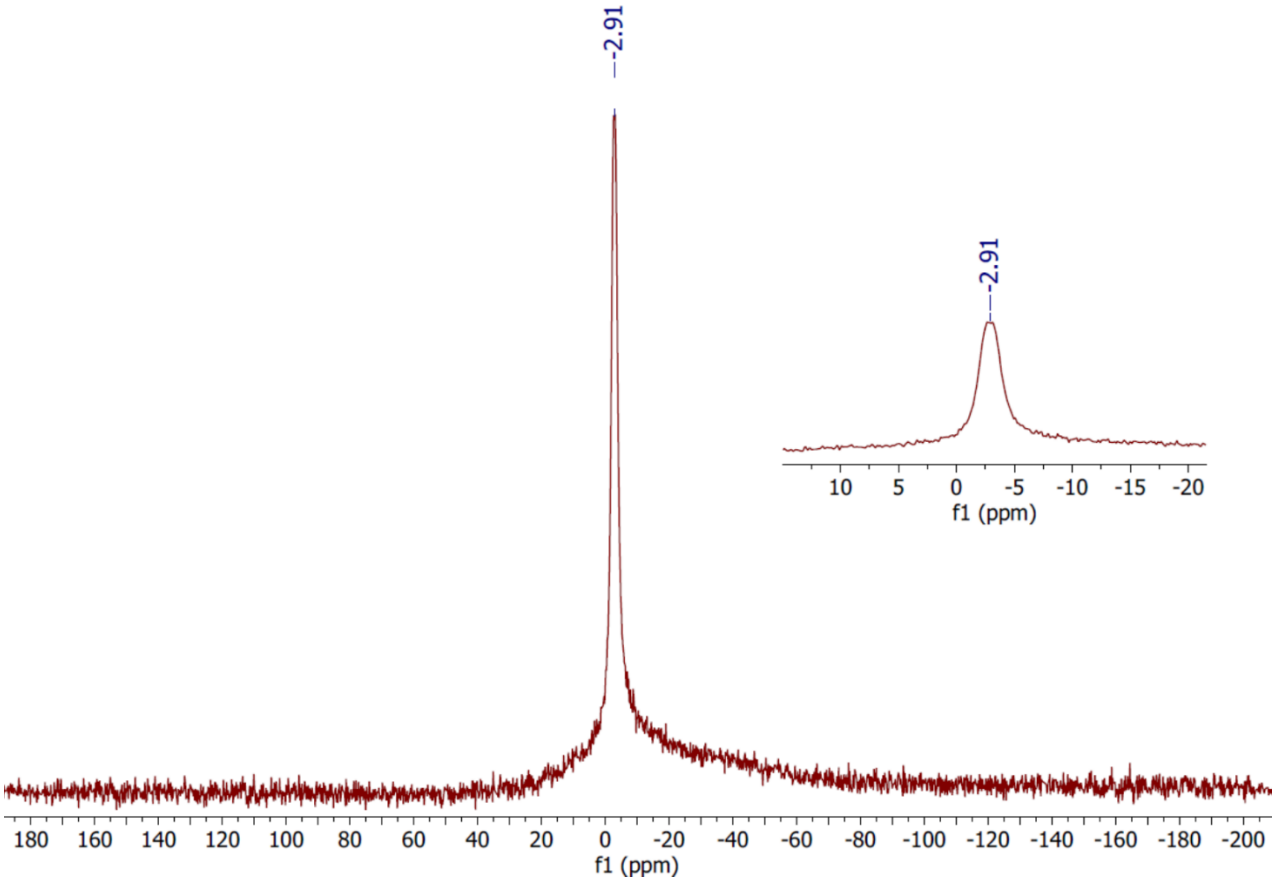

Figure S 65. ^{11}B NMR of [Y(Tp)$_2$(OAr)] **5-Y**, recorded in d_6-benzene.

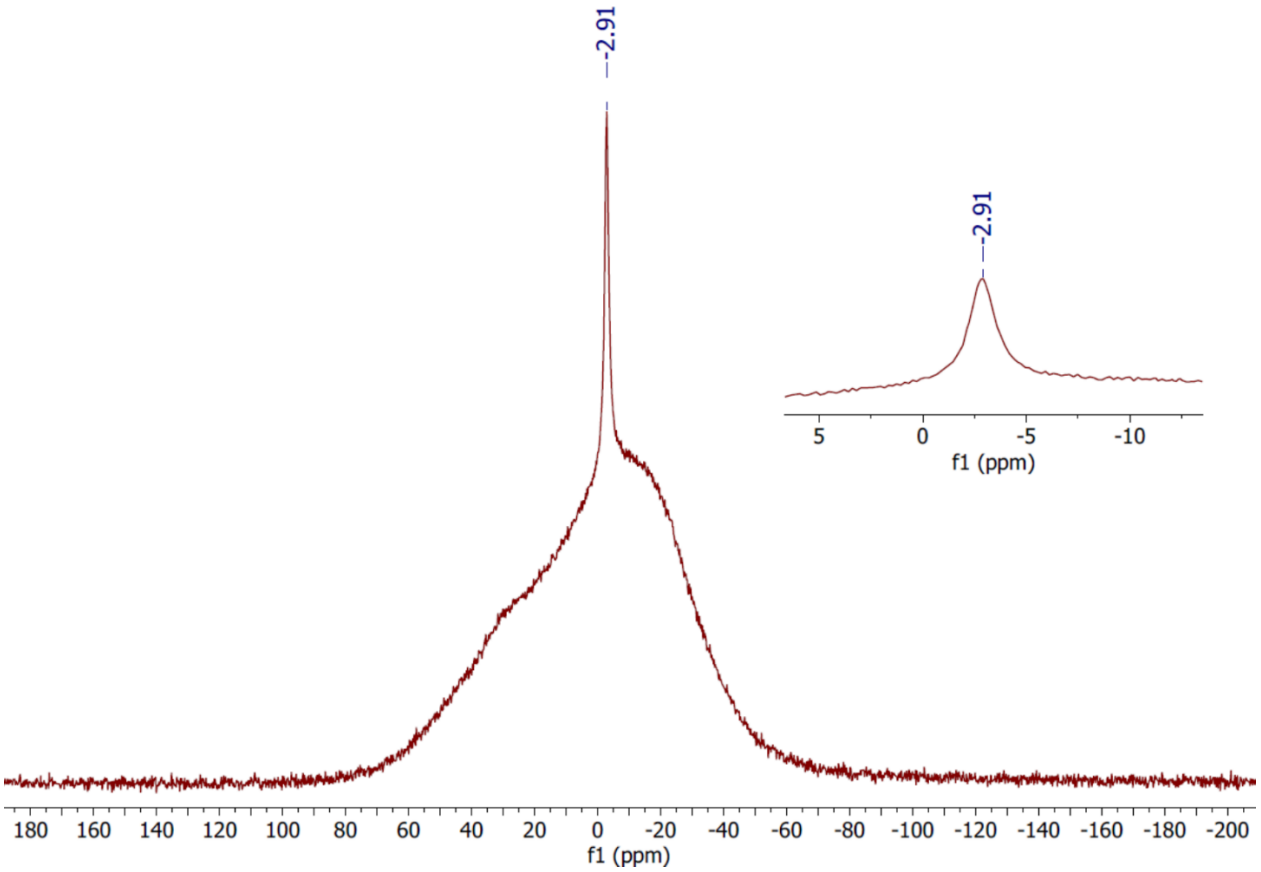

Figure S 66. $^{11}B\{^{1}H\}$ NMR of $[Y(Tp)_2(OAr)]$ **5-Y**, recorded in d_6-benzene.

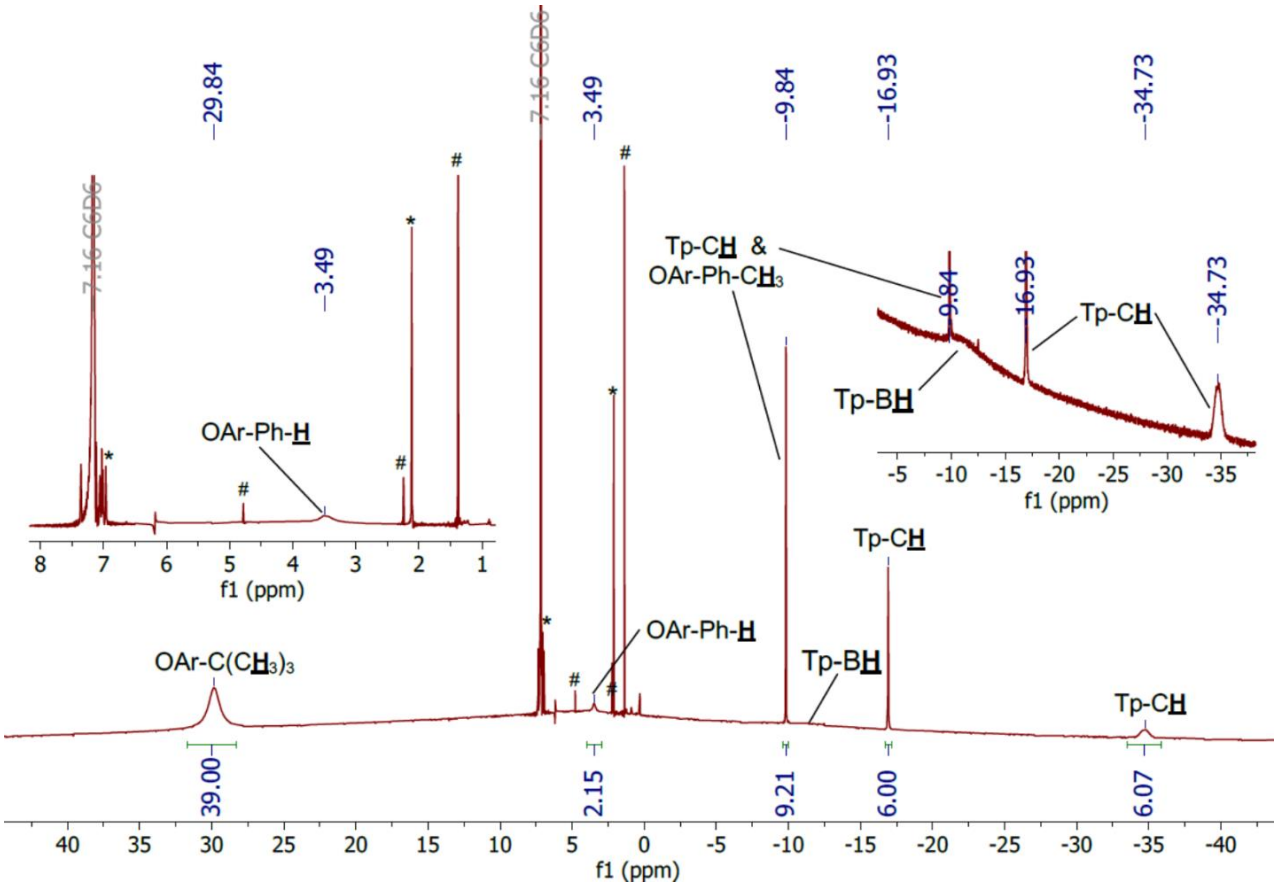

Figure S 67. ^{1}H NMR of $[Yb(Tp)_2(OAr)]$ **5-Yb**, recorded in d_6-benzene. Toluene of crystallisation is denoted with * and H(OAr) from adventitious decomposition of **5-Yb** to H(OAr) is denoted with #.

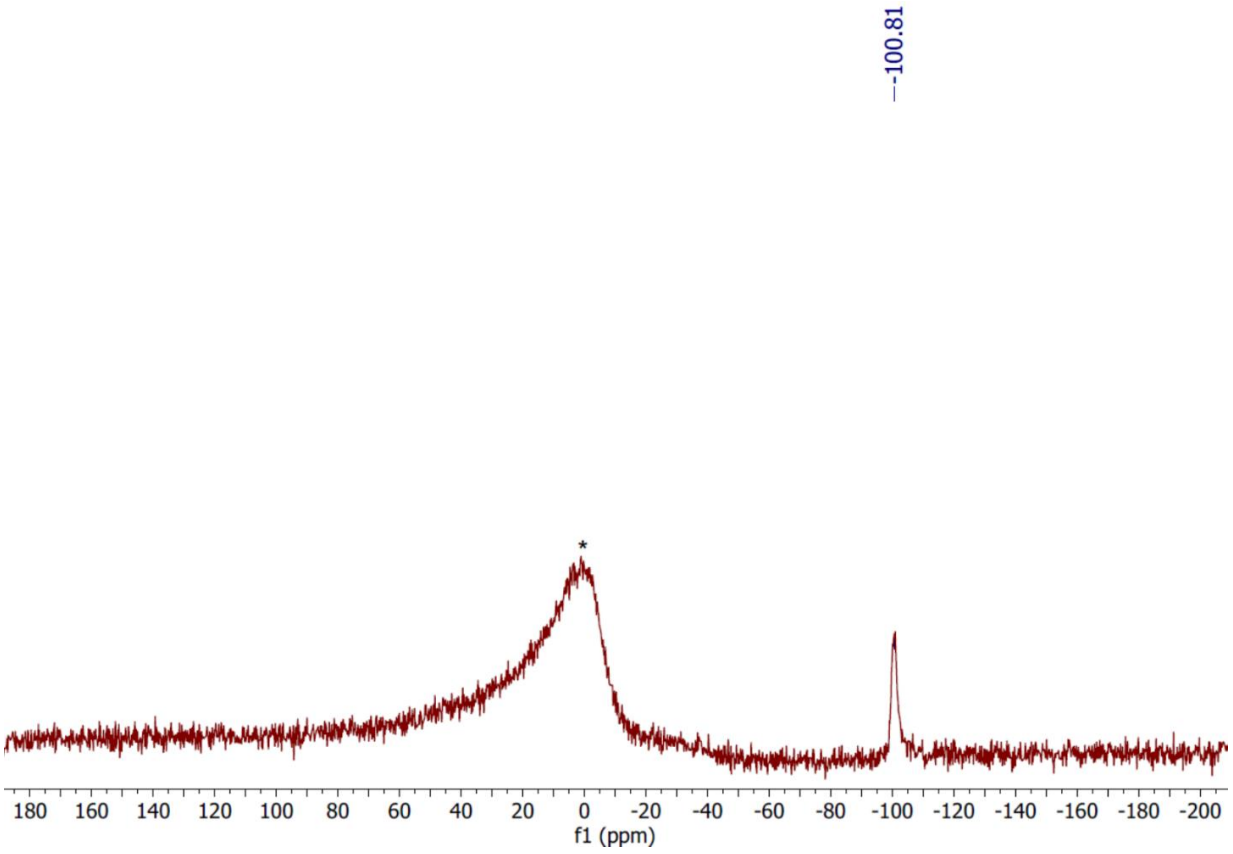

Figure S 68. ^{11}B NMR of [Yb(Tp)$_2$(OAr)] **5-Yb**, recorded in d_6-benzene. Borosilicate glass is denoted by *.

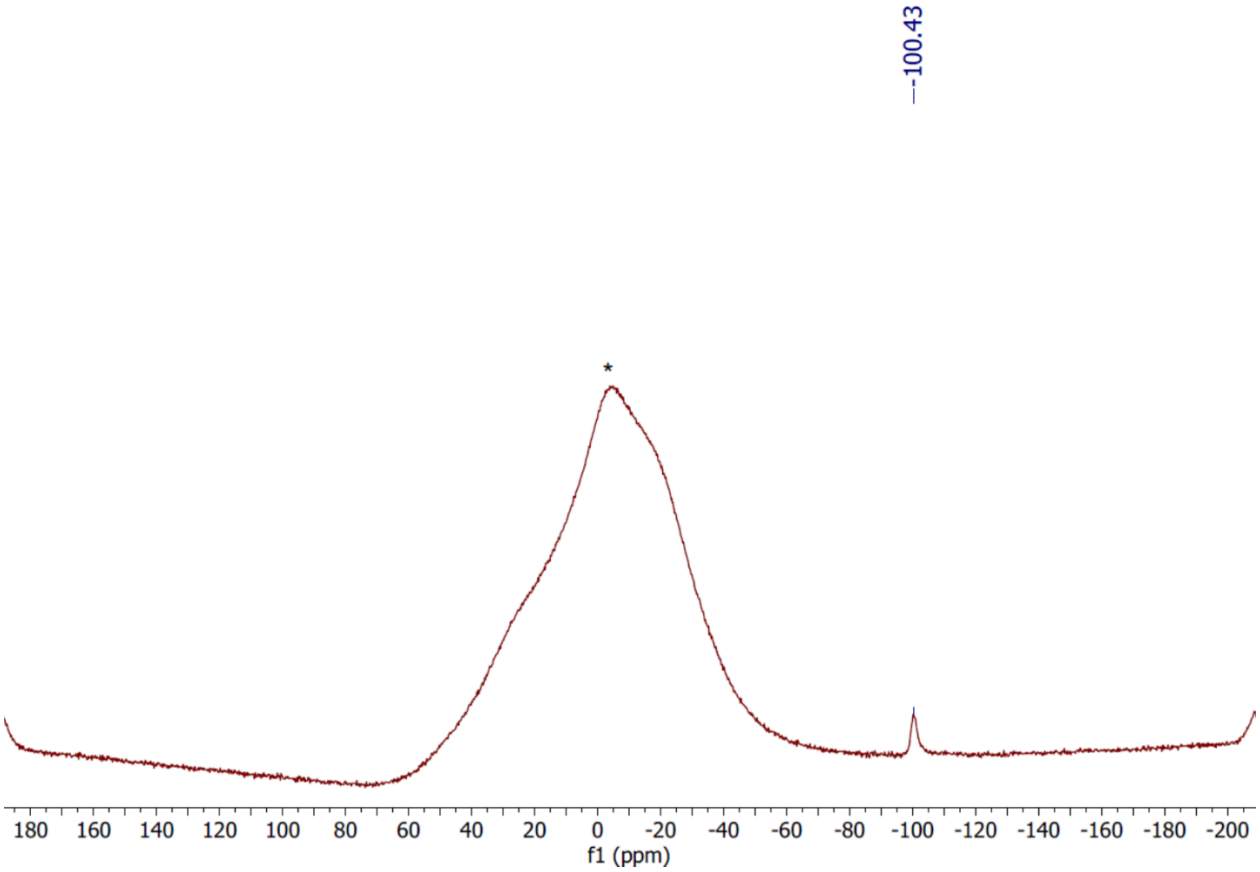

Figure S 69. ^{11}B{^{1}H} NMR of [Yb(Tp)$_2$(OAr)] **5-Yb**, recorded in d_6-benzene. Borosilicate glass is denoted by *.

S2 Infrared (IR)

S2.1 K(Tp)

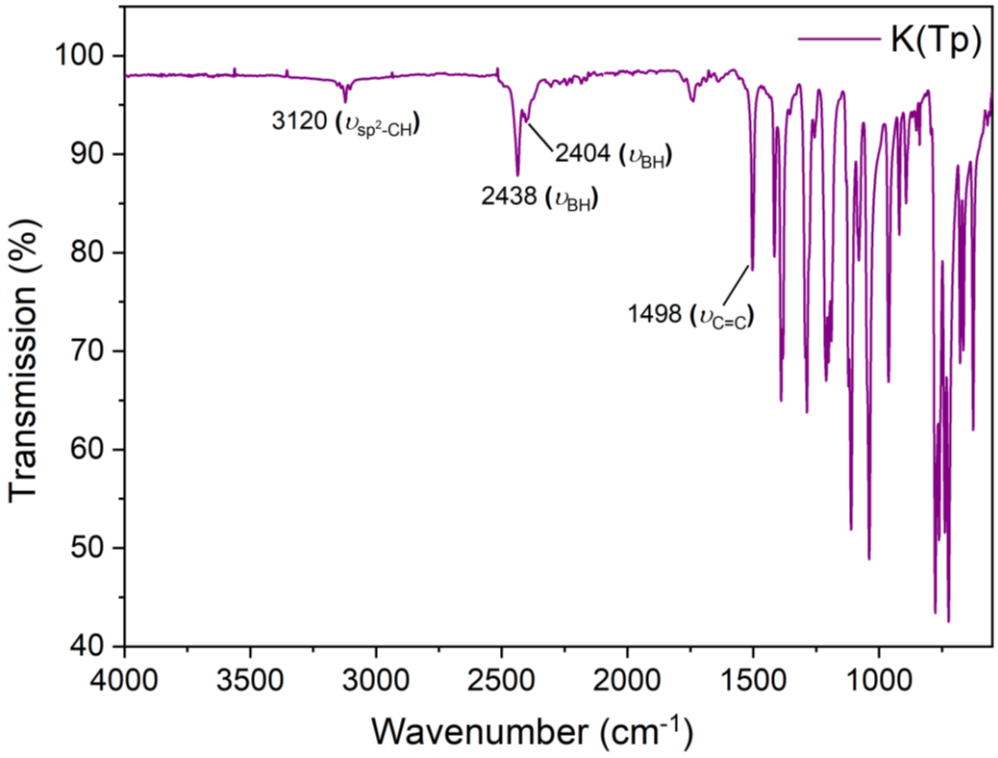

Figure S 70. ATR-IR spectrum of K(Tp), recorded at 298 K.

S2.2 $Ln(OTf)_3$ (Ln = Y, Eu, Gd, Yb)

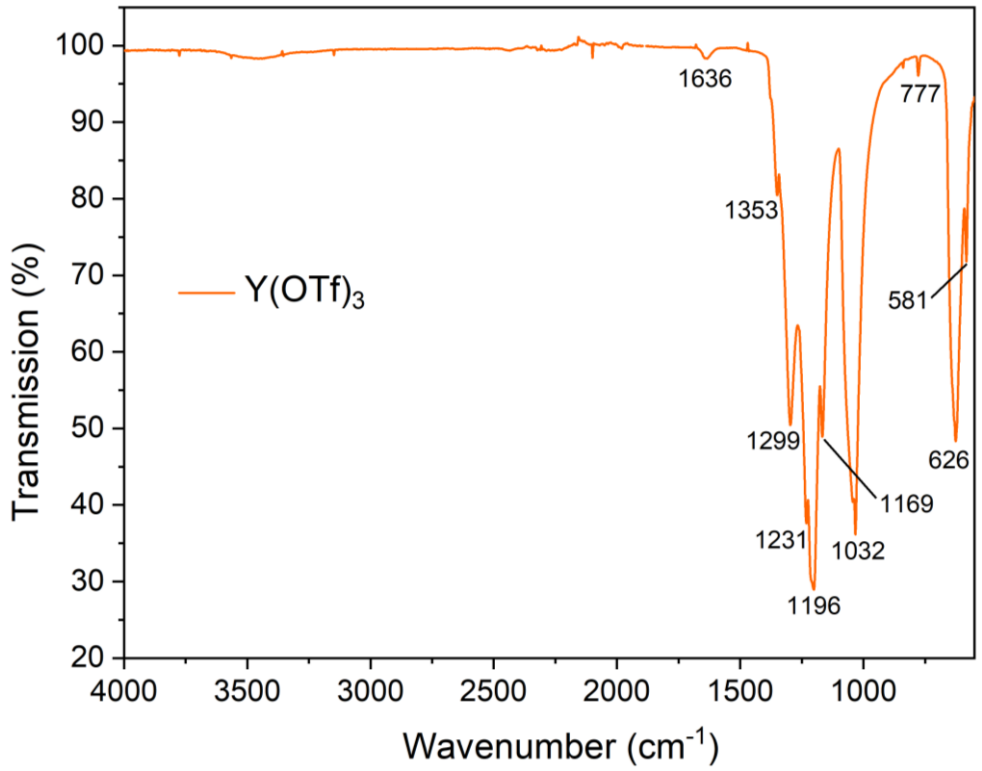

Figure S 71. ATR-IR spectrum of $Y(OTf)_3$, recorded at 298 K.

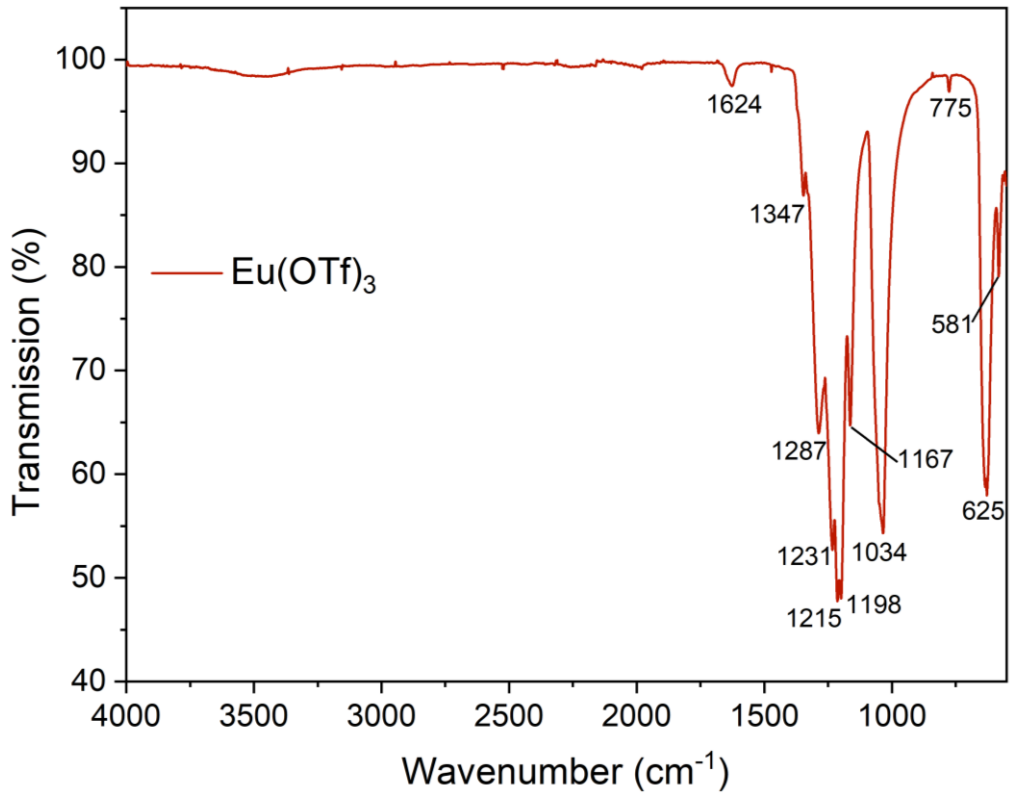

Figure S 72. ATR-IR spectrum of $Eu(OTf)_3$, recorded at 298 K.

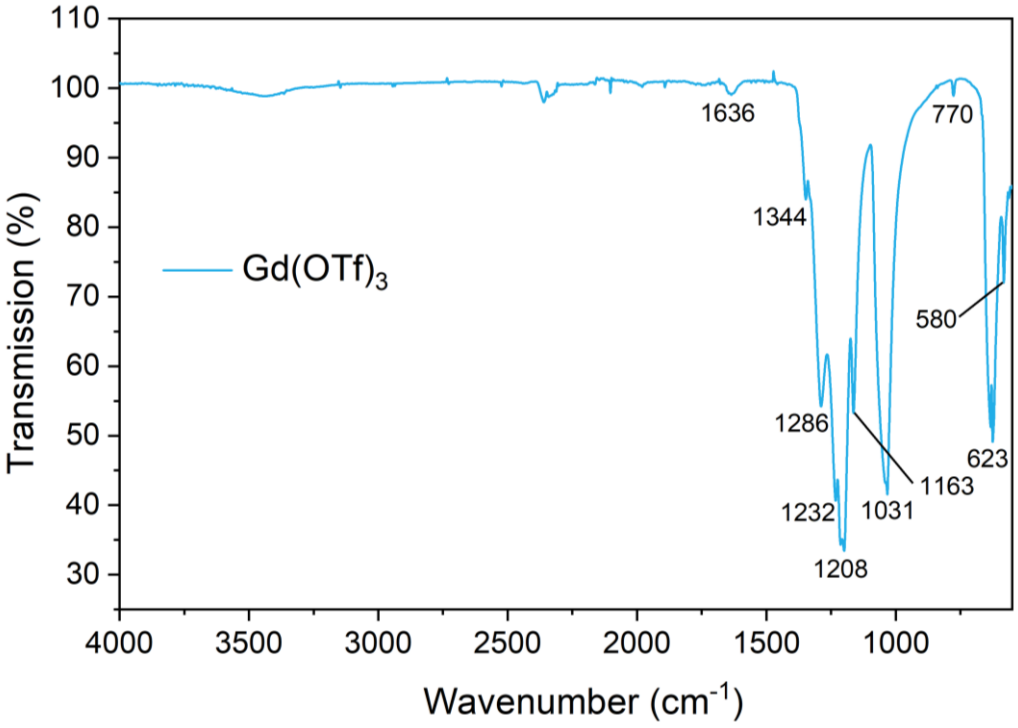

Figure S 73. ATR-IR spectrum of $Gd(OTf)_3$, recorded at 298 K.

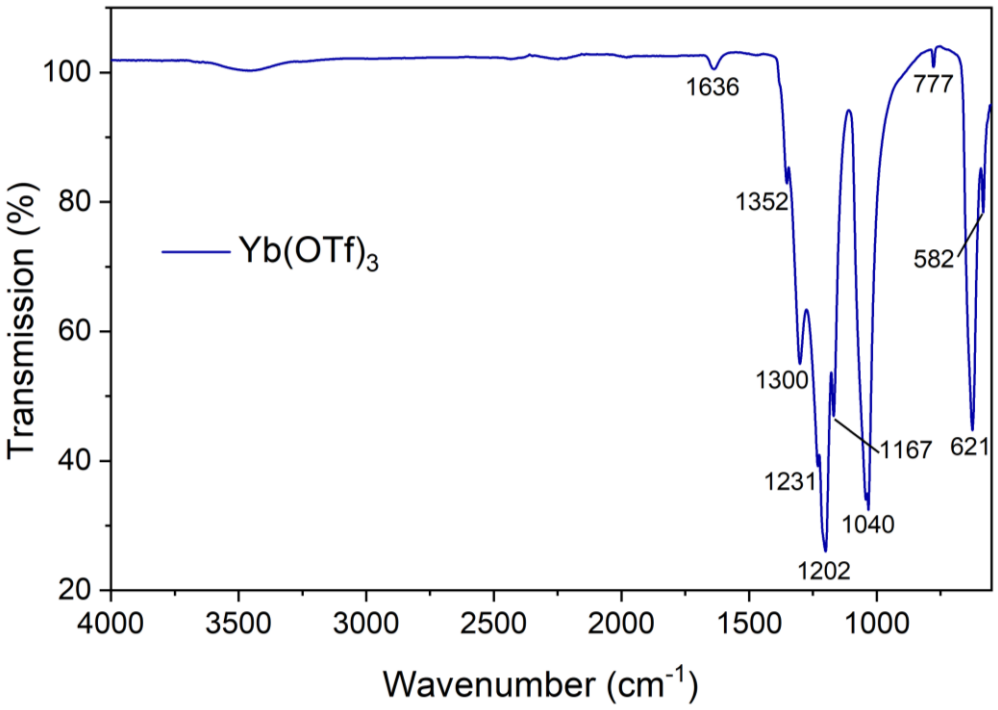

Figure S 74. ATR-IR spectrum of $Yb(OTf)_3$, recorded at 298 K.

S2.3 [Ln(Tp)$_2$(OTf)] 1-Ln (Ln = Y, Eu, Gd, Yb)

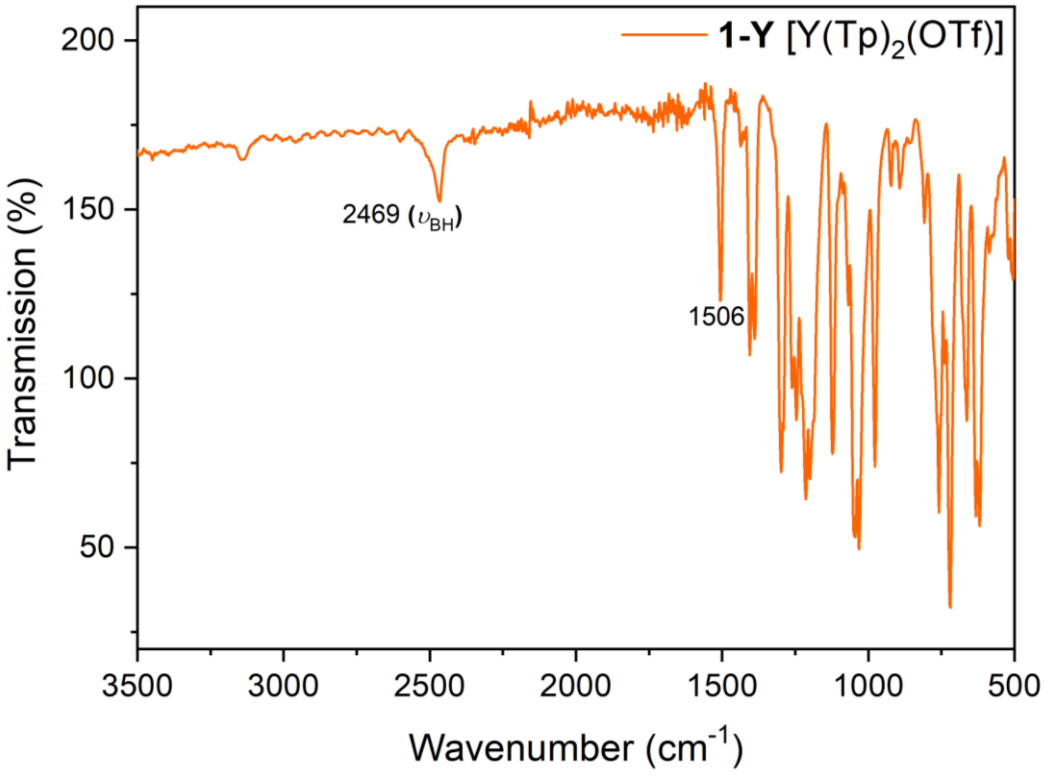

Figure S 75. ATR-IR spectrum of [Y(Tp)$_2$(OTf)] **1-Y**, recorded at 298 K.

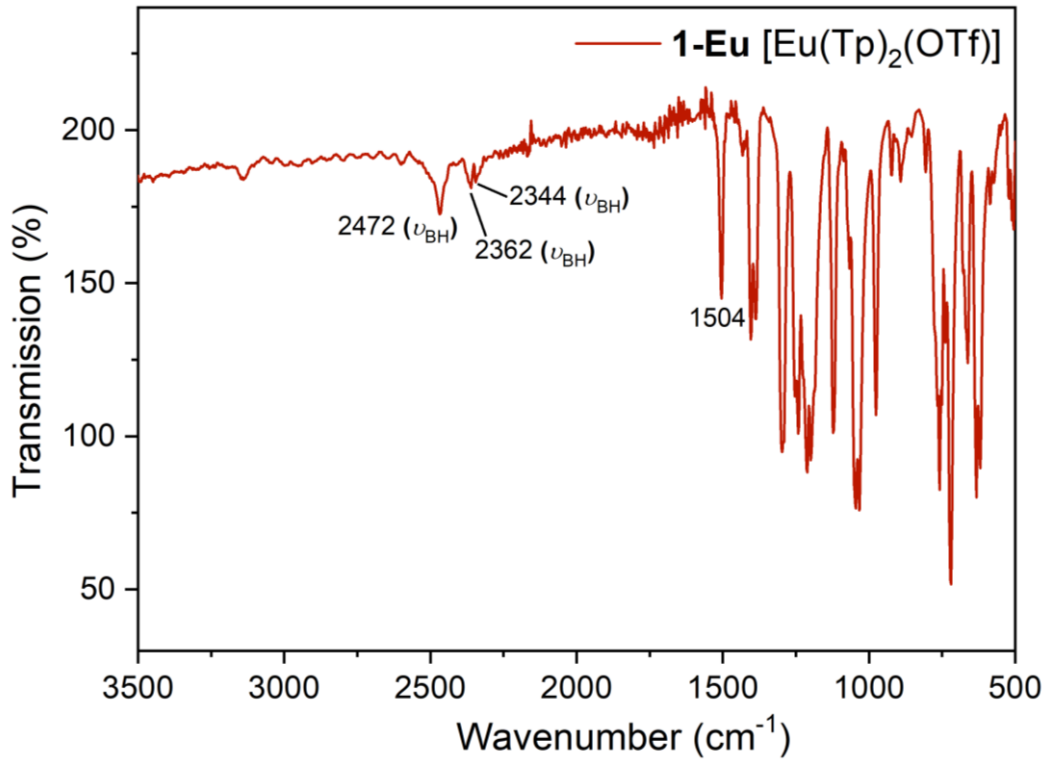

Figure S 76. ATR-IR spectrum of [Eu(Tp)$_2$(OTf)] **1-Eu**, recorded at 298 K.

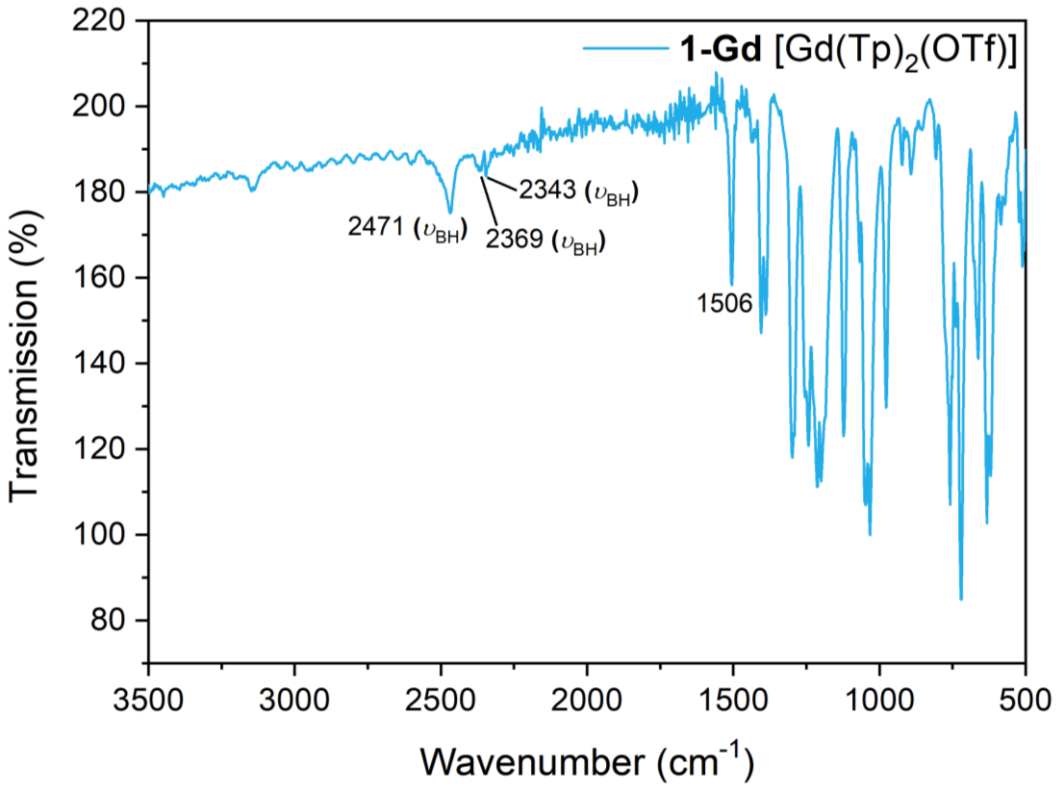

Figure S 77. ATR-IR spectrum of [Gd(Tp)$_2$(OTf)] **1-Gd**, recorded at 298 K.

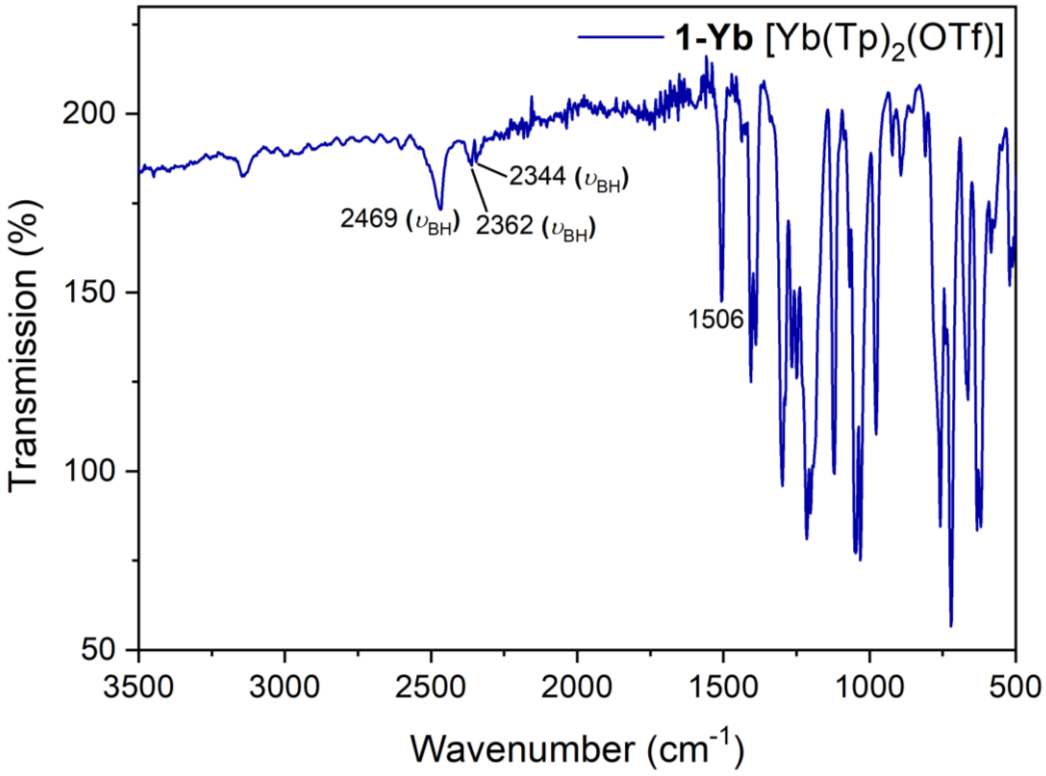

Figure S 78. ATR-IR spectrum of [Yb(Tp)$_2$(OTf)] **1-Yb**, recorded at 298 K.

S2.4 [Ln(Tp)$_2$(hfac)] 2-Ln (Ln = Y, Eu, Yb)

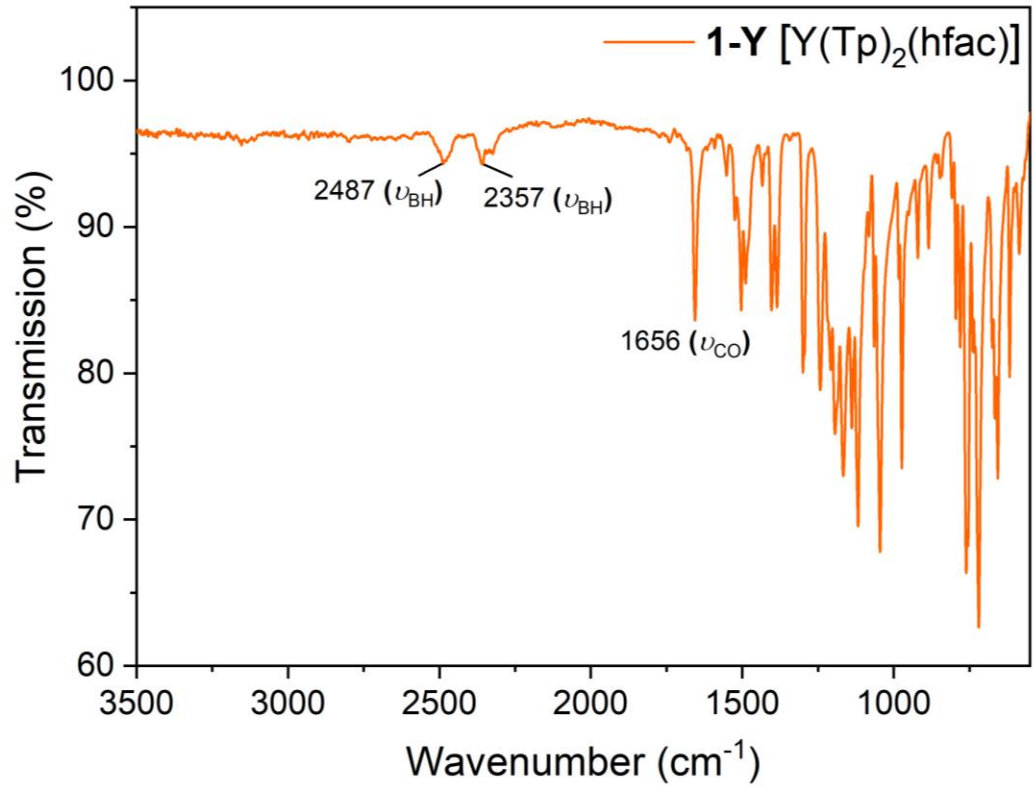

Figure S 79. ATR-IR spectrum of [Y(Tp)$_2$(hfac)] **2-Y**, recorded at 298 K.

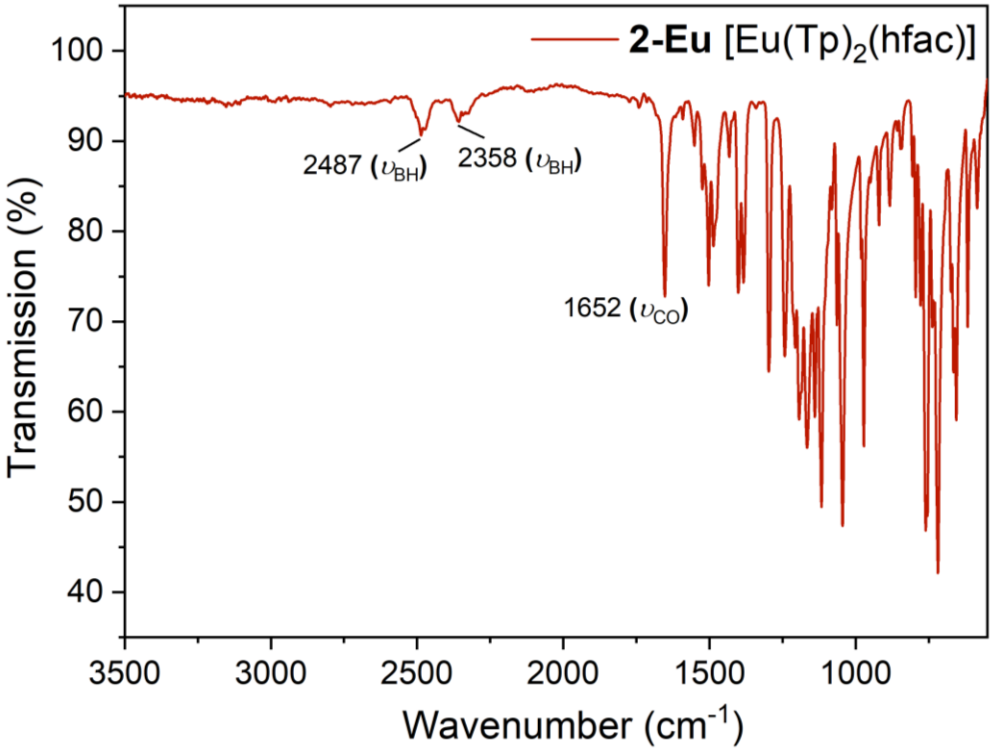

Figure S 80. ATR-IR spectrum of [Eu(Tp)$_2$(hfac)] **2-Eu**, recorded at 298 K.

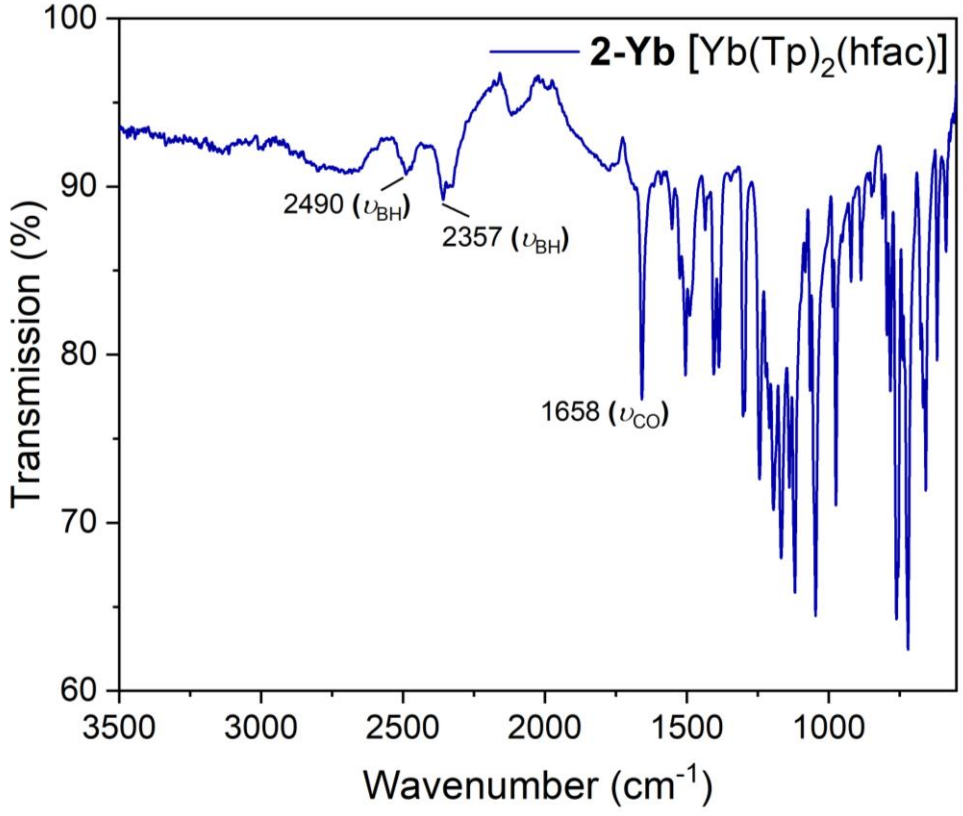

Figure S 81. ATR-IR spectrum of [Yb(Tp)$_2$(hfac)] **2-Yb**, recorded at 298 K.

S2.5 [Ln(Tp)$_2$(N'')] 3-Ln (Ln = Y, Yb)

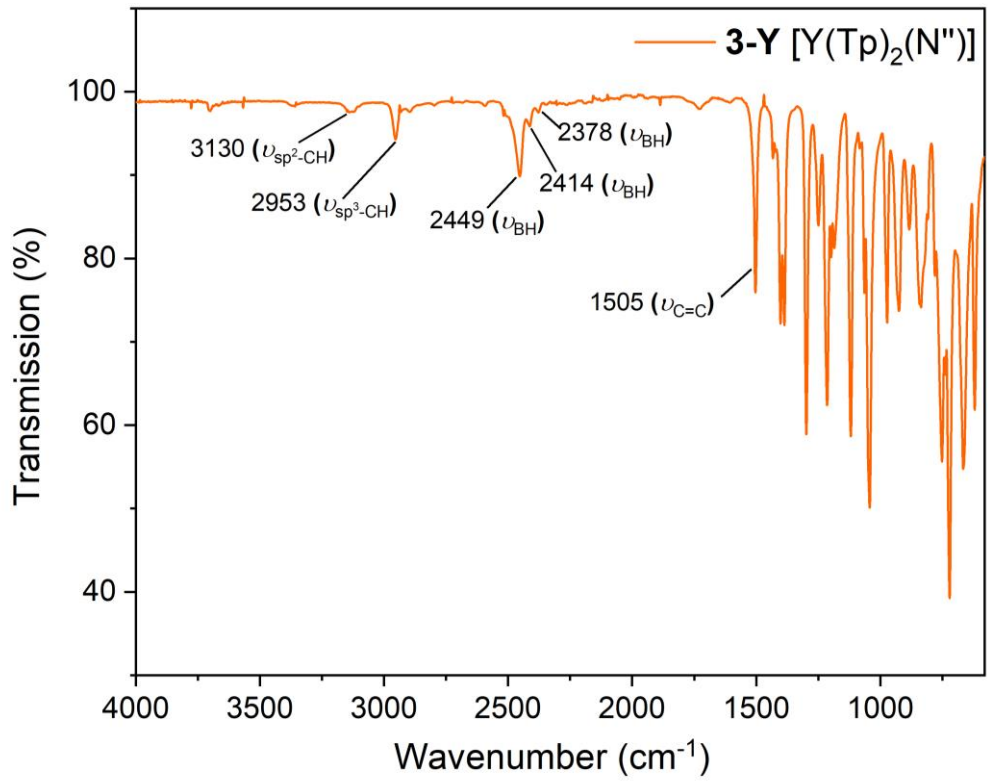

Figure S 82. ATR-IR spectrum of [Y(Tp)$_2$(N'')] **3-Y**, recorded at 298 K.

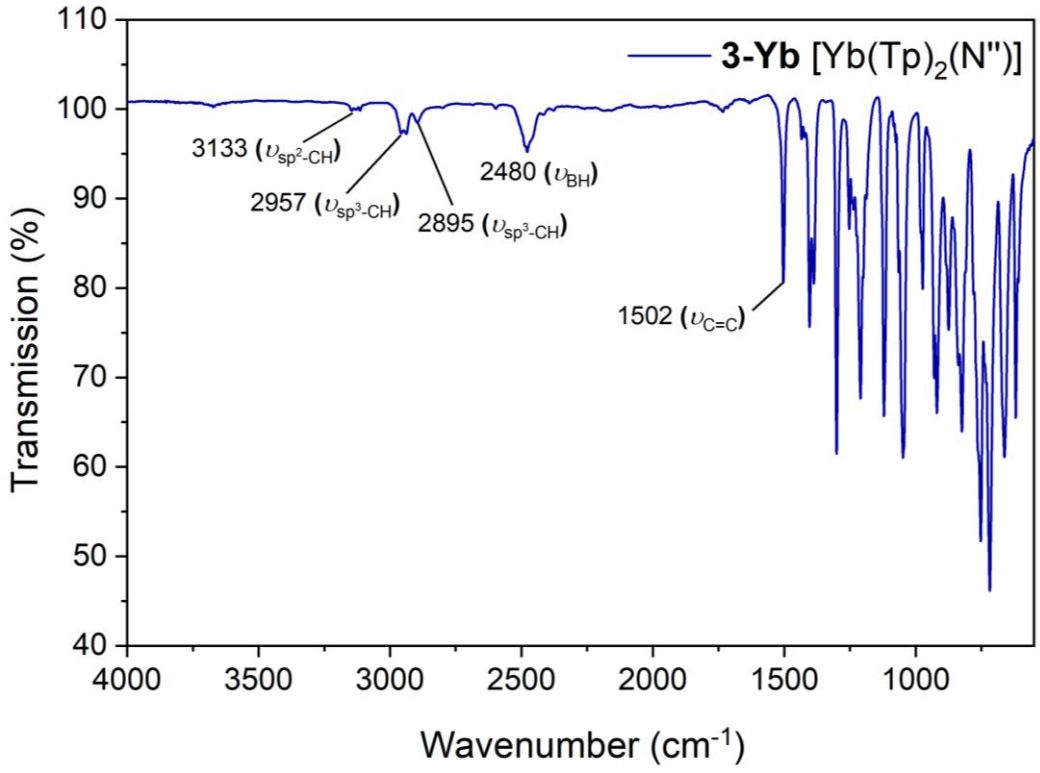

Figure S 83. ATR-IR spectrum of [Yb(Tp)$_2$(N'')] **3-Yb**, recorded at 298 K.

S2.6 [Ln(Tp)$_2$(OAr)] 5-Ln (Ln = Y, Yb)

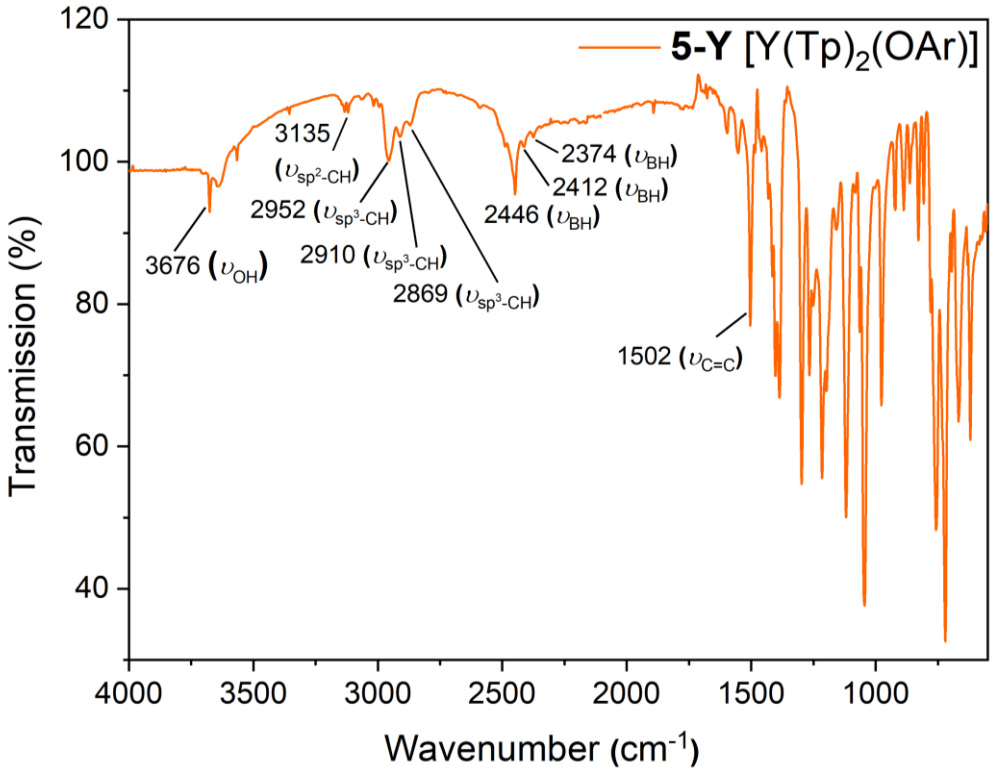

Figure S 84. ATR-IR spectrum of [Y(Tp)$_2$(OAr)] **5-Y**, recorded at 298 K.

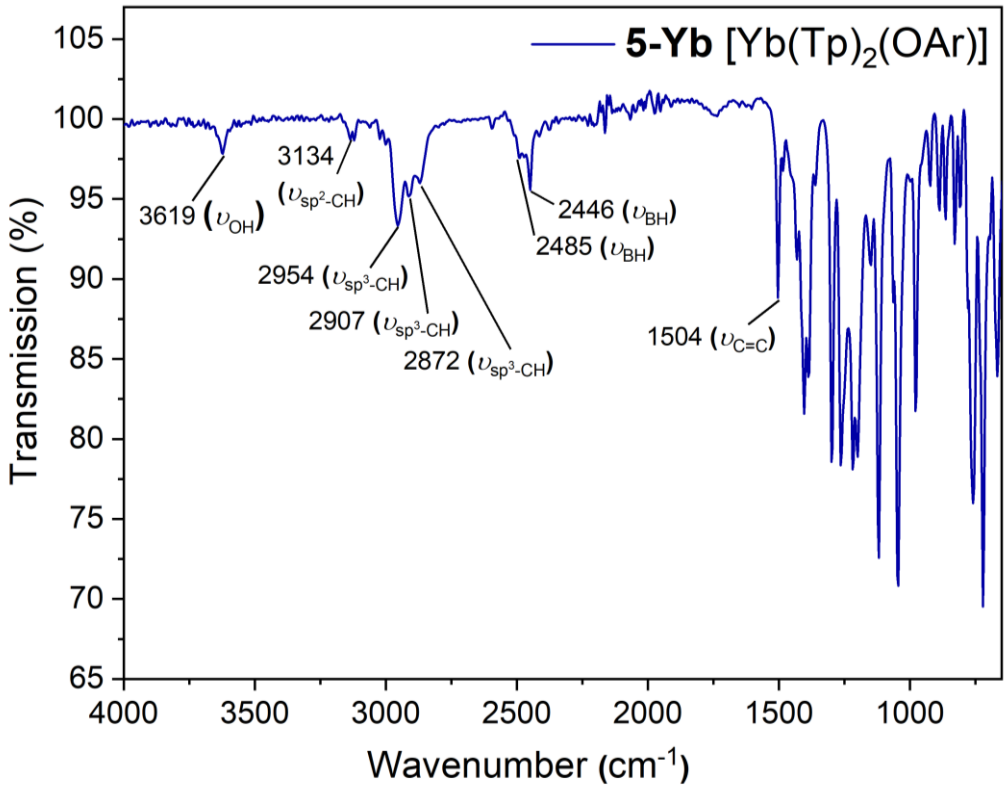

Figure S 85. ATR-IR spectrum of [Yb(Tp)$_2$(OAr)] **5-Yb**, recorded at 298 K.

S3 Electronic absorption (UV-Vis-NIR) of $Ln(Tp)_2(hfac)$ 2-Ln (Ln = Y, Eu, Yb)

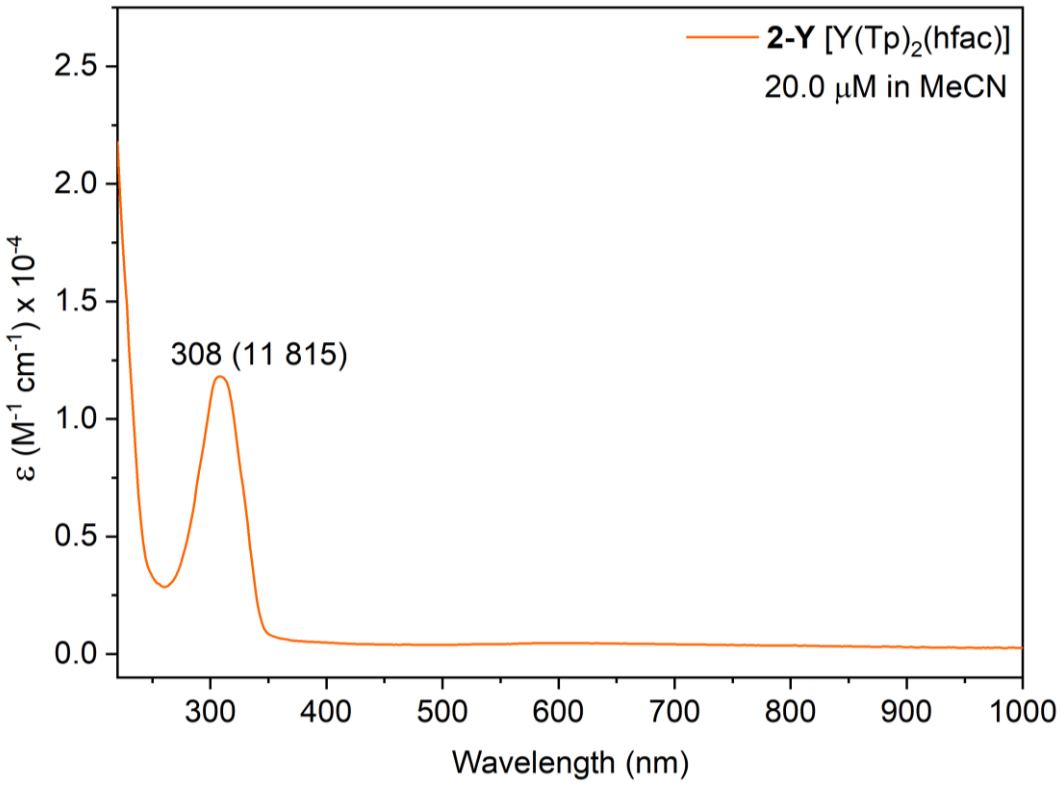

Figure S 86. UV-vis-NIR spectra of $[Y(Tp)_2(hfac)]$ **2-Y**, recorded in MeCN (20.0 μM) at 298 K.

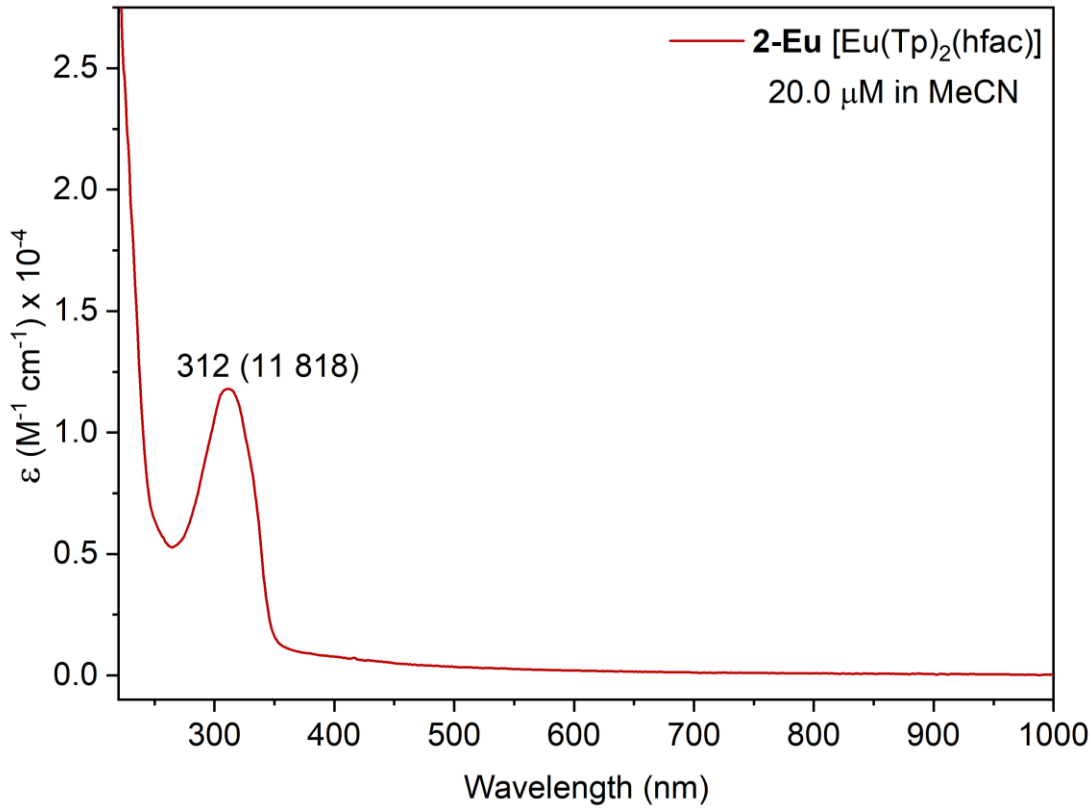

Figure S 87. UV-vis-NIR spectra of $[Eu(Tp)_2(hfac)]$ **2-Eu**, recorded in MeCN (20.0 μM) at 298 K.

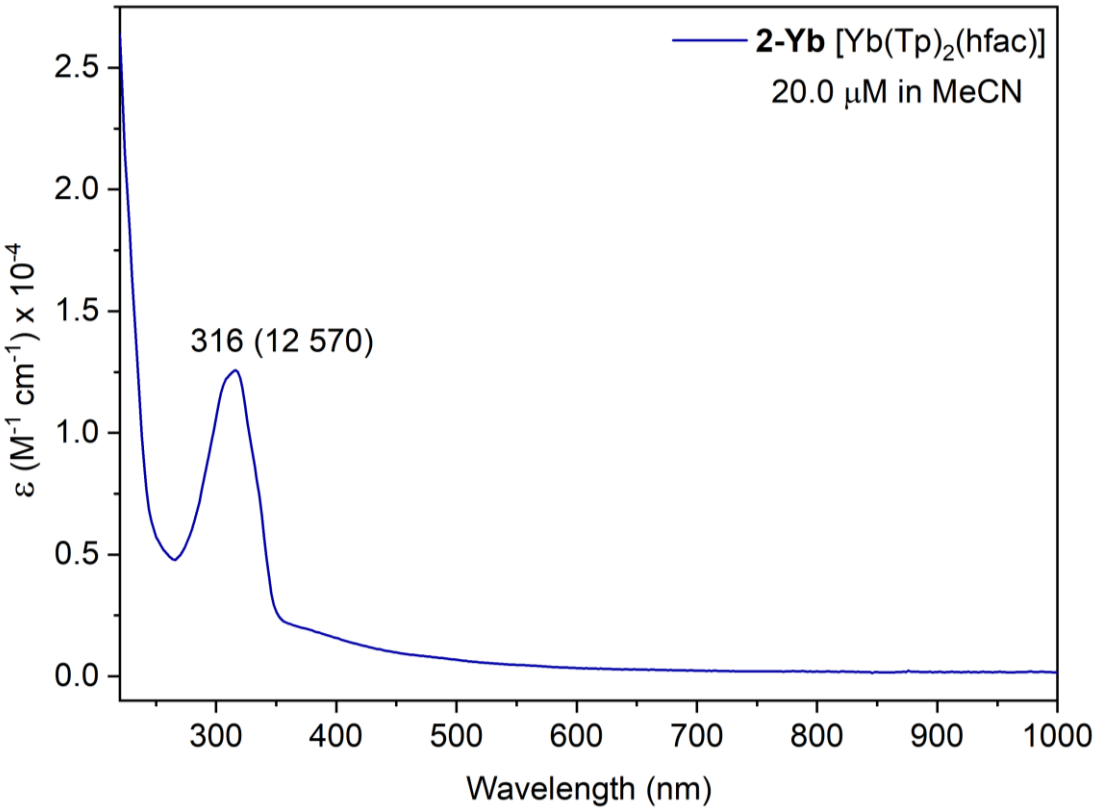

Figure S 88. UV-vis-NIR spectra of [Yb(Tp)$_2$(hfac)] **2-Yb**, recorded in MeCN (20.0 μM) at 298 K.

C. References

[1] S. Trofimenko, J. R. Long, T. Nappier and S. G. Shore, *Inorganic Syntheses* **1970**, 99-109. DOI: 10.1002/9780470132432.ch18

[2] A. B. Simas, V. L. Pereira, C. B. Barreto Jr, D. L. d. Sales and L. L. d. Carvalho, *Química Nova* **2009**, *32*, 2473-2475. DOI: 10.1590/S0100-40422009000900042

[3] R. Inoue, M. Yamaguchi, Y. Murakami, K. Okano and A. Mori, *ACS Omega* **2018**, *3*, 12703-12706. DOI: 10.1021/acsomega.8b01707